

Master thesis, LiTH-IFM_Ex 860

Interactions between [poly(R)-3-hydroxybutyrate] (PHB) and *in vitro* cultured macrophages and fibroblasts

Peter Gennemark and Martin Nyman



Linköping University

Master thesis, LiTH-IFM_Ex 860
Linköping University,
Department of Physics and Measurement Technology
SE-581 83 Linköping, Sweden

Linköping 2000

Contents

1 INTRODUCTION.....	3
1.1 PROJECT BACKGROUND.....	3
1.2 AIM.....	3
1.3 PROJECT OVERVIEW.....	3
1.4 RESTRICTIONS.....	4
2 THEORY.....	5
2.1 WOUND HEALING.....	5
2.2 POLYMERS.....	8
2.2.1 General features.....	8
2.2.2 Poly[(R)-3-hydroxybutyrate] (PHB).....	9
2.2.3 Biodegradation of PHB.....	11
2.2.4 Host response.....	11
2.3 PROCESSING.....	13
2.3.1 Film formation by solvent evaporation.....	13
2.3.2 Film formation by melt pressing.....	14
2.3.3 Particle formation.....	14
2.4 MODIFICATIONS.....	14
2.4.1 Chemical modification.....	14
2.4.2 Plasma modification.....	15
2.4.3 Sterilisation and bulk modification by radiation.....	16
2.5 CHARACTERISATION.....	16
2.5.1 Viscosimetry.....	16
2.5.2 Contact angle.....	18
2.5.3 Fourier transform infrared spectroscopy (FTIR).....	20
2.5.4 Electron spectroscopy for chemical analysis (ESCA).....	21
2.5.5 Gel permeation chromatography (GPC).....	22
2.5.6 Scanning electron microscopy (SEM).....	24
2.5.7 Atomic force microscopy (AFM).....	25
2.5.8 Coulter counter.....	26
2.6 CELL CULTURE.....	26
2.6.1 Fibroblasts and cell adhesion.....	26
2.6.2 Fibroblast viability tests.....	30
2.6.3 Macrophages and cell activation.....	31
3 MATERIALS AND METHODS.....	37
3.1 PHB PROCESSING.....	37
3.1.1 Film formation by solvent evaporation.....	37
3.1.2 Film formation by melt pressing.....	38
3.1.3 Particle formation.....	40
3.2 MODIFICATIONS.....	40
3.2.1 Chemical modification.....	40
3.2.2 Plasma modification.....	41
3.2.3 Sterilization and bulk modification.....	41
3.3 PHB CHARACTERISATION.....	42
3.3.1 Viscosimetry.....	42
3.3.2 Contact angle.....	44
3.3.3 Fourier transform infrared spectroscopy (FTIR).....	45
3.3.4 Electron spectroscopy for chemical analysis (ESCA).....	45
3.3.5 Gel permeation chromatography (GPC).....	45
3.3.6 Scanning electron microscopy (SEM).....	47
3.3.7 Atomic force microscopy (AFM).....	47
3.3.8 Coulter counter.....	47
3.4 CELL EXPERIMENTS.....	48
3.4.1 General materials used in cell experiments.....	48
3.4.2 Fibroblasts and cell adhesion.....	49
3.4.3 Macrophages and cell activation.....	55
3.5 STATISTICS.....	58

4 RESULTS.....	60
4.1 PHB CHARACTERISATION.....	60
4.1.1 Viscosimetry.....	60
4.1.2 Contact angle.....	61
4.1.3 Fourier transform infrared spectroscopy (FTIR).....	64
4.1.4 Electron spectroscopy for chemical analysis (ESCA).....	68
4.1.5 Gel permeation chromatography (GPC).....	70
4.1.6 Scanning electron microscopy (SEM).....	74
4.1.7 Atomic force microscopy (AFM).....	77
4.1.8 Coulter counter.....	79
4.2 CELL EXPERIMENTS.....	79
4.2.1 Fibroblasts and cell adhesion.....	79
4.2.2 Macrophages and cell activation.....	89
5 DISCUSSION.....	93
6 CONCLUSIONS.....	100
7 FUTURE DIRECTIONS.....	101
8 ACKNOWLEDGEMENTS.....	102
9 REFERENCES.....	103
10 APPENDICES.....	108

1 Introduction

1.1 *Project background*

A film structure consisting of the biodegradable polymer, poly[(R)-3-hydroxybutyrate] (PHB) is intended for use as a material in medical devices by Astra Tech AB. PHB can for example work as a protective coat and tissue scaffold after heart and lung surgery. Another application may be the treatment of severe skin wounds, where PHB works as a wound dressing. PHB will degrade to an endogenous substance *in vivo*. The degradation is mainly a result of enzymatic activity and is an extremely slow process, which takes one year or more. The extended degradation period makes studies of the biocompatibility hard to conduct, especially interactions on the cellular level are complicated to follow. However, by variations of the molecular weight *in vitro*, and by adding PHB to an isolated cell culture system, the degradation process can be simulated. Furthermore, interactions on the cellular level can be studied.

1.2 *Aim*

The aims of this diploma work were to fabricate and modify films of the polymer PHB, and to study biological effects at the cellular level during biomaterial (PHB) degradation. The fibroblast attachment and viability on PHB were to be studied by viability assays. The activation of macrophages was to be studied by measuring cytokine production. Furthermore, the cellular degradation of the polymer was to be studied with different surface and bulk sensitive analysis instruments.

1.3 *Project overview*

Films made of poly[(R)-3-hydroxybutyrate] (PHB) were manufactured by melt pressing and solvent evaporation. The film surfaces were modified in three different ways: chemical modification with KOH, plasma modification with O₂ (g) and with CHF₃ (g). In addition fibre patches of PHB were studied. Characterisation of the PHB-films was performed by viscosimetry,

contact angle measurements, Fourier transform infrared spectroscopy (FTIR), electron spectroscopy for chemical analysis (ESCA), gel permeation chromatography (GPC), scanning electron microscopy (SEM) and atomic force microscopy (AFM).

Human macrophages and human fibroblasts were further on exposed to the films. Cell adhesion and proliferation of the fibroblasts and the production of cytokines from macrophages were quantified.

Microspheres of PHB and PLG were also exposed to macrophages. The spheres were studied in SEM.

1.4 Restrictions

The main restriction in this diploma work is that PHB is intended to be used *in vivo*, while all experiments are performed *in vitro*. Therefore, the number of biological agents (cells, proteins, etc.) that can influence the degradation of PHB is limited.

2 Theory

The theoretical part of this work provides an introduction to the cellular events following an injury, for example caused by a surgical operation followed by the implantation of a biomaterial. Furthermore, a section about polymers with focus on PHB is presented. The following sections give a background to instruments and analyses used, with a subsequent part about fibroblasts and macrophages.

2.1 *Wound healing*

When skin, tissue or an organ is damaged there is a sequence of events taking place in the body to prevent further injury and to facilitate the healing process, a process which itself is highly dynamic and flexible depending on type of injury and site of injury. There is also a difference when remainders, for example an implant, is left behind at the site of injury. This causes the body in some way to neutralise, wall off or dilute the injurious agent itself. That is, an inflammatory process.¹

Immediately after an injury, changes occur in vascular flow, caliber, and permeability. Fluid, proteins, and blood cells escape from the vascular system into the injured tissue in a process called exudation. The fluid formed is called exudate. Following changes in the vascular system, which also include changes induced in blood and its components, cellular events occur and characterise the inflammatory response.¹ Inflammation is thus a cellular and vascular response that serves to dispose of microbes, foreign material, and dying tissue in preparation for repair.²

The inflammatory response

When an implant is placed into the human body, there are numerous of mechanisms that initiate to heal the injury caused by the surgical scission. The implant itself causes an inflammatory response that serves to contain, neutralise or wall off the injurious agent. The inflammation involves the migration of certain cells to the site of injury. These cells include both leukocytes, monocytes and fibroblasts, that respond to chemical mediators at the early stages of injury. The general sequence of events after an injury can be seen in figure 1.

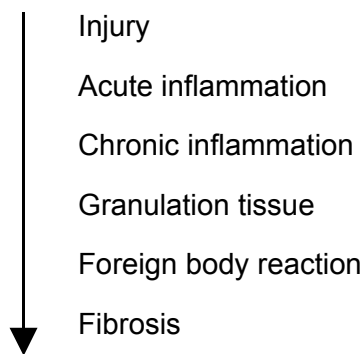


Figure 1. Sequence of events following injury caused by an implantation.¹

The *acute inflammation* lasts for minutes up to days. The dominant cell type around the implant is the neutrophil, which react to serum proteins called opsonins. These opsonins are substances that adsorbes to foreign surfaces, for example bacterial cell walls or biomaterials. The specific attachment of neutrophils to opsonins causes these cells to attempt to phagocyte the foreign material. As the biomaterials often are much to large to phagocyte, the neutrophils will release extracellular products in an attempt to degrade the foreign material. These products comprise reactive oxygen species (ROS) and enzymes.¹

Chronic inflammation involves the presence of monocytes, macrophages, lymphocytes and fibroblasts at the implant site. Renewal of blood vessels and the formation of connective tissue are initiated. The most important cell type during the chronic inflammation is probably the macrophage, with its huge production of biologically active substances. Some of these substances stimulate fibroblasts to produce collagen, and hence tissue remodeling around the implant.¹

Granulation tissue is a specialised form of tissue, composed of fibroblasts, collagen, small blood vessels and other species such as macrophages. The granulation tissue formed can be seen as a hallmark of healing inflammation. Fibroblasts are active, proliferate and excrete collagen that forms a fibrous capsule around the implant. Granulation tissue may be seen from 3-5 days following an implant.¹

The *foreign body reaction* is characterised by the presence of foreign body giant cells (FBGCs) and the components of granulation tissue. The exact composition of species in this reaction is to some extent determined by surface properties of the biomaterial. The reaction may persist for the lifetime of the implant.¹

Fibrosis, or fibrous encapsulation, is generally the last event following an implantation. The implant and the foreign body reaction become isolated from the rest of the body. Though, this ending might seem different depending on the biomaterial and site of implant. The repair of the implant site is mainly determined by the proliferative abilities of the cells present. Tissues composed of "permanent cells" (e.g. nerve cells and some muscle cells) often give rise to fibrosis. Tissues composed of "stable cells" (e.g. parenchymal cells, fibroblasts and epithelial cells) may reconstitute to a normal tissue structure, thus displaying the biomaterial as a more or less permanent constituent of the body. Depending on the implant type, one might want the implant to degrade, i.e. initiate a controlled prolonged foreign body reaction; or firmly attach, i.e. get a regeneration of the normal tissue at the site of implant. This might to a vast extent be determined by the implanted material and its surface composition.¹

Skin wound healing

As the outermost protection of the body, the skin is daily exposed to normal wear and stresses. In addition, severe burns and leg ulcers may disrupt the integrity of the skin.

The skin is composed of two main layers; *epidermis* and *dermis*, divided by a basement membrane. Epidermis is the outer layer and consists mainly of keratinocytes and melanocytes. These cells produce keratin respectively melanin, both protective substances stored in the skin. Epidermis itself is divided into five layers, of which the outer ones are composed of dead keratinocytes filled with keratin. The inner layers are mainly stem cells dividing into keratinocytes, and keratin-producing cells.²

In an epidermal wound, a portion of the epidermal layer is scraped off and basal epidermal cells in the area of the wound break their contacts with the

basement membrane. These cells then enlarge and migrate across the damaged area until they encounter another similar cell. This causes contact inhibition of proliferation and the cells change direction of migration. Finally, when one cell is surrounded by other epidermal cells on all sides, it settles. From this initial layer of new epidermis the cells begin to divide, thus thickening the layer.²

2.2 Polymers

2.2.1 General features

Polymers are long-chain molecules that are built up of small repeating units, monomers. They can be produced synthetically, but lots of polymers, like cellulose and starches, are produced naturally. In polymer synthesis, a distribution of molecular weights is often achieved. Two statistically useful definitions of molecular weight are the number average (\overline{M}_n) and weight average molecular weights (\overline{M}_w), see equations 1 and 2.¹

$$\overline{M}_n = \frac{\sum N_i M_i}{\sum N_i} \quad \text{(Equation 1)}$$

$$\overline{M}_w = \frac{\sum N_i M_i^2}{\sum N_i M_i} \quad \text{(Equation 2)}$$

where N_i is the number of moles of species i , and M_i is the molecular weight of species i . The polydispersity index is equal to the ratio of \overline{M}_w and \overline{M}_n . It is used as a measure of the breadth of the molecular weight distribution.

Polymers containing one type of monomer are called homopolymers, while copolymers have two or more different repeating units. Copolymers can be alternating, random or block copolymers depending on reaction conditions, see figure 2.¹

Homopolymer	-A-A-A-A-A-A-A-A-
Random copolymer	-A-B-B-A-A-A-B-A-B-
Alternating copolymer	-A-B-A-B-A-B-A-B-A-

Block copolymer

-B-B-B-B-B-A-A-A-A-

Figure 2. Possible monomer arrangement in polymers.¹

Due to asymmetric centres on the polymer, different configurations are possible. Chains in which all substituents have the same configuration are isotactic, while syndiotactic chains have substituents alternating from one side to the other. In the atactic arrangement, the substituent groups alter randomly along the chain, see figure 3.¹

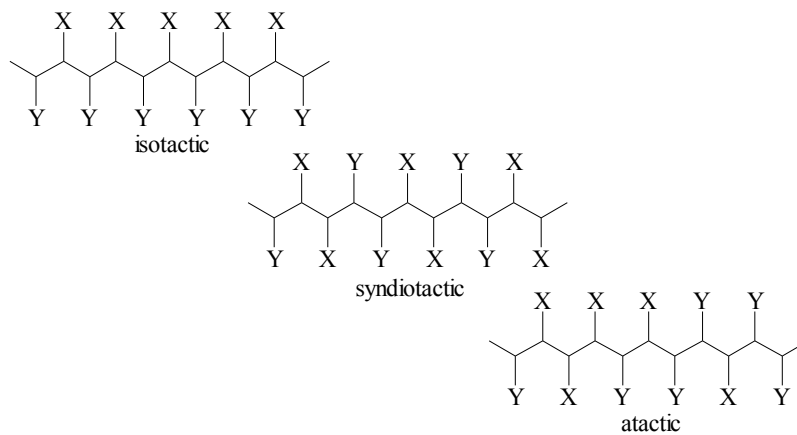


Figure 3. Schematic picture of isotactic, syndiotactic and atactic configurations of polymers.³

Polymers are either totally amorphous or semi-crystalline. Because of lattice defects that form disorders, a polymer can never be completely crystalline. Crystalline polymers tend to be tough and ductile. They can be melt processed and become rigid again upon cooling. The glass transition temperature (T_g) is a measure of the thermal properties of polymers. Below T_g , polymers tend to be hard and glassy, while they are rubbery above T_g .¹

2.2.2 Poly[(R)-3-hydroxybutyrate] (PHB)

Poly[(R)-3-hydroxybutyrate] (PHB) was first characterised in 1925 and is a natural storage product (energy reserve) in bacteria and algae.⁴ The chemical structure of the repeating unit in PHB, is shown in figure 4.

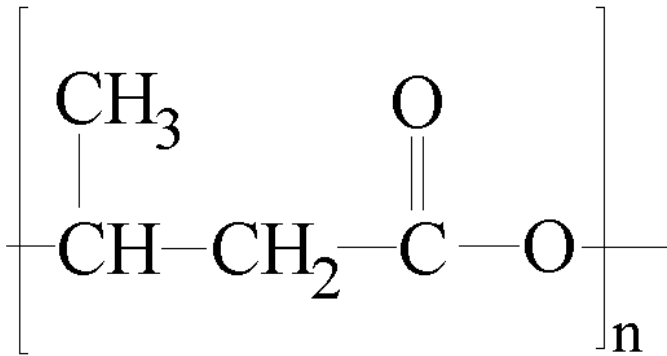


Figure 4. Chemical structure of PHB.

Natural PHB has only one configuration (R) and is therefore isotactic. PHB compares well with polypropylene in terms of molecular weight, melting point, crystallinity and tensile strength. The melting point of PHB is 177°C and the glass transition temperature is 15°C. The crystallinity is 80% and the tensile strength is 40 MPa.⁵

PHB is a ubiquitous component in cellular membranes of bacteria, plant and animals. Furthermore, PHB with a M_w about 14 000 g/mole is found in human plasma. The concentrations ranged from 0.60 to 18.2 mg/l in an experiment performed by Reusch et al.⁶

Current industrial production of PHB employs the microorganism *Alcaligenes eutrophus*, but other microorganisms can also be used. *Alcaligenes eutrophus* accumulates PHB at up to 80% dry weight, when growing on glucose as carbon source. Furthermore, the copolymer poly[(R)-3-hydroxybutyrate-co-(R)-3-hydroxyvalerate] can be produced if propionic acid is added to the glucose feedstock.⁵ It is also possible to synthesise PHB in a laboratory. However, it is not preferred since the chemicals needed are expensive and toxic.⁴

PHB used by Astra Tech AB is composed of approximately 0.15% poly[(R)-3-hydroxyvalerate] and is therefore a copolymer, poly(HB-co-HV) (99.85/0.15).³

2.2.3 Biodegradation of PHB

What is biodegradation? One definition might be:¹

"The chemical breakdown of materials by the action of living organisms which leads to changes in physical properties."

Thus, biodegradation is not limited to processes occurring when inserting a material into the human body; rather does it extend to the entire biosphere. As an example, plastic recycling has become a very important part of environmental preservation. Instead of inventing new methods for recycling, a promising solution to plastics disposal might be the use of biosynthesised polymers, of which the poly(hydroxyalkanoates) (PHAs) are of certain interest. PHB belongs to the PHAs and is a high molecular weight polymer involved in carbon and energy storage by a variety of bacteria. As such, it can be completely aerobically degraded into carbon dioxide and water, which is a most attractive feature. The monomer of PHB is 3-hydroxybutyric acid (i.e. 3-hydroxybutyrate), which also is the product of PHB hydrolysis. Extracellular degradation of PHB yields this monomer, which is small enough to passively diffuse through the cell wall, where it is completely oxidised to carbon dioxide and water.⁵

The specific enzymatic degradation by bacteria can be very fast, reducing the polymer (PHB) content in the cell from 60-70% of dry cell weight to 10-15% just within a few hours.⁴

The human body does not normally host bacteria or fungi able to degrade PHB. Though, there are mechanisms in the body to "defend" the living organism from foreign (invading) substances.

2.2.4 Host response

When an implant is placed into the body, there are numerous of adsorption and absorption processes taking place at the implant site. If, for example, a polymeric surface comes in contact with body fluids, this is likely to occur:¹

1. An initial protein-deposition to the surface
2. A water/protein/lipid-absorption into the bulk of the material
3. Cells that specifically and nonspecifically recognise the attached proteins will adhere to the surface and initiate chemical processes to dispose of the foreign material. These processes are mainly

(i) Hydrolysis

(ii) Oxidation

PHB is subject to normal alkaline hydrolysis (as for all esters) when placed in the body. Under optimal conditions (high pH, high temperature) *in vitro*, this degradation can be quite rapid. Normal body conditions (neutral pH, body temperature), though, make this degradation proceed very slowly. Hydrolysis of PHB *in vitro* at the same temperature and pH as prevalent in the human body displays a significantly slower rate than *in vivo* hydrolysis. This emphasises the humoral catalyse of the process from non-specific esterases and lysozymes secreted by the immune-system.⁴

The hydrolysable group in PHB is the ester-linkage. Hydrolysis of this linkage proceeds as described in figure 5.

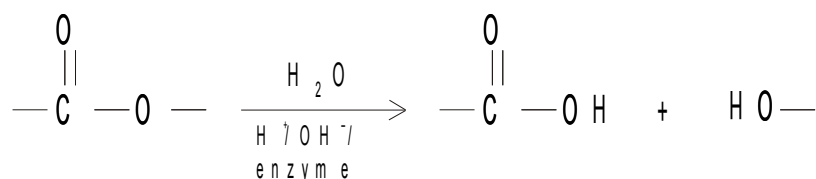


Figure 5. Hydrolysis of an ester-linkage.¹

Both neutrophils and monocytes respond to chemical mediators at the wound site within the early stages of injury. In vicinity of the wound the monocytes differentiate into macrophages, which later may form foreign body giant cells (FBGCs). Activated phagocytic cells excrete reactive species as a response to the implant. These phagocytic cells include polymorphnuclear neutrophils (PMNs), monocytes, macrophages and FBGCs. They metabolise O_2 to form O_2^* , the superoxide anion. This anion might, in a series of reactions, be converted to highly reactive intermediates such as HOCl and OH^* , which serve as oxidants. This excretion of species can be prolonged since the implant often remains for a longer period of time, causing a futile attempt to phagocyte the device. This is called exocytosis or frustrated phagocytosis. Macrophages can reside as FBGCs, or in a collagenous capsule, for several months around the implant.¹

2.3 Processing

2.3.1 Film formation by solvent evaporation

Polymer film formation by solvent evaporation is an easy and fast method to make thin films of a desired polymer.

The polymer is dissolved in a suitable solute, that necessarily has to be evaporable. A few droplets of the solution are put on a surface, which roughness can be varied in order to obtain a desired surface-structure of the film. The solution is evenly distributed using a tool that makes it possible to modulate the thickness. After the solute has evaporated the film can be loosened and allowed to dry completely. Note that the two faces of the formed film usually have different surface characteristics, due to the main evaporation taking place on the side facing air. The thickness of the film can also be varied by trying out different polymer concentrations.⁷

2.3.2 Film formation by melt pressing

Melt pressing is a method for creating polymer films with smooth surfaces and controlled thickness. Hydraulic platen presses have been used in the rubber, plastic, laminating and plywood industry. The press is composed of a basic press frame, a motor pump, two electrically heated platens (maximal temperature usually 300°C). Furthermore, it is possible to program time and pressure cycles.⁸ The polymer, e.g. in powder form, is placed between two press plates. In order to achieve desired films three variables are modulated; pressure, temperature and time.⁷

2.3.3 Particle formation

Particles made of a biodegradable polymer with an incorporated drug can be used in drug delivery applications. Different fabrication methods can be applied to afford controlled drug release from particles. The solvent evaporation method is particularly useful for water-insoluble drugs. The method involves dissolving the polymer (oil phase) in a volatile organic solvent and adding the drug to the organic phase. An emulsifying agent, e.g. polyvinylalcohol, is dissolved in water (aqueous phase). An emulsion of oil droplets is created by homogenisation of the oil phase in the aqueous phase. The emulsifying agent surrounds the oil droplets and has two major functions: It stabilises the biodegradable polymer by steric hindrance and it increases the viscosity, which leads to slower diffusion of the polymer. These two advantages decrease the attachment of particles to each other. During the formation of microspheres, the organic solvent diffuses into the water phase and evaporates.⁹

A disadvantage of the solvent evaporation technique is that the solvent may not completely evaporate. Experiments performed on poly(hydroxybutyrate-co-hydroxyvalerate) (P(HB-co-HV)) showed that residual solvent (methylene chloride) ranged from 3.4 to 58.4 ppm.¹⁰

2.4 *Modifications*

2.4.1 Chemical modification

Chemical modification of a polymer is a versatile method that allows specific modifications in the bulk and of the surface of e.g. a polymer-film. These modifications may consist of introducing functional groups, cleavage of the polymer chain or else.

The method described here applies for alkaline chemical hydrolysis. Hydrolysis is the cleavage of susceptible molecular functional groups by reaction with water. It can be catalysed by acids, bases, salts or enzymes.¹ The reaction-rate can be increased by usage of e.g. potassium hydroxide (KOH); that is, a base. This will essentially introduce carboxyl groups and hydroxyl groups in the polymer chain and render the surface more hydrophilic. Chemical hydrolysis is described in section 2.2.4, figure 5.

The susceptibility of a polymer to hydrolysis is a combination of its chemical structure, its morphology and its dimensions.¹ Properties of PHB that tend to increase the rate of hydrolysis are its high proportion of hydrolysable groups in the main chain, its low or negligible cross-link density and the shape used in this study; thin films, providing a high ratio of exposed surface area to volume.

2.4.2 Plasma modification

Plasma is formed when a gas is supplied a large amount of energy. Neutral atoms or molecules of the gas are broken up by energetic collisions to produce electrons, ions (positive or negative) and other species like radicals. The mix of particles is called plasma. In order to perform a plasma modification on a polymer, a high frequency electromagnetic power is coupled into an evacuated enclosure back-filled with process gas. The enclosure also contains the sample to be treated. The gas becomes ionised into plasma generating the mix of particles and UV radiation, which react with the surface of the sample. In order to achieve functional surfaces by plasma modification, different gases are used. Examples of gases which are used for creation of hydrophilic surfaces are O₂, N₂ and air. Methane and CHF₃, on the other hand, are used for creation of hydrophobic surfaces.¹¹

In this project, low-pressure plasma was employed. At low pressure, collisions are relatively infrequent and the species in the plasma differ a lot in temperature. The free electrons are hot (thousands of Kelvin), while the neutral and ionic species remain cool. Because the free electrons have almost negligible mass, the total system heat content is low, close to room temperature. This makes it possible to process sensitive materials, such as polymers. However, the hot electrons create, through high-energy collisions, radicals and excited species with a high chemical potential energy. Thus, the combination of low temperature and high reactivity makes the method powerful.¹¹

Typically, low-pressure plasma has sufficient energy to break C-H and C-C bonds, which allow reactive group addition, cross-linking and unsaturation reactions to occur.¹²

2.4.3 Sterilisation and bulk modification by radiation

The main purposes by irradiating a polymer sample are to lower the molecular weight in a known fashion and to sterilise the sample.

Several reactions occur within a polymer that is exposed to radiation. The radiation produces reactive free radicals in the sample, which catalyse the addition of molecules (cross-linking, polymerisation) and scission of molecular bonds (degradation, chain scission for polymers). The outcome of the process is determined by a competition between the reactions.¹³

For a sample to be sterilised, a minimal total dosis of β -radiation is set to 25 kGy. This value is based on quite old (1959) research. This value has later been redefined to a Safety Assurance Level (SAL), as “the expected maximum probability of an item or unit being non-sterile after exposure to a valid sterilisation process”. A SAL set to 10^{-6} is defined as a maximum of one in a million survival rate of microorganisms.¹³ The standard of today is that the entire procedure of irradiating a sample must be validated, in order to prove that at most one sample in a million is non-sterile. This implies that no certain dosis can be defined to sterilise a unique sample. Rather is the dosis of radiation individual for every type of sample.¹⁴ The organisms are probably killed due to the damage induced by the radiation to their DNA.¹³

High-energy β -radiation (i.e. electrons) is sent to the sample. The energy level of the electrons is in the range 0,2 – 10 MeV. The maximal energy is restricted to 10 MeV why a radiation-induced radioactivity in the sample is impossible. By irradiating the sample from two (or more) directions, a minimal loss of dosis to the package is obtained.¹³

2.5 *Characterisation*

2.5.1 Viscosimetry

Viscosimetry is a method for determination of the viscosity average molecular weight (\overline{M}_v) of a polymer. \overline{M}_v can then be related to M_n and M_w (for definitions, see section 2.2.1).

The intrinsic viscosity $[\eta]$ [dl/g] can, at a constant temperature and specified solvent, be related to the polymer's viscosity average molecular weight, as¹⁵

$$[\eta] = K^* M_v^\alpha \quad \text{(Equation 3)}$$

, where K and α are the Mark-Houwink constants of a polymer. These are functions of the solvent as well as the polymer type. This relationship is valid for linear polymers¹⁶ and for $0.5 < \alpha < 1.0$.¹⁵ From this equation, a linear relationship between M_v and $[\eta]$ can be calculated as

$$\log(M_v) = \frac{1}{\alpha} (\log([\eta]) - \log(K)). \quad \text{(Equation 4)}$$



Figure 6. Ubbelohde-viscosimeter.

The height is about 30 cm.¹⁷

If a polymer is dissolved in a solvent, the resulting solution will have a viscosity proportional to the \bar{M}_v of the polymer. A higher \bar{M}_v gives a more viscous solution, according to equation 3.

One way to measure the viscosity is by using a viscosimeter, see figure 6.

The time is measured in seconds for a fixed volume of liquid to flow under gravity and at a closely controlled temperature through the capillary of a calibrated viscosimeter. The kinematic viscosity is the product of the measured flow time and the calibration constant of the viscosimeter.¹⁷ This viscosity can then be related to a molecular weight by using a standard curve prepared with molecular weight fractions for each substance. Thus, a number of approximations and simplifications have been done from the scope of equations 3 and 4. Having a correctly prepared standard curve, one can obtain \bar{M}_w by calculations.

2.5.2 Contact angle

Contact angle measurements are useful in order to characterise the surface energy of a polymer. Hydrophilic materials exhibit low contact angle to water. They also possess a high surface energy and have the ability to form hydrogen bonds with water. Hydrophobic materials exhibit high contact angle to water. They possess low surface energy and lack active groups in their surface chemistry for formation of hydrogen bonds with water.¹² There are many methods available for measuring contact angles. A common method is to photograph a small drop of liquid that has been applied to the solid surface of interest. The contact angle θ , between the solid surface and the liquid drop, is determined, by placing a tangent to the drop at its base,¹ see figure 7.

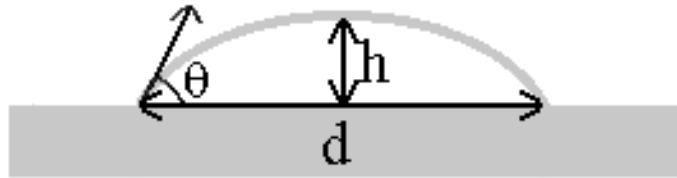


Figure 7. Method for contact angle measurement.¹⁹

The angle θ is calculated using equation 5.¹⁹

$$\tan \frac{\theta}{2} = \frac{2d}{h} \quad \text{(Equation 5)}$$

where h is the height of the liquid drop and d is the length of the base of the liquid drop.

The energy of the surface (γ_{sv}) can be expressed as in Young's equation involving the contact angle (θ). See equation 6.

$$\gamma_{sv} = \gamma_{sl} + \gamma_{lv} \cos\theta \quad \text{(Equation 6)}$$

where subscript **s** refers to solid, **v** to vapour and **l** to liquid. γ_{lv} is the liquid-vapour surface tension of the liquid drop and γ_{sl} is the interfacial tension between the solid and the drop.¹ The components are visualised as vectors in figure 8.

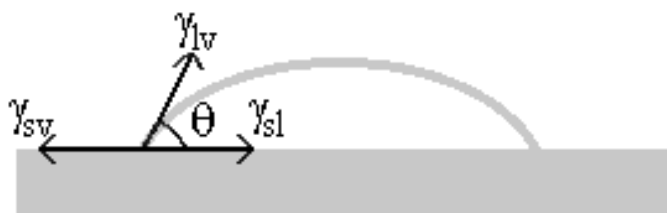


Figure 8. *The components in Young's equation.*¹

The surface energy of the solid (γ_{sv}) can not be directly obtained since the equation contains two unknowns (γ_{sl} and γ_{lv}). Therefore, γ_{sv} is usually approximated by different mathematical methods.¹ An example of such a method is the harmonic-mean method. It uses the contact angles of two testing liquids, Young's equation and the harmonic-mean equation in order to achieve the surface energy. Usually, water and methylene iodide are used as testing liquids. In this method, the surface energy is expressed as two components; a dispersion and a polar. The sum of these components is equal to the solid surface tension. The methylene iodide contact angle mostly influence the dispersion component of the surface energy, while the water contact angle mostly influence the polar component.²⁰

2.5.3 Fourier transform infrared spectroscopy (FTIR)

Infrared spectroscopy provides information about vibrations of atomic and molecular bonds. It can thus be used to analyse a sample, bulk or surface, for certain molecular structures. Information can also be obtained about the orientation of structures.¹

Light of infrared wavelength is sent to the sample. When the frequency of the light is the same as the frequency of a chemical bond within the sample, light is absorbed. The energies of vibration and rotation modes of chemical bonds are often very specific. By Fourier transformation data are presented as a spectrum.²¹

Different types of FTIR-supplements have been evolved. One example is SplitPea™. This is a setup that can analyse solid surfaces, powders as well as liquids.

2.5.4 Electron spectroscopy for chemical analysis (ESCA)

Electron spectroscopy for chemical analysis (ESCA) is a powerful method for determination of the atomic composition of a surface. It is also referred to by its alternative name; X-ray photoelectron spectroscopy (XPS).

The sample to be studied is subject to irradiation from a monochromatic beam of photons (X-rays), usually from a Mg-source or an Al-source. This causes core level (inner shell) electrons from the surface atoms to be ejected. The energies of these electrons are measured and since their respective binding energies are characteristic for the elements in question, the surface elements can be identified. Several types of electrons from the same element are also possible to analyse, originating from different atomic orbitals. In addition, information can be obtained about what type of chemical bonding a certain element is involved in (e.g. carbonyl or carboxyl as for carbon).²²

The basic energy balance used in ESCA is shown in equation 7.

$$E_b = h\nu - E_k \quad \text{(Equation 7)}$$

where E_b is the binding energy of the electron (the value desired), $h\nu$ is the energy of the X-rays (known value), and E_k is the kinetic energy of the electron (measured in the ESCA spectrometer).²² Knowledge about the binding energies allows interpretation of the spectra obtained.

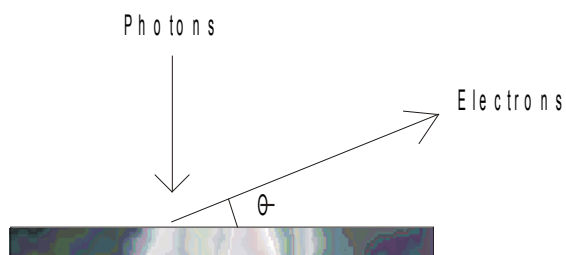


Figure 9. Schematic drawing of the angle of detection (θ) in ESCA.

The X-ray beam (or the detector, as in figure 9) is usually set at a grazing angle to the surface to emphasize the contribution from surface atoms. Most of the signal originates from within nanometers of the surface.²²

2.5.5 Gel permeation chromatography (GPC)

Gel permeation chromatography (GPC) is a technique for determining molecular weights of particularly high-molecular-weight species. A mobile phase, with dissolved molecules of interest, is run through a column with a constant flow. Column packing for GPC consists of small (diameter about 10 μm) silica or polymer particles containing a network of uniform pores into which solute and solvent molecules can diffuse. In the pores, molecules are effectively trapped and removed from the flow of the mobile phase. There are no other interactions between the sample and the column material, the separation depends on the size of the molecules. The smallest molecules diffuse longest into the pores and therefore elute last. Molecules that are larger than the average pore size are excluded and are the first to be eluted. The eluted molecules can be detected by a differential refractometer, which measures the differences in refractive index between the column eluent and a reference stream of pure mobile phase. The detector is highly temperature sensitive and must be maintained at a constant temperature.²¹ A block diagram of a GPC set-up is shown in figure 10.

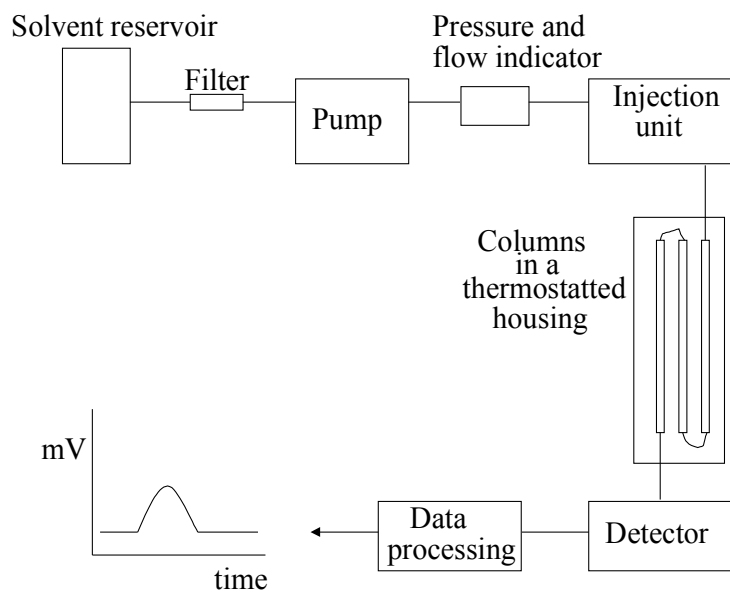


Figure 10. Block diagram of a GPC.³

To get quantitative results from GPC, a standard curve must be constructed. This is accomplished with monodisperse polymer standards, usually made of polystyrene (PS). By translating the standard curve, it can be applied for other polymers. For this purpose the Mark-Houwink equation is used, see equation 8.²³

$$[\eta] = K \cdot M^\alpha \quad \text{(Equation 8)}$$

where $[\eta]$ is the intrinsic viscosity of the polymer solution, K and α are the Mark-Houwink constants for the polymer in a certain solution and M is the molecular weight of the polymer.

If the same solvent is used for both the standards and the polymer of interest, equation 9 is valid.

$$[\eta]_{st} * M_{st} = [\eta]_s * M_s \quad \text{(Equation 9)}$$

where subscript **st** refers to standard and subscript **s** refers to sample.

Combination of equations 8 and 9 gives equation 10.

$$M_s = \left([\eta]_{st} * \frac{M_{st}}{K_s} \right)^{\left(\frac{1}{1+\alpha_s} \right)} \quad \text{(Equation 10)}$$

To calculate the number average molecular weight, \overline{M}_n , and the weight average molecular weight, \overline{M}_w , the height (h) of the peak in the elution curve needs to be measured. By taking the height for several elution times under an elution peak and calculate the corresponding molecular weights according to equation 10, \overline{M}_n and \overline{M}_w can be calculated using equation 11 and 12.³

$$\overline{M}_n = \frac{\sum h_i}{\sum h_i / M_i} \quad \text{(Equation 11)}$$

$$\overline{M}_w = \frac{\sum h_i M_i}{\sum h_i} \quad \text{(Equation 12)}$$

In practice, GPC software tools easily perform all calculations.

2.5.6 Scanning electron microscopy (SEM)

Scanning electron microscopy (SEM) is a useful technique when systems of colloidal dimensions (or smaller) are to be studied. Surfaces can be characterised and observed directly with high resolution and three-dimensional structures are often visualised.

The resolving power of a microscope is limited mainly by the wavelength of the light used for illumination. When extremely small structures are to be visualised, the wavelength of the radiation used must be reduced considerably below that of visible light. Electron beams, focused by electromagnetical lenses, can be produced with wavelengths in the order of 0.01 nm. The scanning electron microscope scans the sample with a fine

beam of electrons. These electrons produce a variety of signals from the sample such as backscattered electrons, secondary emitted electrons and X-rays, which can be detected, displayed on a fluorescent screen and photographed.²²

Before observations, a sample often needs to be coated with a metal. This is done to increase the electron density at the surface and hence detectable signal in SEM. This is usually obtained by applying a thin layer of gold.²⁴

2.5.7 Atomic force microscopy (AFM)

Atomic force microscopy (AFM) makes it possible to create a topographic map of a surface. The technique uses the fact that the forces interacting between a surface and a very small tip are distance dependent. AFM is a lens-free microscope where a tip is mounted on the end of a cantilever, see figure 11. As the sample is scanned, small forces of interaction between tip and surface, cause the cantilever to deflect, revealing the topography of the sample in a three-dimensional way. Typical forces between tip and sample range from 10^{-11} to 10^{-6} N. Deflections as small as 0.001 nm can be detected. AFM can be run in three different modes; contact, tapping and dynamic force mode, which allow the detection of lateral, magnetic, electrostatic and Van der Waals forces.²⁵

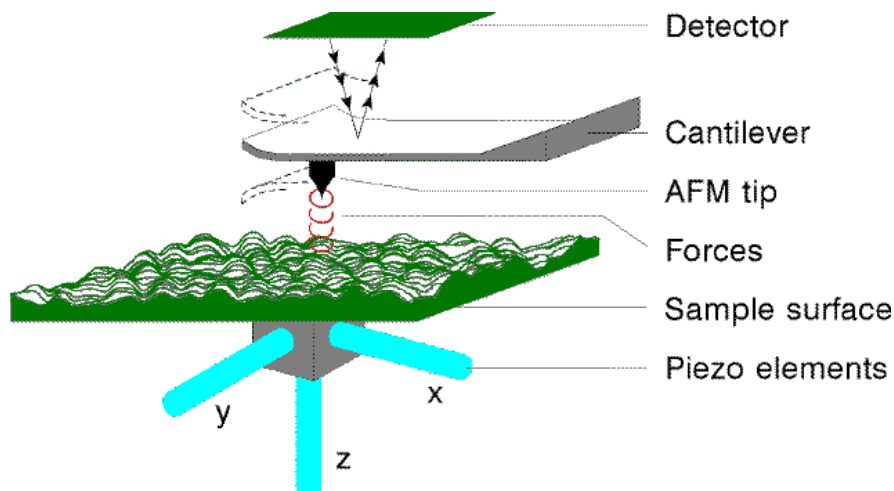


Figure 11. Overview of atomic force microscopy.²⁵

Tapping mode is used to achieve high resolution without inducing destructive frictional forces, which are encountered in the AFM technique. In the tapping mode technique, the cantilever is oscillated near its resonant frequency as it is scanned over the sample surface. The probe is brought closer to the sample surface until it begins to intermittently contact (tap) the

surface. This contact with the surface causes the oscillation amplitude to be reduced, which is detected by a split photodiode using a laser beam, which bounces off the cantilever.²⁶

2.5.8 Coulter counter

Particle size can be measured by the laser diffraction method. The method uses the fact that small particles in the path of a light beam scatter the light in a characteristic, symmetrical pattern, which can be viewed on a screen. Given a certain pattern of scattered light intensity as a function of angle to the axis of the incident beam, the distribution of particle sizes can be deduced. These flux patterns obey the rule of linear superposition. In other words, the pattern from a mixture of several dispersions of particles can be constructed by adding the intensity functions of the constituent particles in the mixture. Thus, the goal of a laser diffraction particle size measurement is to measure the flux pattern in order to determine the distribution of particles.²⁷

2.6 *Cell culture*

2.6.1 Fibroblasts and cell adhesion

As one of the early cells arriving to an implant site, the fibroblast reaction to a biomaterial is important. Fibroblasts seem to thrive even in harsh, solitude environments (e.g. injuries) why they are often used as subjects for cell biological studies.²⁸

The fibroblasts, see figure 12, belong to the connective tissue cells and constitute the architectural framework of the body, partly by secretion of the collagenous matrix. Connective tissue cells play important roles in the repairment of damaged tissue or organs. They are highly adaptable and interconvertible within their family. Fibroblasts may convert to bone cells (osteoblasts/osteocytes), cartilage cells, fat cells or smooth muscle cells (myofibroblasts), thereby facilitating the specialised repairment of different damages within the body.²⁸

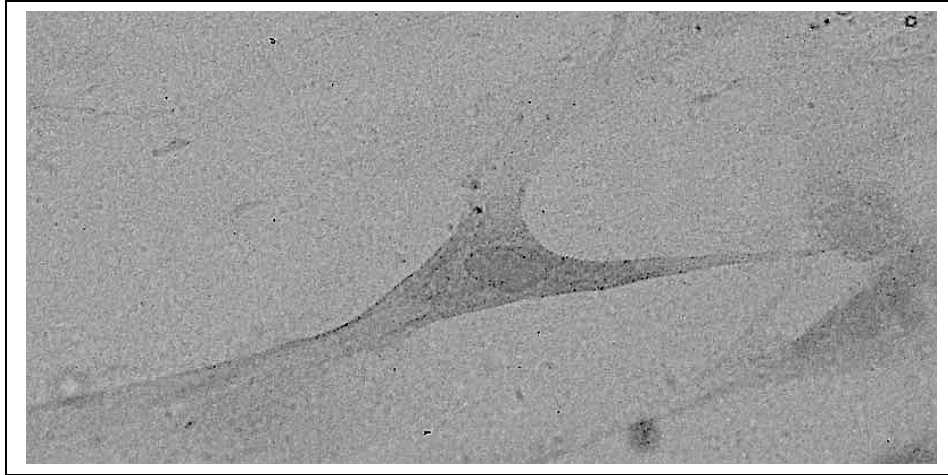


Figure 12. A fibroblast seen in a light microscopy. Magnification 200x.

Fibroblasts secrete collagen type I and III as constituents of the extracellular matrix (ECM). When a tissue is damaged, nearby fibroblasts migrate to the wound, proliferate and produce large amounts of collagenous matrix. This helps to isolate and repair the injured tissue.²⁸

In a defined connective tissue there might exist different types of fibroblast lineages with differing capabilities of transforming into other cells. An immature fibroblast, that can develop into a variety of mature cell types, is called a *mesenchymal cell*. Differentiation of mesenchymal cells is (at least partly) controlled by factors in the ECM, for example transforming growth factor β (TGF- β) and bone morphogenic proteins (BMPs). These substances are found in high concentrations in bone matrix, where they are powerful regulators of growth, differentiation and matrix synthesis by connective tissue cells.²⁸

Fibroblast adhesion

The normal fibroblast is an *anchorage-dependent cell*, i.e. it needs a surface to proliferate. When cultured in suspension, unattached, the cell is rounded up and almost never divide. Though, if a fibroblast form a *focal contact* with a surface it will readily divide and spread. As the cell becomes more spread out the frequency of division increases. A focal contact is the site of attachment, where intracellular actin filaments form anchorages to extracellular matrix molecules.²⁸ Studies have proposed that the metabolic

machinery of the cell is closely coupled to the cytoskeletal network and thus the cell structure after attachment.²⁹

Fibroblasts mediate their adhesion through specific cell-surface receptors directed against molecules in surrounding tissue or adsorbed to the artificial substrate. Such molecules are for example the serum proteins vitronectin and fibronectin.³⁰ It should be noted that already adhered fibroblasts secrete proteins (collagen, fibronectin), which might also have important effects on the local environment of the cell and subsequent adhesion of other cells.³¹

When the fibroblast establish contact with a surface, there is an initial *lag-phase* of proliferation, where the cell does not divide. Rather does it adapt to the surface and spread out. This lag-time can last for several hours. The next event is termed *log-phase*, or proliferative phase, where the cells divide and multiplies. The speed and longevity of this sequence is for example determined by the type of cell and nutrition supply in the surrounding medium. Finally, a state of *confluence* is reached where no proliferation takes place. This is valid for most cells and occurs when the cell is surrounded by and in contact with neighboring cells, also termed *contact-inhibition*. After this state there is a monolayer of cells.²⁸

Fibroblast activation

In order to claim biocompatibility of a material, one must for example show that it does not inhibit normal cell activity such as extracellular expression of substances. Activated fibroblasts normally produce various extracellular matrix proteins such as collagen and fibronectin.³² This activation can be due to macrophages at the site of injury, presenting fibroblast growth regulatory molecules such as interleukin-1 (IL-1). IL-1 regulates fibroblast growth and proliferation and can also induce collagen production.³³

How polymers affect fibroblasts

Characteristics of a material that affect its feasibility for inflammatory cell adherence and activation are important for the biocompatibility of the material. The behaviour of the adhesion and proliferation of cells on polymeric materials depends on various surface characteristics, such as wettability (hydrophilicity/ hydrophobicity or surface free energy), chemistry, topography and the material itself. When studying cell-interactions with a polymer often only one or two parameters are considered why reported results may be somewhat controversial. Certainly, different types of cells

react differently to similar surfaces. This is of extreme importance in implant design, since more than one cell type is expected to interact with the surface.³⁴

Surfaces can be modified in fairly exact manners to display a desired characteristic. Functional groups can be introduced in order to change for example chemistry, wettability and charge. Molecules can be deposited onto the surface by for example plasma modification or by pre-immobilisation of proteins.

Since fibroblasts are anchorage-dependent cells, the substrate onto which they are cultured is of certain importance. They mediate their adhesion through specific cell-surface receptors directed against molecules in surrounding tissue or adsorbed to the artificial substrate. It is therefore likely to believe that adhesion of fibroblasts to artificial substrates is mediated by an initial protein-deposition on the surface. Proteins and other molecules originating from the culture-medium (serum) will quickly (before cell arrival) adsorb to the surface and therefore should be regarded as important for the initial cell-adhesion. This implies that characteristics of the surface concerning its affinity for certain proteins should be evaluated and later referred to the cell-adhesion.¹

Generally, a good surface for fibroblast adhesion should have pre-immobilised molecules such as collagen or fibronectin.³¹ This is not always possible to maintain in all applications of a biomaterial, why the material itself should present a suitable surface. If necessary, the material surface can be processed from chemical modification or other techniques.

Wettability

Fibroblast growth, proliferation and collagen-synthesis depend on the water wettability of the surface, that is the contact angle of water. Optimal condition seems to be when the surface is moderately hydrophilic, that is having a contact angle around 55 degrees.^{34,35} This is not an absolute truth since a study has shown optimum fibroblast affinity for surfaces with contact angles up to 70 degrees.³¹

Surface energy

Relative cell spreading is proposed to be dependent on the surface free energy of the material. Cells show a notable increase in spreading when the surface energy exceeds approximately 50 mN/m.¹

Chemistry and rigidity

Polymers having oxygen-containing diacids in their backbone are uniformly good fibroblast growth substrates, irrespective of hydrophobicity. This

correlates well with reports telling that incorporation of oxygen species into the surface by plasma glow discharge can improve cell growth.³⁶

Pre-adsorbed proteins

Surfaces with pre-immobilised collagen have been shown to present the most favourable conditions for fibroblasts due to minimised lag-time for proliferation. Fibroblasts can proliferate without delay once they come into contact with these surfaces. In contrary, the amount of collagen synthesised relative to the number of cells is highest for surfaces with poor qualities when concerning adhesion and proliferation.³¹

Topography and porosity

Roughness on the level of cell adhesion can be said to be in the order of 1 μm .¹ Fibroblasts have been cultured on polycarbonate (PC) membranes with different micropore sizes, ranging between 0.2 and 8.0 μm in diameter. It was shown that smaller pores favoured cell-adhesion and proliferation. This might be due to a progressive hindrance from large pores.³⁴ Other studies tell that optimal pore size is in the range of 1-2 μm .¹

2.6.2 Fibroblast viability tests

In order to study fibroblast adhesion, viability tests such as Neutral Red and MTS can be employed.

Neutral Red (NR)

Neutral Red (NR) is a colorimetric method for the determination of viable cells in a sample. Basically, it involves the pinocytotic uptake of Neutral Red, which is a red dye. The dye is stored intracellularly in endosomes and by lysing the cells with e.g. ethanol the NR will be released. The total amount of Neutral Red absorbed reflects the number of cells. Neutral Red absorbs light at 540 nm and can therefore be quantified.³⁷

MTS

The MTS test is a colorimetric method for the determination of viable cells. A tetrazolium compound, MTS (3-(4,5-dimethylthiazol-2-yl)-5-(3-carboxymethoxy phenyl)-2-(4-sulfophenyl)-2H-tetrazolium, inner salt), and an electron coupling reagent, PMS (phenazine methosulfate), are mixed in a ratio of 20:1 and added to the cell culture. MTS is then bioreduced to formazan due to the action of dehydrogenase enzymes found in metabolically active cells. Formazan is a brownish soluble compound that absorbs light at 490nm and therefore can be quantified. This quantity is directly proportional to the number of living cells.

One factor that can be varied in the MTS assay is the incubation time, which should be chosen proportional to the number and type of cells. The time-interval should be between 1 and 4 hours.³⁸

2.6.3 Macrophages and cell activation

Monocytes/macrophages

Macrophages are believed to be the primary component controlling the inflammatory and healing responses of biomaterials. They play several roles:³⁹ They perform phagocytosis, they produce growth factors for fibroblasts and other cells, they are also a source of angiogenesis factors (stimulates blood-vessel renewal) and they can modulate the production of connective tissue matrix proteins by other cells (e.g. fibroblasts).

There are two different types of macrophages; fixed macrophages, which reside in a particular tissue, and migrating macrophages, which gather at sites of infection or inflammation.² It is only the migrating macrophages that are derived from monocytes (they are sometimes called monocyte-derived macrophages). They lack proliferative potential and are relatively short lived. Different inflammatory factors stimulate the monocytes to migrate into tissues. Examples of those factors are:⁴⁰ Monocyte chemoattractant

protein-1, -2 and -3 (MCP-1, -2 and -3), macrophage stimulating factor (M-CSF), granulocyte- macrophage stimulating factor (GM-CSF), tumor necrosis factor (TNF) and transforming growth factor α .

Monocytes and macrophages are also highly secretory. Some substances are produced constitutively and others, like TNF, IL-1, IL-6, reactive oxygen metabolites and a variety of growth factors, are induced upon activation.²⁸ Macrophages can be activated to display different characteristics based on their degree of activation and the type of stimulus producing the state. Thus, a single monocyte may give rise to cells with varying properties, depending upon their environment.¹

Phagocytosis is the main function of macrophages. It is seen as a three-step process in which the injurious agent undergoes recognition and cell attachment, engulfment and finally killing or degradation. Biomaterials are not generally phagocytosed by macrophages, because of the disparity in size. The medical device is often several times larger than macrophages. However, certain events in phagocytosis may occur.¹

Recognition and cell attachment takes place when the injurious agent is coated by naturally occurring serum factors called opsonins. The two major opsonins are immunoglobulin G (IgG) and the complement-activated fragment C3b. Both of those plasma-derived proteins are known to adsorb to biomaterials. Macrophages have corresponding cell membrane receptors for these opsonins. These receptors may also play a role in the activation of attached cells. Since engulfment is impossible on an implant, frustrated phagocytosis may occur. The cells release products (e.g. oxygen radicals) in an attempt to degrade the biomaterial.¹

Persistent presence of a foreign material may support an cytokine-induced fusion of macrophages and sometimes also monocytes. The large multinucleated cells are called foreign body giant cells (FBGCs) and their goal is to phagocytose the material.^{1,41}

Cytokines

Cytokines are a group of proteins involved in regulating the cellular response of the immune system.¹ They are quite small (100 to 200 amino acids) glycoproteins produced by red bone marrow cells, leukocytes, macrophages and fibroblasts. They act as local hormones to maintain normal cell functions and to stimulate proliferation.²

Cytokines are often involved in communication between leukocytes. That is the reason why many cytokines have been given the name interleukin (IL). Cytokines act in the range of picomolars through specific cell surface

receptors. Often their activity is synergistic or antagonistic when tested together. There are three principal areas of cytokine activity:¹

- As growth factors for immune cells
- As regulators of the immune response
- As mediators of inflammation

Macrophages are antigen presenting cells (APCs). They process antigens and present them to T-cells. During this process, the macrophages also produce interleukin-1 (IL-1). IL-1 is the most studied cytokine. IL-6 and TNF- α have many functions in common with IL-1.¹

IL-1 is induced by e.g. endotoxin, C5a and TNF/IL-1. It promotes coagulation and cellular accumulation at an inflammatory site and it activates fibroblasts to synthesis collagen. Furthermore, IL-1 stimulates T-cells to produce IL-2. In turn, IL-2 helps T- and B-cells to proliferate and differentiate. IL-6 production is induced by e.g. IL-1 and endotoxin. IL-6 is a T-cell activating factor and it helps activated B-cells to proliferate and secrete immunoglobulines (Ig).^{1,42} TNF- α is e.g. induced by fragments from complement activation and it is proved to have anti-tumour and anti-viral activity. TNF- α also promotes coagulation.³³

IL-1, IL-6 and TNF- α can induce the production of each other and they often produce synergistic effects.¹ Those three cytokines are also the principal mediators of the acute phase response.³³

How polymers affect macrophages

Adherence and cell activation of inflammatory cells on a polymer surface can be taken as an important factor of biocompatibility. However, the degree of activation (e.g. cytokine production) should not be too large. When the stimulus to inflammation is particularly severe or resistant to elimination, a specialised form of inflammatory tissue, granulation tissue, may develop. The consequence of a chronic inflammation is that the tissue response may never be totally resolved and the tissue may always contain inflammatory cells as well as collagen and blood vessels.³³

Cell adhesion depends on the surface characteristics of the polymer. Important factors are wettability, electrical properties, chemical composition and morphology.⁴³ It should also be pointed out that the initial protein adsorption plays an important role. In general, cell adhesion to a solid substrate is divided into three steps:⁴⁴

1. Adsorption of proteins.
2. Specific recognition of these proteins by cell surface receptors.
3. Non-specific interaction of cell surface molecules (oligosaccharides) with adsorbed proteins and substrate.

Wettability

It is difficult to create a general rule concerning wettability and cell adhesion to polymers. Different studies give different answers. Some of the discrepancies found can probably be explained by the fact that different parameters (adhesion, spreading, growth) were investigated and that different cell types or additional adhesive proteins were used. There are two common measurements of the wettability in the literature; contact angle to water and surface energy. A rule of thumb concerning surface energy and cell adhesion is reported. Materials have usually good cell adhesive properties if the surface energy is higher than 40 mN/m.¹ A non-adhesive zone between 20 and 30 mN/m is also reported.⁴⁵ However, in a number of cases, this minimum has not been observed.¹

Concerning contact angle measurements, non-ionic and hydrophilic (or very hydrophobic) surfaces lead to low levels of cell adhesion in general.^{33,41} The cells prefer moderately hydrophobic or ionic surfaces. Studies indicate that incorporation of ionic charge on hydrophilic polymer surfaces increases protein adsorption and monocyte adhesion.⁴¹ Furthermore, Jirousková et al. have showed that monocytes adhere very strongly to positively charged polymers.⁴⁴

Hydrophobic polymers readily adsorb serum proteins that may mediate subsequent cell adhesion or cell activation. Vitronectin and fibronectin are examples of proteins that mediate cell adhesion.³⁰ The adsorbed proteins may also include opsonins (e.g. IgG), which lead to cell activation. On the other hand, hydrophilic materials tend to favour macrophage activation (cytokine production), according to one study. Hydrophobic materials (like polyurethane and silicon) are less likely to initiate an inflammatory response.⁴⁶

Other studies do not report any correlation at all between wettability and cell adhesion and activation.^{32,47}

Chemical modification

The level of macrophage activation has been shown to depend on the occurrence of functional groups (e.g. dimethylamino-, hydroxy- and carboxy-) on the polymer surface.⁴⁴ As an example, Rouxhet et al. have increased the surface concentration of –COOH in poly(hydroxybutyrate-co-hydroxyvalerate), by alkaline hydrolysis (KOH). This treatment results in increased adhesion of macrophages. However, it is not clear if the effect comes from the change in morphology or from the change of chemical surface groups.⁴³

Pre-adsorbed proteins

Studies where different proteins have been preadsorbed to a polymer have been reported. It is shown that the cellular response to the polymer can be modulated by use of different proteins. Pre-adsorption of fibronectin leads to increased cell attachment and spreading. Pre-adsorption of collagen enhances attachment and growth of most anchorage-dependent cells. Albumin preadsorption, on the other hand, prevents cell attachment.³³

Topography

There are few studies made on the morphological effects on macrophage adhesion and activation. Alkaline hydrolysis (KOH) tends to slightly increase the surface area by etching the surface, according to Rouxhet et al. Cell adhesion increased after this treatment as discussed earlier.⁴³

Particles

Macrophages are involved in the biodegradation of foreign materials. After phagocytosis the material may be totally digested or may persist in the form of indigestible residue.³²

Saad et al. have studied the phagocytosis of low molecular weight PHB particles ($M_n=2300$, diameter 1-10 μm). They have shown that macrophages have the ability to phagocytose the particles and that toxic effects and cell activation accompany the process. At high concentrations of PHB particles ($>10\mu\text{g/ml}$), cell damage and cell death occurred. At non-toxic concentration, the number of particles per cell decreased with increased incubation time. This indicates that active biodegradation or exocytosis occurred.⁴⁸

Gangrade and Price have examined particles of PHB and poly(hydroxybutyrate-co-hydroxyvalerate) in SEM. They found that the surface of PHB particles was very rough and that an increase in hydroxyvalerate content gave smoother surface.¹⁰ Studies made at Astra Tech AB show that PHB particles stimulate macrophages *in vitro* to release both $\text{TNF-}\alpha$ and $\text{IL-1}\beta$.⁴⁹

Poly(lactide-co-glycolide) copolymer is easily prepared in a wide range of molecular weights. They undergo hydrolysis forming the non-toxic metabolites, lactic acid and glycolic acids. The degradation pathway is by homogeneous bulk degradation.¹

Zhou et al. have studied the *in vitro* degradation of poly(D,L-lactide-co-glycolide) (90:10) in human serum at 37°C. The surfaces of the microspheres were examined in SEM. No changes were shown up to 60 days, but after 3 months rough and porous surfaces were observed. After 8 months only collapsed micro-spheres were detected. The change in molecular weight was determined by gel permeation chromatography (GPC) and was found to decrease steadily from 70 000 g/mole down to a few thousands g/mole after 8 months.⁵⁰

It has been shown that 50:50 PLG exhibit the fastest biodegradation among the different combinations of lactic and glycolic acid in the polymer.⁹

3 Materials and methods

3.1 *PHB processing*

3.1.1 Film formation by solvent evaporation

A solution of PHB was prepared by dissolving approximately 1,845 g PHB (B333401) in 25 ml of chloroform (Fluka, 25669, EC no. 2006638), which equals to 5 % (w/w) of PHB. This solution was obtained by using a pressure beaker, where PHB was put in a measurement-flask, and chloroform was added to completely soak and cover the polymer. The pressure inside the beaker was adjusted with air to 1 bar. The beaker was then put in a preheated oven at 90°C for 30 minutes, allowed to cool and opened in a fume hood where the volume in the flask was adjusted to 25 ml by adding chloroform.

All materials were washed with ethanol (70%). This was done partly for cleansing, partly to ease the removal of the film from the glass plate.

A few drops of the PHB-solution were put on a smooth glass plate. This solution was immediately evenly distributed on the plate using a film applicator (BYK Gardner, Cat.No. 2040), see figure 13. Four different thicknesses of the smeared solution can be chosen simply by using different faces of the tool. 200 µm was used as an initial thickness. This does however not imply that the ready films will have a thickness in the same range, since the solvent will evaporate.



Figure 13. *Film applicator. The cylindrical part is 60 mm wide.*

The film was allowed to dry (i.e. the chloroform evaporated) for a few minutes, after which it was easily released from the surface and allowed to dry flat on a fluoroethylene copolymer (FEP) foil. The size of the films were approximately 4*6 cm².

The thicknesses of the dried films were measured with a digital micrometer (Testing Machines Inc., model 49-70). An average thickness of 11 μm (st.dev. 2 μm) was obtained.

3.1.2 Film formation by melt pressing

Melt pressed PHB films were manufactured from PHB fibre patches (B333401). A Fontijne hydraulically operated platen press (model TP200) with digital temperature program was used. The temperature and pressure were varied with time. In table 1 the program used is shown.

	Temp (°C)	Load (kN)	Pressure (kPa)	Time (minutes)
Preheating	180	0	0	6
Pressing	180	3	300	5
Cooling	180→50	3	300	45

Table 1. *Temperature and pressure program used for melt pressing.*

Two films of 6*6 cm² were processed each program. The final film size was about 7*7 cm². The thickness was measured with a digital micrometer

(Testing Machines Inc. model 49-70) to 66 μm (st.dev. 4 μm). The total film area in each program was $7*7 \text{ cm}^2 * 2 \text{ films} \approx 100 \text{ cm}^2 = 0.0100 \text{ m}^2$. The pressure can be calculated: Pressure = Load / Area. The set-up of the melt pressing is shown in figure 14.

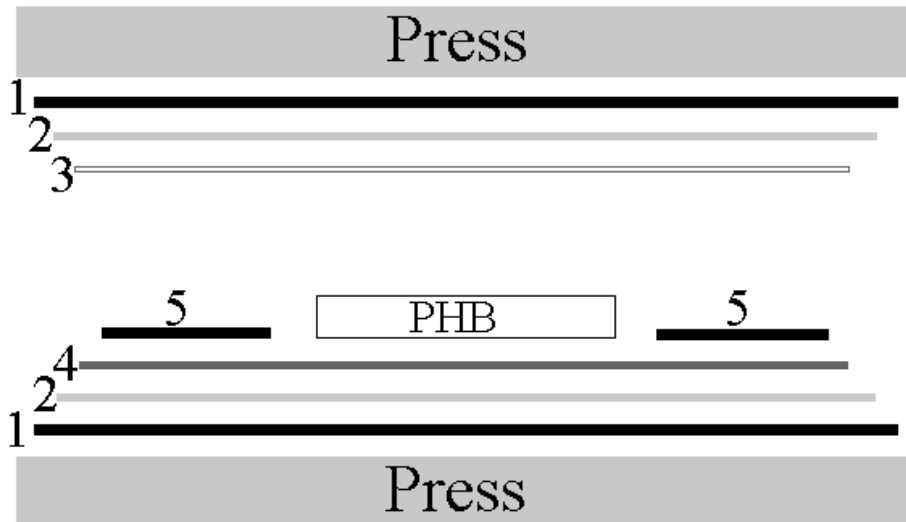


Figure 14. Melt pressing setup, where 1 = Cu-plate, 2 = PTFE, 3 = FEP foil, 4 = Al foil and 5 = Al distances.

Protective Cu-plates were placed closest to the press plates. In order to achieve a smooth surface, a layer of poly(tetra-fluoroethylene) (PTFE) fabrics were then applied. The PHB fibre patches were placed between aluminium foil and a release fluoroethylene copolymer (FEP) foil. Aluminium is relatively inert during melt pressing and was therefore placed closest to the PHB. However, its release properties are not too good. Therefore FEP foil, with better release properties, was applied over the PHB fibre patch. FEP is used instead of PTFE since FEP has lower fluorine content. The risk of fluorine contamination of the PHB is therefore reduced. Distances ($2*18 \text{ cm}^2$) of aluminium were used. The thickness of the distances was about 20 μm . Note that distances may have taken up some of the load, resulting in a lower pressure. All equipment was carefully washed in 70% ethanol before each program. The films were finally packed in plastic bags.

3.1.3 Particle formation

Particles made of PHB and PLG were processed. No drug was incorporated in the particles. PHB (B333401) 3% (w/w) dissolved in chloroform or PLG (RG 506, Boehringer-Ingelheim) 3% (w/w) dissolved in CH_2Cl_2 (Aldrich, 99.6%) worked as oil phase. PVA (poly vinyl alcohol, 13 000-23 000 g/mole, hydrolyse grade 87.88%, Aldrich Chemical Company Inc.) 10% (w/v) dissolved in distilled water served as water phase.

The homogenisation was performed at $6 \cdot 10^3$ rpm for 3 minutes (Polytron PT3100 homogenisator). In each program 3 ml of PHB solution or 5 ml of PLG solution was added to 100 g of PVA solution. Thereafter, the solutions were slowly stirred during the night.

In order to remove surplus of PVA, a washing procedure took place. The solutions were centrifuged at 15 000 rpm for 10 minutes. The pellet, PHB or PLG particles and some PVA, was saved. The supernatant was replaced by 5% (w/w) mannitol (Roquette Frères, France) in water. Mannitol functions as a protective bed around the PHB or PLG particles in the next step, freeze-drying. The mannitol makes it easier to re-suspend the freeze-dried particles. Three centrifugations with mannitol were carried out and the PHB particles were finally freeze-dried over night.

The surface morphology of the microspheres was examined by scanning electron microscope (SEM). The dried microspheres were mounted on metal stubs, coated for 10 minutes under an argon atmosphere with gold and then observed with SEM.

3.2 *Modifications*

3.2.1 Chemical modification

A 2.5 M KOH-solution was made by adding KOH (Tamro Lab AB, 05-400101) to a 50/50 (v/v) mixture of water (MilliQ) and methanol. This solution was cooled to room temperature.

The PHB-films (solvent evaporated as well as melt pressed) were put one by one in a glass-beaker containing approximately 200 ml of the 2.5 M KOH-solution. This content of OH^- ions is in excess compared to the hydrolysable exposed ester-linkages in PHB. The beakers were put in a shaking water bath for 10 minutes at room temperature. The films were collected and one by one put in beakers containing MilliQ-water for the removal of excess KOH. These beakers were put in a shaking water bath for 10 minutes. The water was replaced by fresh MilliQ and the procedure

was repeated once since this was enough for pH to reach 7 or below, tested by dipping a strip of pH-paper into the beaker.

3.2.2 Plasma modification

PHB films fabricated by solvent evaporation and melt pressing were plasma modified (Technics Plasma 440 G with a microwave generator 2.45 GHz) with O₂ (AGA, 3.5 (99.95 %) max 5 ppm H₂O och max 1ppm C_nH_n) and CHF₃ (AGA, 4.5 (99.995 %) max 30 ppm N₂). Two PHB-films (melt pressed films about 7*7 cm² and solvent evaporated films about 4*6 cm²) were modified in each program. Each film was hanging free from a clip in the chamber. The two clips were applied at the ends of a steel wire, which guaranteed that the PHB films would not shelter each other. The pressure was decreased to about 0.15 mbar. The gas (O₂ or CHF₃) was put on, which led to an increase in pressure. Process pressure was 0.5 mbar and the effect was set to 600 W. The plasma treatment started and lasted for 5 seconds. The gas was turned off and the chamber was allowed to ventilate at low pressure and finally at normal pressure. The part of each PHB film that had been sheltered by the clip was removed and the films were put into plastic bags. Before usage, the bags were washed with ethanol (70%) and dried at room temperature.

3.2.3 Sterilization and bulk modification

Five different samples were to be sterilised:

- Solvent evaporated (se) PHB films
- Melt pressed (mp) PHB films
- Fibre patches of PHB
- Particles of PHB (freeze-dried powder)
- Particles of PLG (freeze-dried powder)

Prior to radiation, the molecular weights (\overline{M}_w s) for these samples had been determined by viscosimetry, see section 4.1.1. Approximate values are given in table 2 (M_{w0}).

The \overline{M}_w for particles of PHB was estimated to be the same as for solvent evaporated PHB. That is, no viscosimetry was performed on these particles. The reason for this is the mannitol added to ease the solvation of

the particles after they had been freeze-dried. Mannitol might affect the viscosity of the solution.

The \overline{M}_w for particles of PLG was estimated to be the same as the material from which they had been processed.

An equation previously prepared by Astra Tech was used for calculations of radiation doses.⁵¹

The equation is valid for PHB. An approximation was thus made when it was used for PLG as well. The dose S is given in two sets, with half the total amount on each side of the product to be irradiated. That is, S/2 on the upper side and S/2 on the lower side. The aberration in dose is maximally 5% for each set. The desired \overline{M}_w was 65 000 g/mole. This value was chosen for possible comparisons with future studies and in order to obtain a low molecular weight without losing mechanical strength in the material for future handlings. The calculated values of S are given in table 2.

Type	\overline{M}_{w0} [g/mole]	S [kGy]
se + PHB-part.	460000	88.07
mp	183000	66.13
Fibre patch	470000	88.38
PLG-part.	100000	35.90

Table 2. Results from calculations of radiation doses. \overline{M}_{w0} =molecular weight before radiation.

All total doses presented in table 2 supersede 25 kGy, which is the earlier mentioned demand to ensure sterilisation. Clean room environment in the production of PHB fibre patches had also been applied in order to minimise the number of viable microorganisms in the product. Samples were cut in suitable pieces before packaging in PE/PET envelopes (uncoated Tyvek ID73B), which immediately were melt-sealed. All samples were sent to LR plast, Denmark, for radiation.

3.3 PHB characterisation

3.3.1 Viscosimetry

One way to measure the viscosity of a polymer solution is by using a *viscosimeter*. The one of use in these laborative series was a capillary-

viscosimeter (Ubbelohde-viscosimeter) manufactured from Schott-Geräte (Kebo Lab287.900-6). See section 2.5.1, figure 6.

A solution of PHB was prepared by dissolving approximately 125 mg PHB in 25 ml of chloroform (approximately 0.3% w/w PHB). The amount of polymer and choice of solute are based on the calibration curves previously prepared for PHB at Astra Tech AB. This solution was obtained by using a pressure beaker, where PHB was put in a measurement-flask, and chloroform was added to completely soak and cover the polymer. The pressure inside the beaker was adjusted to 1 bar with air. The beaker was then put in a preheated oven at 90°C for 45 minutes, allowed to cool and opened in a fume hood where the volume in the flask was adjusted to 25 ml by adding chloroform.

The above description applies for fibre patches of PHB. Different kinds of processed PHB require other settings in temperature, time and pressure, see table 3.

Type of PHB	Temperature [°C]	Time [hours]	Pressure [bars]
se films	90	0.5	1
mp films	110	2	2

Table 3. Settings when dissolving PHB in chloroform.

Irradiated, evaporated films dissolved within a few minutes without the need for a pressure beaker. To obtain similar conditions though, the films were exerted for the same treatment as the ones before irradiation.

One should not excessively raise any of the variable parameters (T, t, P), since this might degrade the polymer more than necessary. Hence, screenings were performed to find out the settings presented in table 3.

The solution was filtered (Spectrum Laboratories Inc., DG4P-320-100, 0.45 µm) and poured into a viscosimeter, which was put in a water bath at 25.0°C for 10 minutes. Liquid was sucked into the capillarie and the time for the solution to flow a marked distance was measured. This was repeated three times, after which an average time was calculated. Each sample was prepared in duplicates (two flasks) and the amount from each flask was enough for two separate measurements performed on different viscosimeters. Hence, for each type of modified PHB, four values were obtained, from which an average molecular weight was calculated. For

validation of the results, a tolerance of maximally 5% aberration among the four values of M_w for each type was accepted.

The equations used are:

$$\eta = K * t \quad \text{(Equation 13)}$$

$$\overline{M}_w = 706052 * \eta - 282421 \quad \text{(Equation 14)}$$

, where η is the viscosity [mm^2/s], K is the calibration constant of the viscosimeter [mm^2], t is the average time [s], and \overline{M}_w is the weight average molecular weight. The values in the formula for \overline{M}_w are calculated from a standard curve for PHB previously prepared at Astra Tech AB.¹⁸

Samples were analysed with viscosimetry before and after radiation (no cell incubation) in order to evaluate the effect from the radiation. From each film-type (se and mp), a reference sample and a sample prior subject to chemical modification (KOH) were analysed. The choice of model films is based on the fact that chemical modification might degrade PHB, and hence lower its \overline{M}_w compared to reference pieces. In addition, fibre patches of PHB were analysed.

3.3.2 Contact angle

The water contact angle was measured (DAT1100, Fibro system AB, Sweden). Ten measurements were performed on each type of PHB film. The volume of each drop was 4 μl and the contact angle was measured 1 second after the drop was applied to the surface. Furthermore, the methylene iodide contact angle (VCA 2500 Video contact angle system, Advanced surface technologies Inc.) was measured. On each type of PHB film, 20 measurements were performed. The volume of each drop was about 0.6 μl and the contact angle was measured 1 second after the drop was applied to the surface. Mean values and standard deviations were calculated. The surface energies were calculated using the harmonic mean method and the variances were calculated using Gauss' approximation formula, see appendix 1.

3.3.3 Fourier transform infrared spectroscopy (FTIR)

All samples were analysed using a Perkin Elmer System 2000 FT-IR, supplied with a SplitPea™ (Harrick scientific corp.). Fourier transformations and spectrum visualisation were processed by software from Perkin Elmer (Spectrum v.2.0).

The samples were analysed by applying a pressure of 1 kg on the films. Spectrums were recorded between 4000 – 450 cm⁻¹ and data were presented from 16 scans on each sample. A penetration depth of a few micrometers was obtained.

Irradiated films of all modifications and fibre patches were studied before and after cell exposure. The films studied after cell exposure were prior to IR-analysis subject to the washing procedure as described in section 3.4.1.

3.3.4 Electron spectroscopy for chemical analysis (ESCA)

Electron spectroscopy for chemical analysis (ESCA) was run at a pressure of 3*10⁻⁸ torr, and at an angle of detection of 20 degrees. The analysis area was circular with 0.8 mm diameter. An approximate penetration depth of 20 Å was obtained.

A first study was performed on all samples after surface modifications in order to see if the modifications had been successful.

A second study was performed on surfaces after cell incubations. These surfaces were chosen on basis of performed adhesion studies with fibroblasts and cytokine studies with macrophages. Melt pressed films, CHF₃-modified, and solvent evaporated films, KOH-modified, were used. Essentially, three films of each type (mp CHF₃ and se KOH) were studied; one film that had only been subject to irradiation, one film washed with SDS after cell incubation and one film washed with no prior cell incubation. The last mentioned film was studied to see possible effects on the surfaces from the detergent sodium dodecyl sulphate (SDS) used in the washing procedure. See sections 3.4.1 and 3.4.2 for details.

3.3.5 Gel permeation chromatography (GPC)

Gel permeation chromatography (GPC) was performed on system from Waters (Waters 712 WISP injector, Waters 510 HPLC pump and Waters 410 differential refractometer). The flow was set to 1.0 ml/min and was continuously measured with a flowmeter (Phase separations Ltd.). The temperature of the detector and the columns were set to 30°C. Chloroform (Fluka, 25669, EC no. 2006638) was used as mobile phase. In order to

minimise the risk of air in the system, the chloroform was ultra-sonicated prior use. Furthermore, nitrogen (ADR-class 2, 1A, Air liquid) was bubbled through the solvent continuously.

Three columns, coupled in series and packed with poly(styrene-co-divinylbenzene) particles, were used:

1. Shodex GPC K-805, exclusion limit 4 000 000 g/mole
2. Shodex GPC K-803, exclusion limit 70 000 g/mole
3. Shodex GPC K-805, exclusion limit 1 500 g/mole

A calibration curve of polystyrene (PS) standards (Polymer laboratories) was made. Ten narrow (nearly monodisperse) standards dissolved in chloroform, with molecular weights ranging from 400 g/mole to 4 000 000 g/mole, were prepared. The injection volume was 150 μ l and the concentration was 1 mg/ml. In order to prevent contaminations from reaching the columns, the solutions were filtered through a 25 μ m disposable syringe filter (Advantec MFS, Inc.) prior injection. A standard curve for PHB was calculated using the following Mark-Houwink constants:

$$\text{PS (30}^\circ\text{C):}^{23} \quad \alpha = 0.79 \quad K = 4.9 \cdot 10^3 \text{ ml/g}$$

$$\text{PHB (30}^\circ\text{C):}^4 \quad \alpha = 0.78 \quad K = 1.18 \cdot 10^4 \text{ ml/g}$$

The standard curves for PS and PHB can be seen in appendix 2. Three categories of PHB films and fibre patches were analysed with GPC:

1. PHB films and fibre patches not exposed to cells, but washed in the same 1% SDS program as the cell exposed surfaces, see section 3.4.1.
2. PHB films and fibre patches exposed to fibroblasts for 3 days, see section 3.4.1.
3. PHB films and fibre patches exposed to macrophages for 5 days, see section 3.4.2.

PHB films were dissolved in chloroform according to the method described in section 3.3.1. The concentration was 2 mg/ml (10 mg PHB was solved in 5 ml chloroform) and the injection volume was 200 μ l. Prior injection the solutions were filtered through a 25 μ m disposable syringe filter (Advantec MFS, Inc.). One sample was prepared from each type of PHB film and all

samples were injected two times. \overline{M}_w , \overline{M}_n and polydispersity index were calculated using the PHB standard curve and software tools (Millenium®) belonging to the GPC (Waters). The ratio between exact amount PHB dissolved in chloroform and peak area was also determined. This ratio should be constant if the PHB was properly dissolved in chloroform and not trapped in the 25 μm filter.

3.3.6 Scanning electron microscopy (SEM)

PHB solvent evaporated and melt pressed reference films were studied, before irradiation and cell exposure, in SEM. In addition, particles were studied before and after macrophage incubation.

The dry samples were mounted on metal stubs and inserted into a vacuum chamber where they were flowed with argon gas at a pressure of 1 kPa. This is done to remove oxygen from the atmosphere therein and to clean the sample from adhered gas. The samples were then sputter coated with gold for 10 minutes at a current of 10mA. After this, the coated samples were observed in SEM, with a working distance of 15 mm and at an acceleration voltage of 10 kV. Vacuum was sustained during observations.

3.3.7 Atomic force microscopy (AFM)

Surface morphology was investigated by atomic force microscopy (Digital Instruments, California) in tapping mode. One PHB sample, mp REF exposed to macrophages, see section 3.4.2, was split in two parts. The first part was studied on the side where macrophages had been grown. The other part was studied on the opposite side, which had been facing the tissue culture plate during cell incubation. Pictures were taken at different scanning areas and at different spots on the surfaces.

3.3.8 Coulter counter

The size distribution of the PHB and PLG particles was determined by laser diffraction (Beckman Coulter LS130 with an Argon laser). The diffraction pattern from the laser beam when it hit the particles in water was read by an array of 128 detectors along one axis. The size distribution was mathematically resolved using a model, which assumed spherical and white particles. Furthermore, it took use of two in-parameters; polymer refractive index (1.0) and solution refractive index (1.332).

3.4 Cell experiments

3.4.1 General materials used in cell experiments

- Culture flasks, different sizes; bottom areas of 25, 75 and 150 cm² respectively, TCPS, NUNCLON™, Denmark
- Dulbecco's Modified Eagles Medium (DMEM) with GLUTAMAX, with 4500 mg/l glucose, with pyridoxine, Gibco BRL
- Ethanol (99.5%), Kemetyl, Haninge, Sweden
- Eosin Y (CI no 45380)
- Fetal calf serum (FCS) or fetal bovine serum (FBS) , GIBCO BRL
- Hank's Balanced Salt Solution (HBSS) without phenol red, Gibco BRL
- Hematoxylin, Mayer Hamalun solution, Merck
- Hepes buffer 1M, Gibco BRL
- L-glutamine, GIBCO BRL
- Lipopolysaccharide (LPS), Sigma®
- MRC-5, human lung fibroblasts, ATCC no. CCL-171
- Neutral Red (NR) solution, diluted 80x with DMEM immediately before use
- Paraformaldehyde puriss, MERCK
- Phosphate Buffer Saline (PBS) without calcium and magnesium, without sodium bicarbonate, Gibco BRL
- Penicillin-Streptomycin, 10000IU/ml-10000UG/ml, Life Technologies™, GIBCO BRL
- Phorbol 12-myristate 13-acetate (PMA), Sigma®
- RPMI 1640 medium, Life Technologies™, GIBCO BRL
- Sodium dodecylsulfate (SDS), Sigma®, L-3771
- THP-1, human monocytes, ATCC, American Type Culture Collection, no TIB-202
- Tissue culture plate (6-well, 24-well, 96-well), TCPS, Costar, Corning Inc.
- Trypsin/EDTA, 0.05% Trypsin and 0.02% EDTA from HyClone (Life Technologies™, 35400-027), diluted 1:10 in PBS and kept in a refrigerator before use

3.4.2 Fibroblasts and cell adhesion

All primary work with the cells was done in a sterile environment.

Fibroblast (human lung fibroblasts, MRC-5) cultures were maintained in a 37°C water-jacketed incubator equilibrated with 5% CO₂ and kept at approximately 99% relative humidity. The cells were grown in Dulbecco's modified Eagle's medium (DMEM) supplemented with 10% (v/v) FCS and 1% (v/v) PEST in culture flasks with different sizes. The medium was changed every second day except for weekends. The cells were subcultured (see section Subculturing) with a ratio of 1:5 on 7-day intervals using trypsin-EDTA.

When the cells were subject to experiments, they were routinely trypsinised and the cell-suspension was kept in a Falcon-vial until use. The pieces of film used were squares with an area of approximately 1 cm². The TCPS wells used for culturing (24-well-plates) had a bottom area of 2 cm².

Subculturing

Subculturing is done to multiply the cell-number by avoiding confluence. It was usually performed once a week, and the same procedure was applied when the cells were harvested for experiments.

The culture medium was aspirated from the flask. The flask was rinsed once with PBS to remove protease-inhibitors, i.e. to enhance the effect of trypsin. PBS was withdrawn and trypsin/EDTA solution was added, the flask was shaken and allowed to incubate for about 15 minutes. The flask was visually examined to ensure that most of the cells were released from the surface and DMEM was thereafter added to the flask. The cell-suspension was repeatedly aspirated and flushed against the wall of the flask to break cell-clusters and reach "single-cell suspension". The initial solution was then diluted 5x with DMEM and set in new culture flasks.

Adhesion studies

The most convenient way to calculate cell concentrations, under the circumstances in these studies, is by handling the initial concentration as a function of the surface area of which they adhere to, i.e. cells/cm². This will make it easier to compensate when growing cells on larger areas. This is important since the viability tests used (NR, MTS) detect viable cells on a surface. Since the PHB films commonly were placed in a TCPS well with a bottom area twice as large (2 cm²) as the piece of film (1 cm²), half of the

cells would theoretically adhere to the well bottom. When moving the film in a subsequent step prior to detection of viable cells, half the number of cells (theoretically) would remain undetected in the well. When growing cells on TCPS as positive control, this larger surface area had to be adjusted for, since the viability tests were performed in the well into which the cell suspension initially had been placed. In study 1, 2 and 4 this adjustment was done by doubling the amount of extraction buffer to the TCPS-wells. In study 3 this was done by adding only half the amount of cell suspension initially to the TCPS-wells. Note that cell adhesion to the inner wall of the wells is not accounted for, neither is adhesion to the side of the film facing the well bottom accounted for.

The cell concentrations used in study 0 are based on previous studies using between $4 \cdot 10^4$ and 10^5 cells/cm² for cell adhesion studies.^{30,31,34} This way a suitable interval of concentrations was obtained. The time-intervals chosen should be enough for fibroblast adherence to different degrees.

Study 0

In order to find an optimal initial cell concentration for subsequent studies, a study was performed with different cell concentrations exposed to TCPS. These cells were also exposed for different times to determine when it was suitable to study adhesion initially.

The cells were trypsinised according to the standard protocol described earlier. Cell concentration was adjusted to $3,2 \cdot 10^5$ cells/ml and consequent dilutions were performed by diluting the immediate previous solution with higher concentration in twice the amount of DMEM. This way, 5 suspensions in three-fold diluted steps was obtained. The test was performed in a 96-well TCPS-plate with a well bottom-area of 0.4 cm². The cells were exposed to the wells for five different time-intervals and each measurement (time and concentration) was done in triplicate. This equals to a total of 75 (5 concentrations * 5 times * triplicates) used wells.

The cell-concentrations used were: 158667, 52889, 17630, 5877, 1959 [cells/cm²].

The time-intervals used were: 30, 60, 120, 180, 240 [minutes].

200 µl of cell-suspension was added to each well. When the subject time had elapsed the suspension was aspirated and the wells were washed once with PBS, which then were replaced with fresh DMEM. Cells were then subject to the Neutral Red (NR)-procedure described in section 2.6.2, with amounts changed to 200 µl of NR and extraction-buffer.

Study 1 and study 2, NR

These studies were performed to evaluate cell adhesion to PHB.

The cells were trypsinised according to the standard protocol and the concentration was adjusted to $5 \cdot 10^4$ cells/ml. Films of PHB were placed singularly in wells on 24-well plates. For each time to be studied every type of film was represented in duplicates. Empty wells (TCPS) were used in quadruplicate as positive reference for each time.

1 ml of cell-suspension was added to each film and incubated for different time-intervals. The chosen intervals were 1h, 24h, and 72h. The cell adhesion was tested after the set times with NR described in section 2.6.2.

Study 3, MTS

This study was performed to study cell adhesion to PHB using MTS test, in order to try another viability test. This test should not give rise to any “background-absorbancy” from the films, as the NR-test might do.

The cells were trypsinised according to the standard protocol and the concentration was adjusted to $5 \cdot 10^4$ cells/ml. Films of PHB were placed singularly in wells on 24-well plates. For each time to be studied every type of film was represented in triplicate, except for solvent evaporated KOH due to lack of pieces. This type was instead used in duplicate. Empty wells (TCPS) were used in quadruplicate as positive reference for each time. To compensate for the twice as large area exposed to the cells in the “blank TCPS” compared to the films, only half the amount (0.5 ml) of cell-suspension was added to TCPS. 1 ml of cell-suspension was added to each film and allowed to incubate for different time-intervals. The chosen intervals were 1h, 24h and 72h. The cell adhesion was tested after the set times with MTS as described in section 2.6.2.

Study 4, double cell concentration

This study was performed to evaluate the possible dependence of cell concentration on adhesion to PHB and TCPS. Only one time was studied, 1h, to see initial adhesion. Cell concentration was doubled compared to study 1, 2 and 3.

The cells were trypsinised according to the standard protocol and the concentration was adjusted to $1 \cdot 10^5$ cells/ml. Films of PHB were placed

singularly in wells on 24-well plates. For each time to be studied every type of film was represented in duplicate. 1 ml of cell-suspension was added to each film and allowed to incubate for 1 hour. The cell adhesion was tested with NR as described in section 2.6.2.

Study 5, NR uptake into films of PHB

This study was performed to see a possible NR adsorption to or NR absorption into the PHB films. This is important to know, since a possible uptake causes inadequate values of cell adhesion when comparing the different modifications. No cells were used in this study.

Films of PHB were placed singularly in wells on 24-well plates. For each time to be studied every type of film was represented in duplicate. 1 ml of DMEM was added to each film and allowed to incubate for different time-intervals. The chosen intervals were 1h and 24h. The films were then subject to the NR-procedure described in section 2.6.2.

Preparation of pieces for PHB characterisation studies

The cells were trypsinised according to the standard protocol and the concentration was adjusted to $1 \cdot 10^5$ cells/ml. Films of PHB were placed singularly in wells on 24-well plates. 1 ml of cell suspension was added to each film.

In order to achieve enough solvent evaporated (se) PHB films for GPC studies, larger films (about $3 \cdot 3 \text{ cm}^2$) were incubated in 6-well tissue culture plates. Adding 5 ml of cell suspension compensated for the 5-fold increase in well bottom area. All plates were incubated in 37°C (humidified atmosphere at 5% CO_2) for 72 hours.

In order to remove biological materials (e.g. cells and proteins) from the surfaces after the cell incubation, the films were washed in different solutions:

1. Water, 3 minutes
2. 1% (w/v) sodium dodecylsulfate (SDS), 2 minutes
3. Water, 3 minutes

4. 99.5% Ethanol, 1 minute

Finally the films were air-dried.

Viability tests

Neutral Red (NR)

The method described below applies for a normal piece of film placed in a well with a bottom area of 2 cm² (24-well plate).

The cell suspension was carefully aspirated from the well in order not to demolish the film or the possible cells upon it. Each well was washed once with PBS to remove nonadherent cells and 500 µl of NR-solution were pipetted into each well. The plate was incubated for 3 hours.

Meanwhile, an extraction-buffer was prepared. This was done by mixing equal amounts of ethanol (99,5%) and distilled water. Acetic acid was added to an amount of 1%. This buffer will lyse the cells and release the intracellular Neutral Red.

The NR-solution was removed from the wells, which were washed twice with PBS to remove excess staining dye. Each film was moved to a new well by using a forceps. 500 µl of the extraction buffer was pipetted onto every piece of film. The amount of buffer chosen should be the same for each square portion of sample exposed to cells, since Neutral Red will dissolve in the buffer and give rise to an absorbancy proportional to its concentration therein. To compensate for the twice as large area exposed to the cells in the "blank TCPS" compared to the films, twice the amount of buffer was added to these wells. The plate was put on a micro-plate shaker at 300 rpm for 20 minutes.

From each well, 2*200 µl were pipetted into separate wells on a 96-well plate. This amount should also be carefully regulated in order to take equal amounts for each well. The absorbancies were read at 540 nm on a spectrophotometer.

MTS

Medium was aspirated from each well, which were washed once with HBSS to remove nonadherent cells. The films were moved to a new well into which 500 µl of HBSS and 100 µl of MTS/PMS were added. The plates

were briefly shaken on a micro-plate shaker to evenly distribute MTS/PMS in HBSS and thereafter incubated for 2 hours at 37°C, 5% CO₂.

The plates were once again briefly shaken for evenly distribution of the colour and 2*200 µl were pipetted from each well into separate wells on a 96-well plate. The absorbancies were read at 490 nm using an ELISA plate reader.

Light microscopy; fixation and visualisation

Our aim with the fixation was to preserve cells on the surfaces for later studies. Since we were interested in the morphology of the cells a proper fixation was necessary in order to (i) prevent cell lysis occurring after organism death and (ii) avoid possible changes in structures due to later added staining dyes. Depending on how the fixated cells were to be studied, two different fixation methods were employed.

The specimens were prepared by removal of the culture medium, washed once with PBS and immersed in formaldehyde buffer (formaline) 4%. Incubation time in this buffer varied from 3 hours up to days.

The fixed PHB films were stained with hematoxylin and eosin. 10 g eosin Y was solved in 200 ml water. 800 ml ethanol was added. 150 ml of this solution was mixed with 450 ml 80% ethanol and 3 drops of concentrated acetic acid.

The films were dipped into solutions according to a standard staining protocol:

- Hematoxylin diluted 1:6 in water, 30 seconds
- Washing in water (from tap)
- Water (from tap) 4 min
- Eosin solution diluted 1:2 in distilled water, 30s
- Washing in distilled water
- Storage in distilled water

The films were mounted on glass with glycerine between film and coverslip. The films were studied in light microscope (ZEISS).

3.4.3 Macrophages and cell activation

Human monocytes, THP-1 were cultured in tissue culture flasks made of polystyrene in an incubator with humidified atmosphere at 5% CO₂. The cells were maintained in RPMI 1640 medium supplemented with 10% (v/v) fetal bovine serum, 1% (v/v) Penicillin-Streptomycin (10 000 IU/ml – 10 000 UG/ml) and L-glutamine to a final concentration of 2 mM. The cells were routinely subcultured in new flasks every week by splitting them 1:5. Furthermore, fresh medium was added two times per week.

THP-1 cells were differentiated into adherent macrophage-like cells by adding 100 ng phorbol 12-myristate 13-acetate (PMA) per ml cell suspension into the culture flasks. The suspension was incubated during 48 hours (37°C, humidified atmosphere at 5% CO₂). The treatment led to an adherent cell layer in the cultivation flask. The cells were removed by a standard trypsin/EDTA protocol: The medium was removed and the cells were washed with PBS (without Ca²⁺ and Mg²⁺). 4 ml of Trypsin/EDTA were added and the culture flask was incubated (37°C, humidified atmosphere at 5% CO₂) during 15 minutes. The resulting cell suspension was diluted about 10 times in culture medium.

Cytokine production

For the determination of cytokine production, PHB films (1*1 cm²) were placed in the bottom of each well of a 24-well tissue culture plate. Three PHB samples of each type and four samples of negative and positive controls were run. Single-cell suspension was added to the polymers at a density of 7.5 * 10⁵ cells per well in 1 ml culture medium. Single-cell suspension in an empty well served as negative control and single-cell suspension supplemented with 1 µg/ml lipopolysaccharide was used as positive control. The plate was incubated in 37°C (humidified atmosphere at 5% CO₂) and after 6, 24, 46 and 54 hours 100 µl of the suspension from each well were collected and placed in Eppendorf tubes. The tubes were immediately put in the freezer.

TNF-α, IL-1β and IL-6 levels in the supernatant covering the attached cells were determined using a commercial ELISA-kit (MEDGENIX COMBO TNF-α/IL-1β/IL-6 kit, BioSource Europe S.A., Belgium). The kit is performed on a 96-well microtiter plate and can be divided into four major steps:

1. TNF-α, IL-1β and IL-6 in the sample react with monoclonal antibodies (anti TNF-α, anti IL-1β and anti IL-6) coated on the microtiter well.

2. A mixture of monoclonal antibody (Mab) TNF- α labelled with horseradish peroxidase (HRP) and Mab IL-1 β labelled with alkaline phosphatase (AP) is added. After an incubation period, the microtiter plate is washed and the first sandwich, coated Mab TNF- α / TNF- α / Mab TNF- α HRP is revealed by adding chromogenic solution (tetramethylbenzidine, TMB). The TNF- α levels are determined colourimetrically by reading the microtiter plate at 650 nm.
3. The microtiter plate is washed and another chromogen (p-Nitrophenyl-phosphate, pNPP) for the second sandwich, coated Mab IL-1 β / IL-1 β / Mab IL-1 β AP, is added. The IL-1 β levels are determined colourimetrically by reading the microtiter plate at 405 nm.
4. The microtiter plate is washed and anti IL-6 HRP is added allowing the formation of the third sandwich, coated Mab IL-6/ IL-6/ Mab IL-6 HRP. Chromogenic solution (TMB) is added and the IL-6 levels are determined colourimetrically by reading the microtiter plate at 450 nm.

On each 96-well microtiter plate 15 wells were reserved for triplicates of a five-point standard curve. From this curve the concentrations of the unknown samples were determined. In the experiments performed, the samples were diluted (1:48 for positive control and 1:10 for the others) before analysis. The dilution was done in order to achieve cytokine responses in the range of the standard curve. TNF- α levels were read on Spectra MAX plus (Molecular Devices, AstraZeneca no. 210896), while IL-1 β and IL-6 levels were read on Thermo max microplate reader (Molecular Devices, AstraZeneca no 12726).

Preparation of pieces for PHB characterisation studies

PHB films (1*1 cm²) for FTIR, ESCA, GPC and AFM studies were incubated with differentiated THP-1 cells. The films were placed in the bottom of each well of a 24-well tissue culture plate. Single-cell suspension were added to the polymer films at a density of $7.5 * 10^5$ cells per well in 1 ml culture medium. In order to achieve enough solvent evaporated (se) PHB films for GPC studies, larger films (about 3*3 cm²) were incubated in 6-well tissue culture plates. Adding 5 ml of cell suspension compensated for the 5-fold increase in well bottom area. The plates were incubated in 37° C (humidified atmosphere at 5% CO₂) for 5 days.

In order to remove biological materials from the surfaces, the films were washed in different solutions:

1. Water, 3 minutes
2. 1% (w/v) sodium dodecylsulfate (SDS), 2 minutes
3. Water, 3 minutes
4. 99.5% Ethanol, 1 minute

Finally the films were air-dried.

Light microscopy; fixation and visualisation

Following removal of supernatants, adherent cells on PHB surfaces were rinsed in PBS, fixed in formaldehyde and stained with hematoxylin and eosin. The films were mounted on glass with glycerine between film and coverslip. Eventually, the films were studied in light microscope (ZEISS). The fixation and staining are described in detail in section 3.4.1.

Particles

PHB and PLG particles were incubated with differentiated THP-1 cells. In order to study and compare cellular responses to particles in a standardised manner it is suitable to use the surface area ratio (SAR) method.⁵² The total surface area of the cells divided by the total surface area of the particles was decided to be equal to one in this study. A differentiated THP-1 cell was assumed to be spherical and have a diameter of 30 μm . The particle diameter was determined with a Coulter counter, see section 3.3.8 and 4.1.8. Calculations gave that each differentiated THP-1 cell should be exposed to $1.5 \cdot 10^2$ PHB particles or $3.0 \cdot 10^2$ PLG particles.

In order to remove mannitol from the particles the PHB particles were dissolved in 50 ml sterile water in a 50 ml Falcon tube. The solution was centrifuged (3000 rpm, 5 minutes) and the pellet was resuspended in 50 ml sterile water. Six washing steps were performed. The particle concentration was determined by manual counting in a Bürchner chamber.

16 ml of single-cell suspension ($1.25 \cdot 10^6$ cells/ml) was added to 4 ml of PHB particles ($0.7 \cdot 10^9$ particles/ml) solved in cell culture medium. The result was 20 ml cell-particle suspension ($1.0 \cdot 10^6$ cells/ml, $140 \cdot 10^6$ particles/ml). Furthermore, 16 ml of single-cell suspension ($1.25 \cdot 10^6$ cells/ml) was added to 4 ml of PLG particles ($1.45 \cdot 10^9$ particles/ml) solved in cell culture medium. The result was 20 ml cell-particle suspension ($1.0 \cdot 10^6$ cells/ml, $290 \cdot 10^6$ particles/ml).

The suspensions were incubated in polystyrene flasks (75 cm²) for 5 days. Post incubation the suspension in each flask was removed. The adherent cells in the bottom of the flask were treated with 1% sodium dodecylsulfate (SDS, Sigma®, L-3771) and placed in a Falcon tube. The solutions were centrifuged (3000 rpm, 5 minutes) and the pellet resuspended in water. The procedure was repeated three times. Finally each pellet was resuspended in 2 ml water and removed to a Eppendorf tube (2.5 ml). The samples were dried under vacuum for 6 hours (Integrated SpeedVac® System ISS110, Savant, AstraZeneca no 202095). The surface morphology of the particles was examined in SEM.

In order to study the molecular weights of the particles with GPC, the particles were meant to be dissolved in chloroform.

3.5 Statistics

In order to compare experimental values of two data-sets, Student's T-test has been used in this study.⁵³ If the variances of the two data-sets are considered equal, the equal t-test should be used. Otherwise the unequal t-test should be performed. As a rule of thumb; if the ratio of the variances is larger than 2, the variances should be considered unequal. The formula to calculate the equal variance t statistic is shown in equation 15.

$$t = \frac{\bar{x} - \bar{y}}{\sqrt{s^2 \left(\frac{1}{N_1} + \frac{1}{N_2} \right)}} \quad \text{(Equation 15)}$$

where N_i = number of observations in the i :th data-set, \bar{x} = mean of first data-set, \bar{y} = mean of first data-set, s^2 is the pooled variance refereing to equation 16.

$$s^2 = \frac{s_1^2 * (N_1 - 1) + s_2^2 * (N_2 - 1)}{N_1 + N_2 - 2} \quad \text{(Equation 16)}$$

where s_i = variance of the i :th data-set

The formula to calculate the unequal variance t statistic is shown in equation 17.

$$t = \frac{\bar{x} - \bar{y}}{\sqrt{\frac{s_1^2}{N_1} + \frac{s_2^2}{N_2}}} \quad \text{(Equation 17)}$$

A two-side significant difference on e.g. 95% level ($\alpha=0.05$, $p<0.05$) is accomplished if:

$$|t| > t_{\alpha/2}(N_1+N_2-2)$$

where $t_{\alpha/2}(N_1+N_2-2)$ can be found in a T-table.

4 Results

4.1 PHB characterisation

4.1.1 Viscosimetry

The results from the viscosimetry measurements performed on PHB before and after radiation are presented in table 4. All data is presented in appendix 3.

	Before radiation		After radiation	
	Mw [g/mole]	St. dev.	Mw [g/mole]	St. dev.
Fiber patch	471474	3317	59570	621
se REF	457123	6059	72808	2301
se KOH	464282	4003	72421	3328
mp REF	179990	3307	75391	3849
mp KOH	186867	1689	77941	3024

Table 4. Molecular weights of PHB before and after radiation, obtained by viscosimetry. $N=4$.

Solvent evaporated films as well as melt pressed films originate from fibre patches (\overline{M}_w 471474 g/mole) prior to processing. Solvent evaporation shows no indication to lower the weight average molecular weight (\overline{M}_w). Melt pressing lowers the \overline{M}_w significantly. Chemical modification does not reduce \overline{M}_w to a detectable degree. Rather do these chemically modified films show slightly higher \overline{M}_w than respective reference films, see table 4 and figure 15.

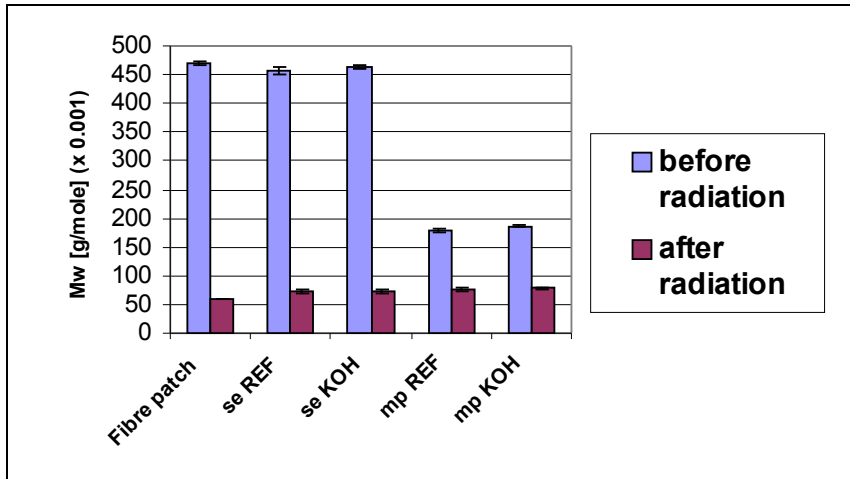


Figure 15. \overline{M}_w before and after radiation.

All types of PHB have a significantly lower \overline{M}_w after radiation. The desired value for all types were 65 000 g/mole as described in section 3.2.3.

Neither the patch nor the films have an \overline{M}_w really close to this desired value. The patch lies approximately 6 000 g/mole below this value, whereas the films lie approximately 7 000 – 13 000 g/mole above this value.

4.1.2 Contact angle

The result from the contact angle measurements is presented in table 6 and graphs can be seen in figure 16 and figure 17.

Sample	Contact angle [degrees]			
	water, n=10		methyleneiodide, n=20	
	mean	st.dev	mean	st.dev
se ref	63.91	1.10	39.40	3.60
se KOH	40.68	3.56	42.35	3.20
se O2	52.29	1.76	44.20	4.10
se CHF3	83.26	6.74	64.20	5.50
mp ref	59.34	1.52	36.90	2.10
mp KOH	44.86	2.62	33.75	3.10
mp O2	55.99	0.51	48.40	4.50
mp CHF3	87.82	1.39	87.75	4.70

Table 5. Contact angle data of different PHB films.

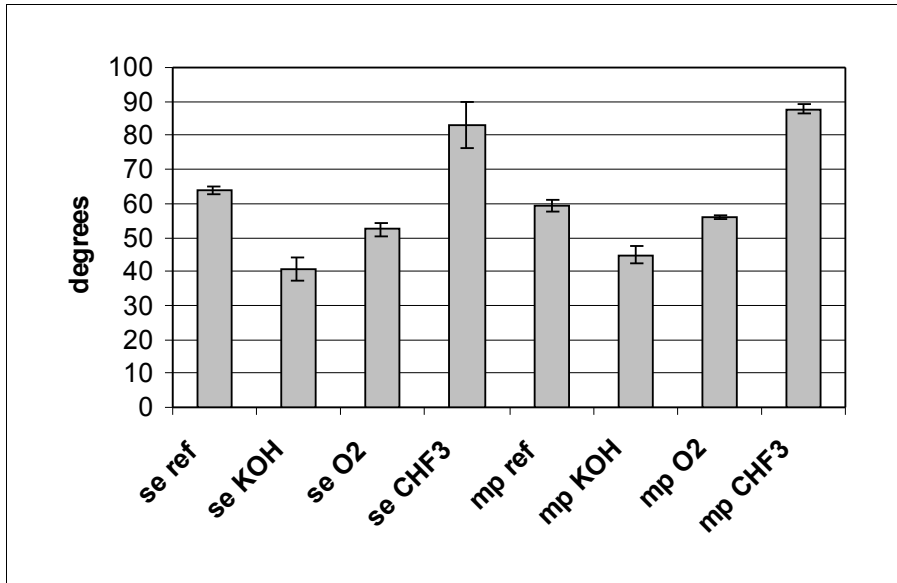


Figure 16. Water contact angles of different PHB films.

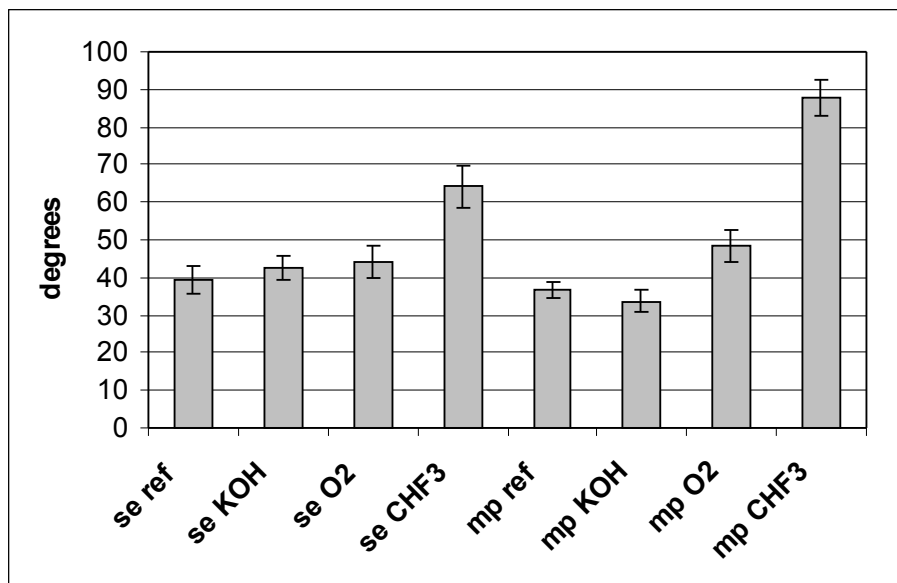


Figure 17. Methylene iodide contact angles of different PHB films.

Surfaces plasma modified by CHF₃ exhibit the highest contact angle. They are thus most hydrophobic. Surfaces chemically modified by KOH exhibit the lowest contact angle. They are thus most hydrophilic.

The water contact angle of the 8 different PHB films, were compared to each other using Student's T-test on 95% confidence level ($p < 0.05$). Since 28 (= 7+6+5+4+3+2+1) comparisons were performed, the α -value was adjusted according to the solution of the equation: $(1-\alpha)^{28} = 0.95 \Rightarrow \alpha = 0.0018$. This gives that the probability is 0.95 that all 28 comparisons are true. All pairs of PHB surfaces but two (se KOH-mp KOH and se CHF₃-mp CHF₃) show significantly different water contact angles.

The same calculations were made for methylene iodide contact angles. In that case, all pairs of PHB surfaces but four (se ref-se KOH, se ref-mp ref, se KOH-se O₂ and se O₂-mp O₂) showed significantly different contact angles. The surface energy of the different PHB surfaces is presented in table 6 and a graph is shown in figure 18.

Sample	Surface energy (mN/m)					
	Total		Dispersion comp.		Polar comp.	
	mean	st.dev	mean	st.dev	mean	st.dev
se ref	47.87	1.11	29.25	1.50	18.61	0.82
se KOH	59.36	2.02	26.41	1.29	32.95	2.20
se O ₂	52.60	1.30	26.27	1.69	26.33	1.36
se CHF ₃	32.40	3.10	20.34	2.83	12.06	3.83
mp ref	50.68	0.91	29.80	0.84	20.88	0.93
mp KOH	58.77	1.49	29.91	1.14	28.86	1.60
mp O ₂	49.66	1.01	24.74	1.24	24.92	0.99
mp CHF ₃	25.87	0.82	10.59	1.81	15.26	1.62

Table 6. Surface energy data of different PHB films.

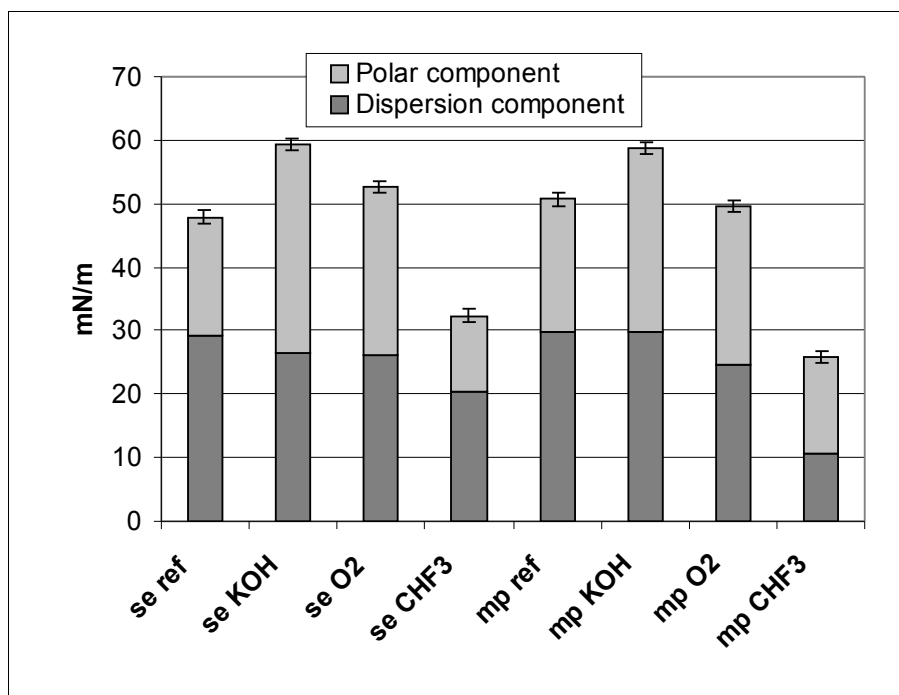


Figure 18. Surface energies of different PHB films.

The surface energies of the 8 different PHB films were compared to each other using Student's T-test on 95% confidence level ($p < 0.05$). Since 28 comparisons were performed, the α -value was adjusted to 0.0018. This gives a probability of 95 percent certainty that all 28 comparisons are true.

The surface energies of mp KOH and se KOH were not significantly different. However, these two surfaces had significantly different polar components of the surface energies. All other pairs of PHB surfaces showed significantly different surface energies.

4.1.3 Fourier transform infrared spectroscopy (FTIR)

In order to characterise the modified PHB films, FTIR analyses were performed. Figure 19 shows the solvent evaporated films.

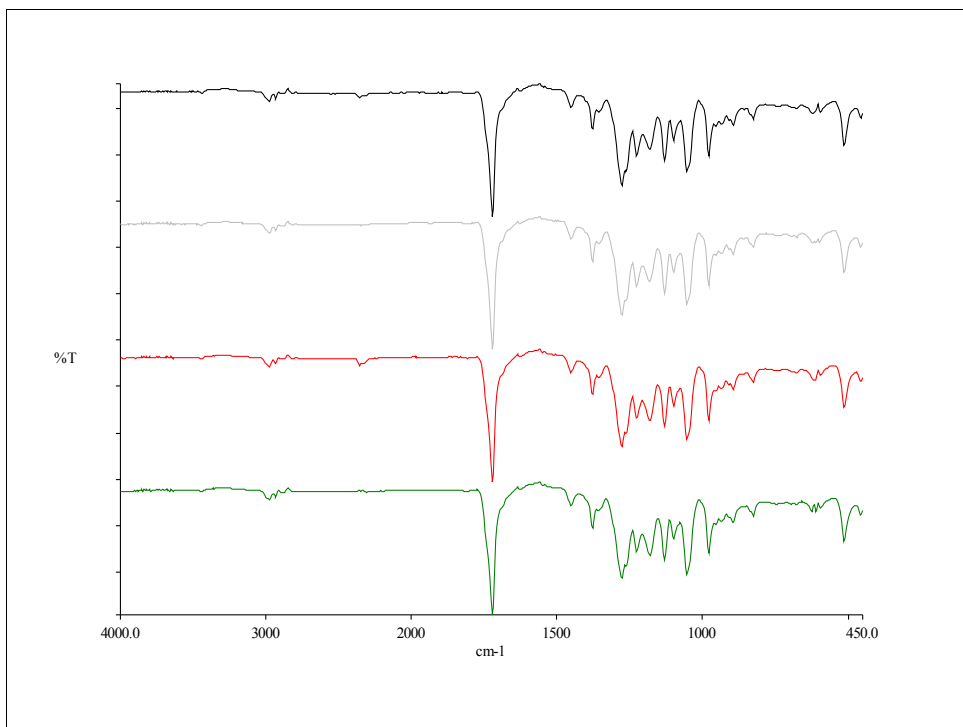


Figure 19. FTIR spectra of solvent evaporated (se) PHB films before cell incubation, from above: se ref, se KOH, se O₂ and se CHF₃.

The spectra are almost identical. Noise from water and CO₂ in the atmosphere can be seen at 3500 cm⁻¹ and 2400 cm⁻¹ respectively. Figure 20 shows the melt pressed films.

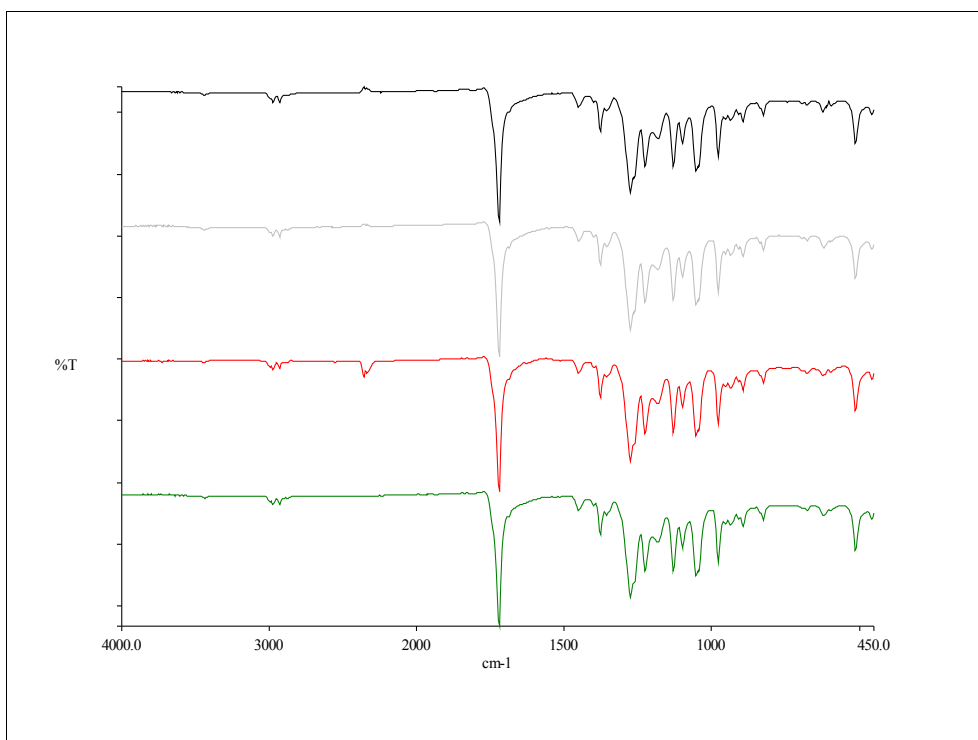


Figure 20. FTIR spectra of melt pressed (mp) PHB films before cell incubation, from above: mp ref, mp KOH, mp O2 and mp CHF3.

The spectra of melt pressed PHB films are also almost identical. Thus, the modifications do not lead to any detectable changes in FTIR. When comparing solvent evaporated films to melt pressed films, no differences can be observed. The PHB fibre patch also gives the same spectra.

PHB films incubated with cells were studied with FTIR. It has previously been shown that enzymatic degradation of PHB leads to one peak at 1530 cm^{-1} and one at 1660 cm^{-1} .⁵⁴ The peaks are due to vibrations in carboxylate ions (1530 cm^{-1}) and carbonyl-groups (1660 cm^{-1}). Furthermore, a peak at 1568 cm^{-1} has also been reported, arising from carboxylate ions due to cleavage of the ester bonds within the polymer chain.⁵⁵

Two representative spectra (see ref and mp ref) are shown in figure 21 and figure 22. Spectra of the other types of PHB films can be seen in appendix 4.

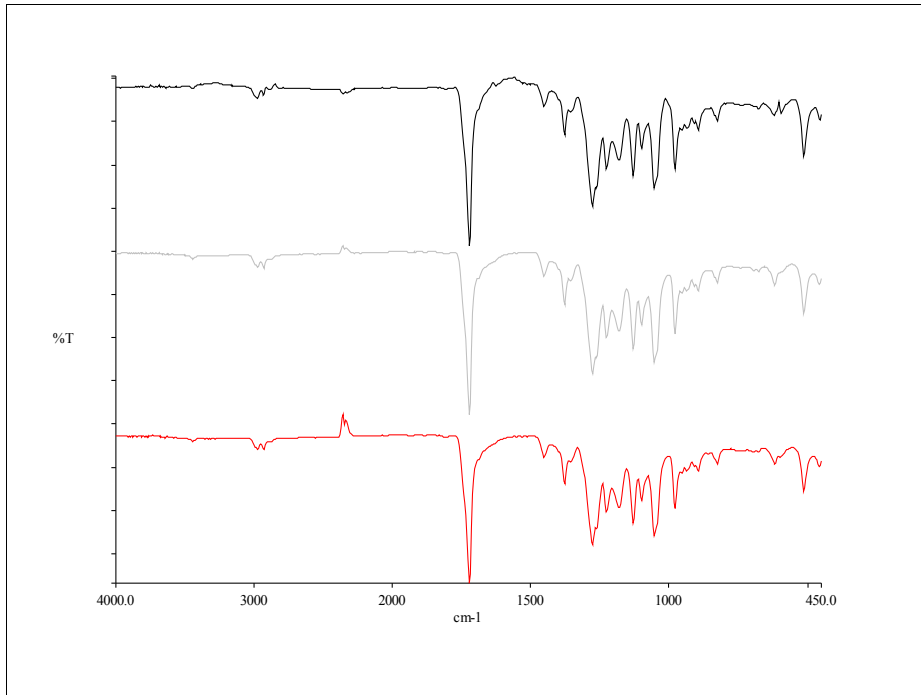


Figure 21. FTIR spectra of solvent evaporated (se ref) PHB films, from above: before cell incubation, after fibroblast incubation and after macrophage incubation.

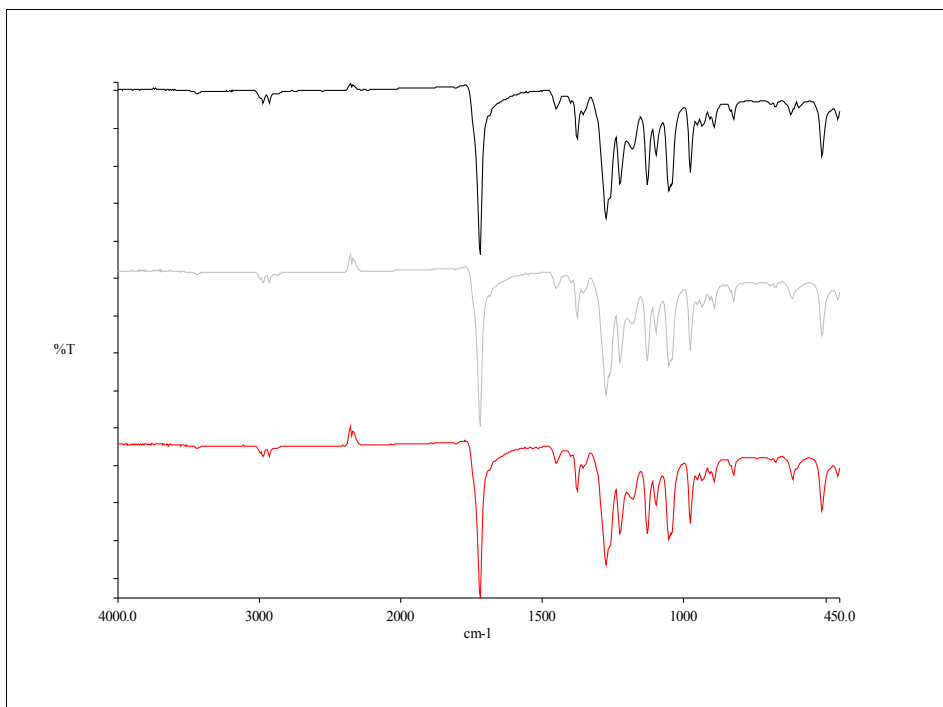


Figure 22. FTIR spectra of melt pressed (mp ref) PHB films, from above: before cell incubation, after fibroblast incubation and after macrophage incubation.

The spectra are almost identical. Thus, the cell incubations do not lead to any detectable changes in FTIR.

4.1.4 Electron spectroscopy for chemical analysis (ESCA)

PHB films were run in ESCA before cell experiments in order to characterise the surface modifications. The results are shown in table 7 and table 8.

Sample	Atomic percent				
	C1s	O1s	F1s	N1s	Ca1s
se ref	71.4	28.6			
se KOH	69.4	30.6			
se O2	69.1	30.9			
se CHF3	60.6	22.2	15.6	1.7	
mp ref	70.0	30.0			
mp KOH	70.2	29.5			0.3
mp O2	68.3	30.0	1.4		0.2
mp CHF3	57.9	20.6	20.8	0.9	

Table 7. Atomic percent of PHB.

Sample	Percentage carbon with different binding energies (Eb)				
	288 eV	290 eV	292 eV	295 eV	296 eV
se ref	56.6	25.1	18.3		
se KOH	56.6	25.1	19.0		
se O2	52.3	25.3	22.4		
Se CHF3	59.4	23.8	16.8		
mp ref	54.0	23.6	22.4		
mp KOH	53.7	24.8	21.6		
mp O2	50.7	28.6	20.7		
mp CHF3	49.0	22.9	20.5	5.8	1.8

Table 8. Percent carbon with different E_b .

The carbon peak for each PHB film type was examined in detail. The carbon peak is built up of four smaller peaks, since PHB consists of four carbon atoms with different electron withdrawing surroundings. It was possible to divide the peak into several parts using the software belonging to the ESCA instrument. The peak with greatest binding energy ($E_b=292$ eV) corresponds to the carbon atom named **a** in figure 23. The two oxygen atoms in its neighbourhood have the ability to withdraw electrons from the carbon atom. Carbon atom **b** in figure 23 is affected by one oxygen atom

and has therefore the second greatest E_b (290 eV). The two carbon atoms referred to as **c** in figure 23 have no oxygen neighbours and approximately the same surroundings. It was not possible to distinguish their peaks. They exhibit the smallest E_b (288 eV).

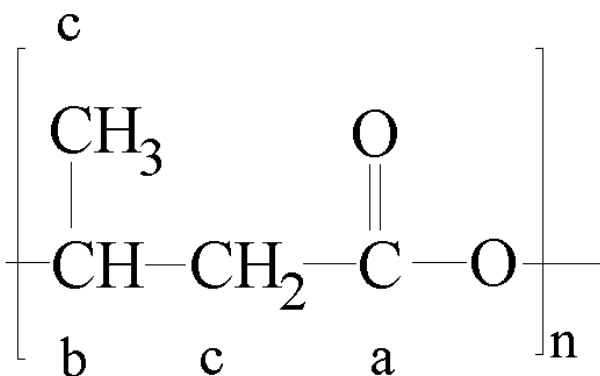


Figure 23. Repeating unit of PHB, **a** refers to the carbon atom with greatest E_b , **b** refers to the carbon atom with medium E_b and **c** to the two carbon atoms with smallest E_b .

Concerning solvent evaporated (se) surfaces, both se KOH and se O2 show a small increase in oxygen content, compared to se ref. In both cases, the content of carbon atom **a** is increased. This indicates that carboxyl-groups have been formed during surface modification. The se CHF3 surface shows a large fluorine content. Nitrogen is also present.

The melt pressed (mp) surfaces do not exhibit the same pattern. The oxygen content in mp KOH and mp O2 is not increased, compared to mp ref. No increase in carboxyl-groups is observed. Traces of calcium are present in mp KOH and mp O2. Furthermore, mp O2 exhibit a content of fluorine. The mp CHF3 surface shows a large fluorine content. The carbon peak for mp CHF3 was built up of five smaller peaks. The two peaks with highest E_b (296.4 eV and 294.83 eV) are probably $-\text{CF}_3$ and $-\text{CF}_2-$ groups, since fluorine exhibit a greater electron withdrawing effect than oxygen.²¹

The results of PHB films run in ESCA after washing with SDS and after cell incubation are shown in table 9 and table 10.

Sample	Atomic percent					
	C1s	O1s	F1s	N1s	S2p	Na1s
mp CHF3	60.6	24.0	14.5	1.0		
mp CHF3, SDS	57.9	16.1	24.4	1.6		
mp CHF3, macrophage, SDS	84.7	12.1	0.0	0.9	2.3	
mp CHF3, fibroblast, SDS	73.7	18.2	0.5	6.3	1.3	
se KOH	69.1	28.8		1.1		0.5
se KOH, SDS	68.9	30.3		0.2		0.6
se KOH, fibroblast, SDS	73.8	20.7		3.4	0.7	0.4

Table 9. Atomic percent of PHB not incubated and incubated with cells. Furthermore, se KOH exhibited 0.6% Ca2p and se KOH fibroblasts, SDS exhibited 1.0% Si2p.

Sample	Percentage carbon with different binding energies (Eb)					
	285.5	287.5	288.5	290-291	293	295
	eV	eV	eV	eV	eV	eV
mp CHF3		53.0	28.1	18.9		
mp CHF3, SDS		53.9	24.0	14.1	4.5	3.6
mp CHF3, macrophage, SDS		85.4	14.6			
mp CHF3, fibroblast, SDS		70.8	19.2	10.1		
se KOH	5.7	55.7	24.2	14.5		
se KOH, SDS		54.1	23.0	22.9		
se KOH, fibroblast, SDS	20.0	58.5	14.2	7.4		

Table 10. Percent carbon with different E_b .

The results show that washing with SDS does not remove the surface layer of fluorine. Furthermore, no sulphur is added.

The mp CHF3 surface incubated with macrophages has lost all its fluorine content. Furthermore, the oxygen content is reduced and the carboxyl carbon atoms are not detectable. The mp CHF3 surface incubated with fibroblasts has lost almost all of its fluorine content. A small decrease of carboxyl carbon atoms can also be observed.

4.1.5 Gel permeation chromatography (GPC)

\overline{M}_w , \overline{M}_n and polydispersity index for the different types of PHB films were determined with GPC. Data are shown in appendix 5. The ratio between exact amount PHB dissolved in chloroform and peak area was relatively constant. This indicates that the PHB was properly dissolved in chloroform. In figures 24-27, values of \overline{M}_w and \overline{M}_n for PHB films not exposed to cells and PHB films exposed to fibroblasts or macrophages are compared.

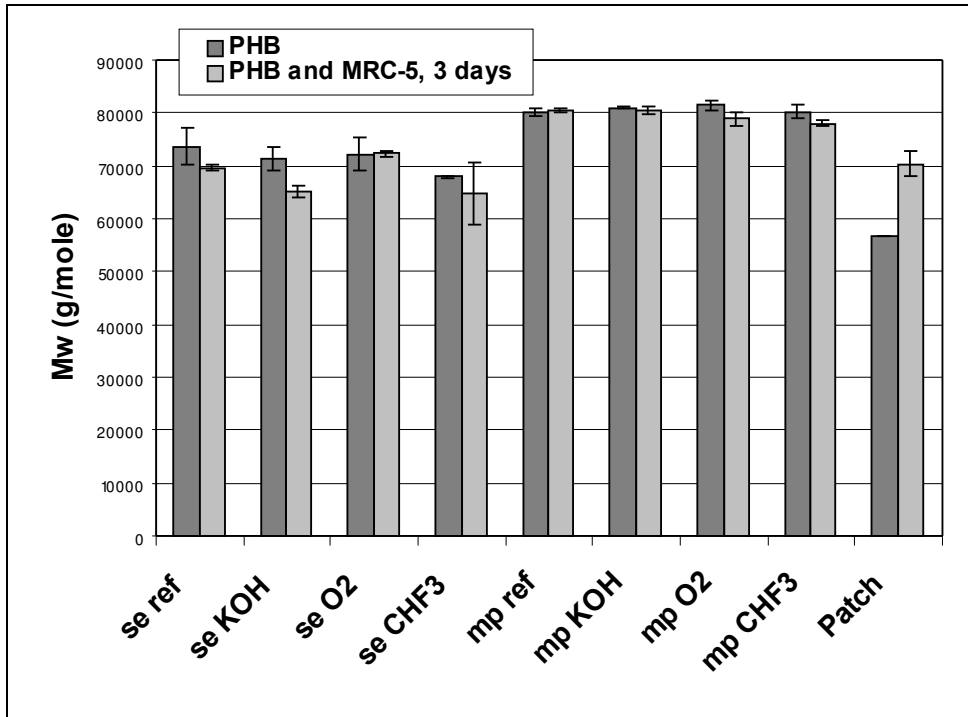


Figure 24. \overline{M}_w from GPC, comparison of different types of PHB films not exposed to fibroblast and PHB films exposed to fibroblasts (MRC-5) for 3 days.

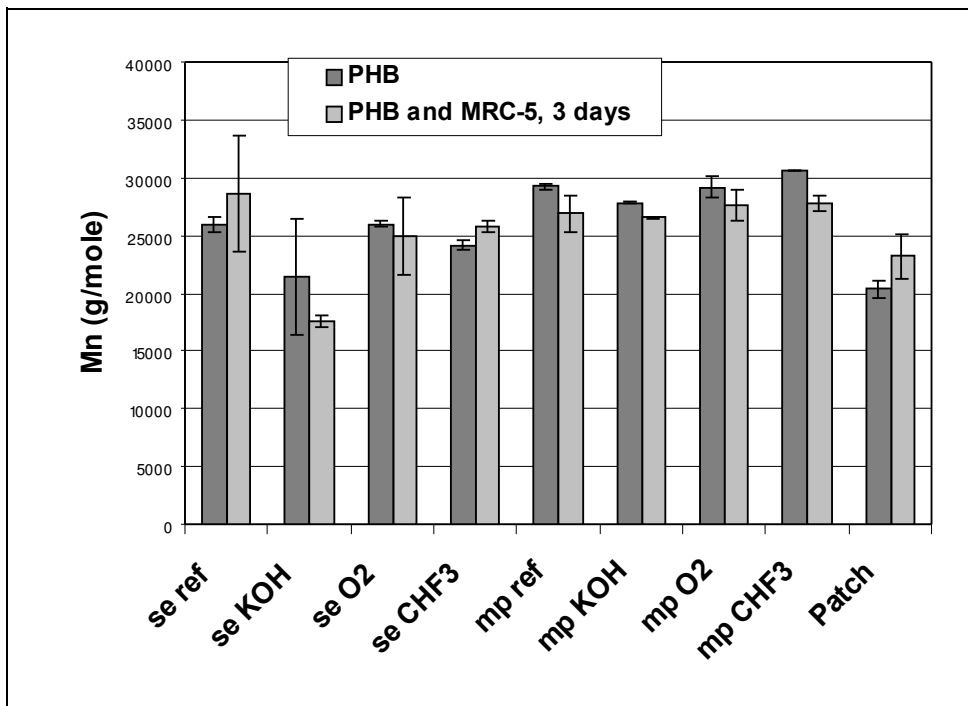


Figure 25. \overline{M}_n from GPC, comparison of different types of PHB films not exposed to fibroblast and PHB films exposed to fibroblasts (MRC-5) for 3 days.

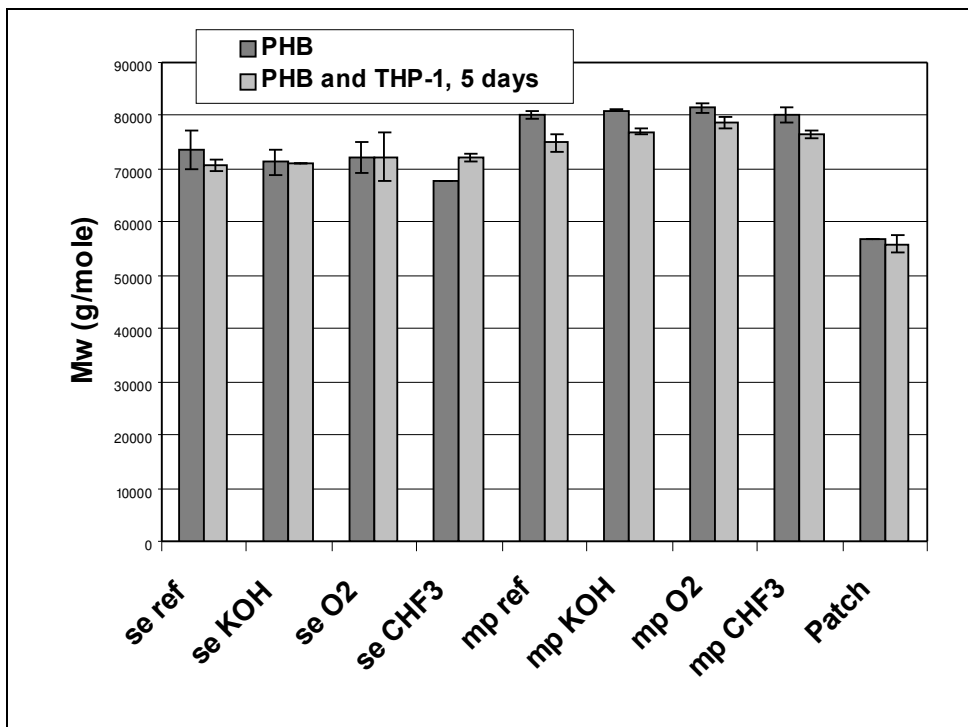


Figure 26. \overline{M}_w from GPC, comparison of different types of PHB films not exposed to macrophages and PHB films exposed to macrophages (THP-1) for 5 days.

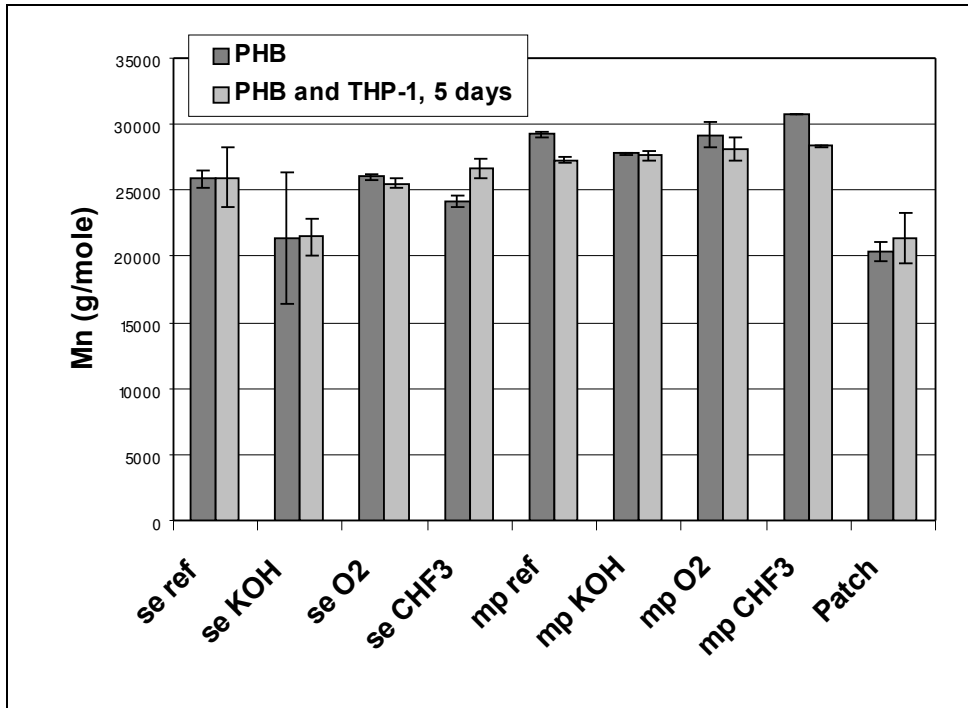


Figure 27. \overline{M}_n from GPC, comparison of different types of PHB films not exposed to macrophages and PHB films exposed to macrophages (THP-1) for 5 days.

The results show that no big changes in molecular weights (\overline{M}_w and \overline{M}_n) have occurred during cell incubation. Some indications of decreasing molecular weights can be observed. Concerning fibroblasts, \overline{M}_n for PHB mp KOH decreases about 5% during cell incubation. Macrophage incubation leads to a decrease of \overline{M}_w for se REF and mp KOH, 4% and 5% respectively. Furthermore, \overline{M}_n of both mp REF and mp CHF3 decreases about 7%. However, in some cases the molecular weight increases during cell incubation.

It turned out to be impossible to dissolve the PHB and PLG particles in chloroform. Thus, no results were obtained.

4.1.6 Scanning electron microscopy (SEM)

PHB melt pressed and solvent evaporated reference films were studied, before radiation and cell exposure, in SEM. The solvent evaporated surface is shown in figure 28. The melt pressed surface is shown in figure 29.

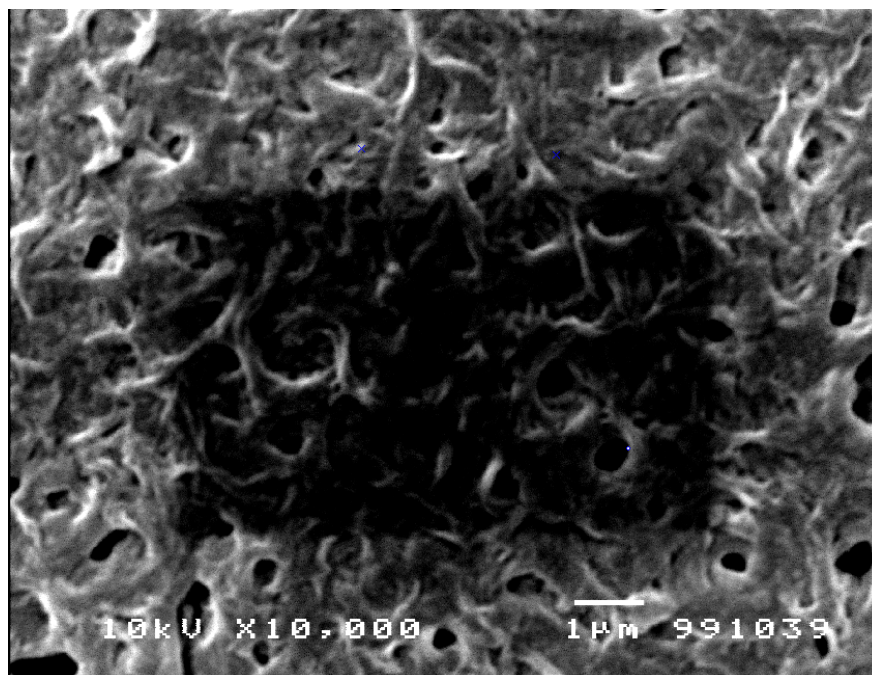


Figure 28. *Solvent evaporated reference film, before radiation.*

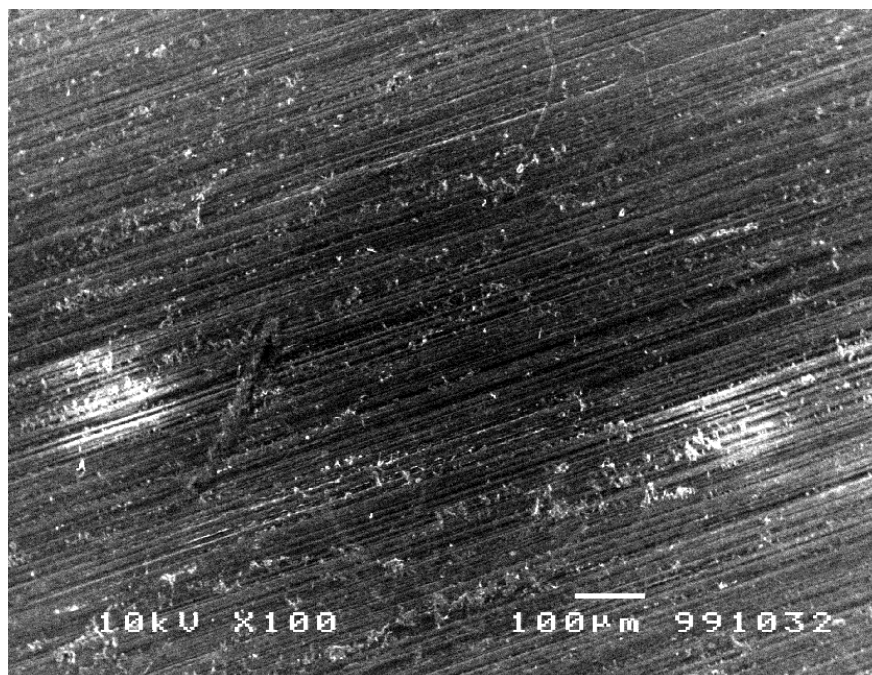


Figure 29. Melt pressed reference film, before radiation.

PHB and PLG particles were studied in SEM. The PHB particles before cell exposure are shown in figure 30. The PHB particles after macrophage incubation are shown in figure 31.

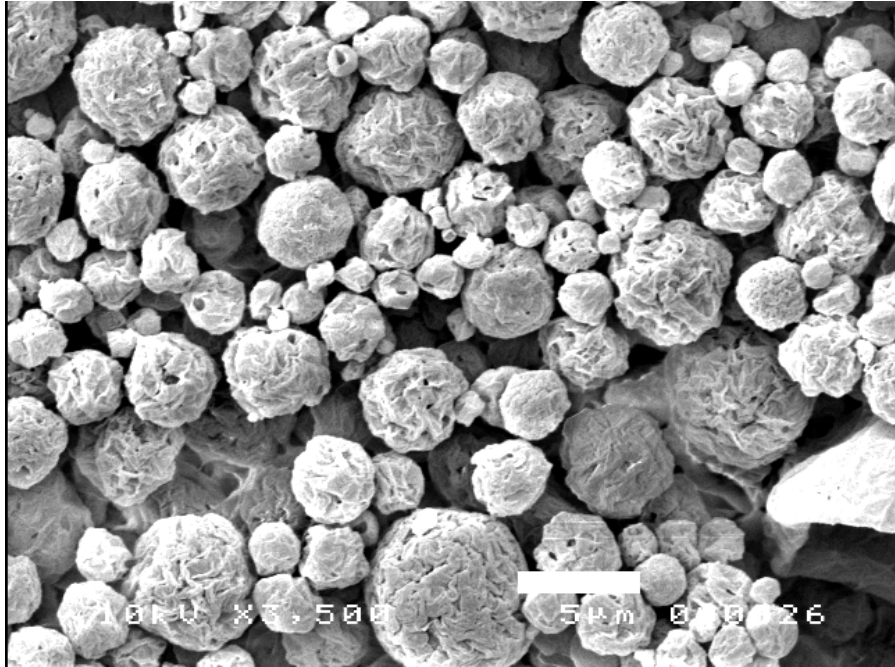


Figure 30. PHB particles before cell exposition. The white bar has a length of 5 μm .

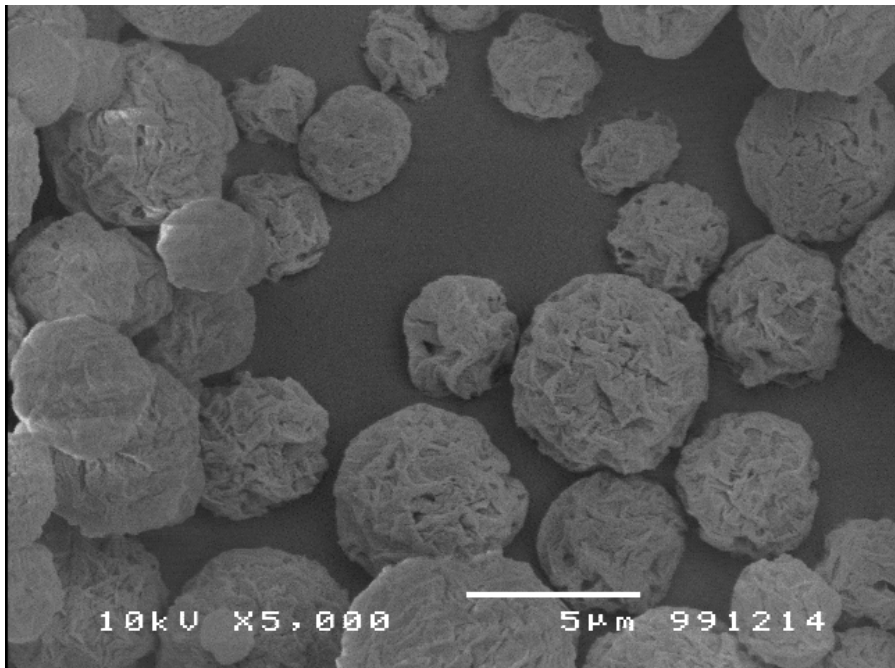


Figure 31. PHB particles incubated with THP-1 cells (macrophages) for 5 days.

The PLG particles before cell exposure are shown in figure 32. The PLG particles after macrophage incubation are shown in figure 33.

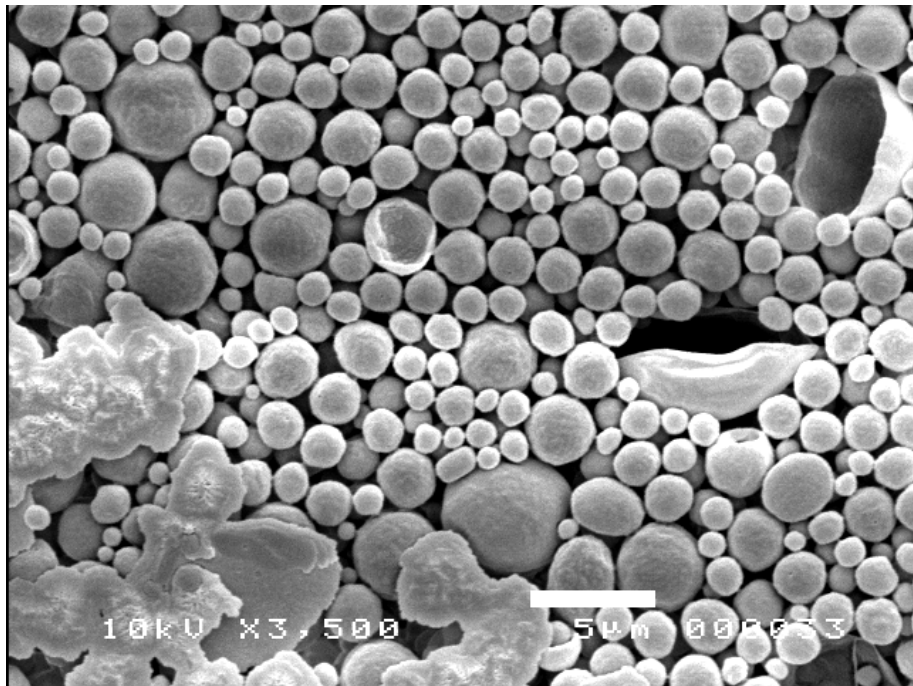


Figure 32. *PLG particles before cell exposition. The white bar has a length of 5 μ m.*



Figure 33. *PLG particles incubated with THP-1 cells (macrophages) for 5 days.*

4.1.7 Atomic force microscopy (AFM)

Two typical AFM-pictures are shown below in figure 34 and 35. Figure 34 shows the side of the film, on which macrophages have grown. Figure 35 shows the opposite side, which has been facing the tissue culture plate during cell incubation. The number of peaks and valleys seems to increase during cell incubation.

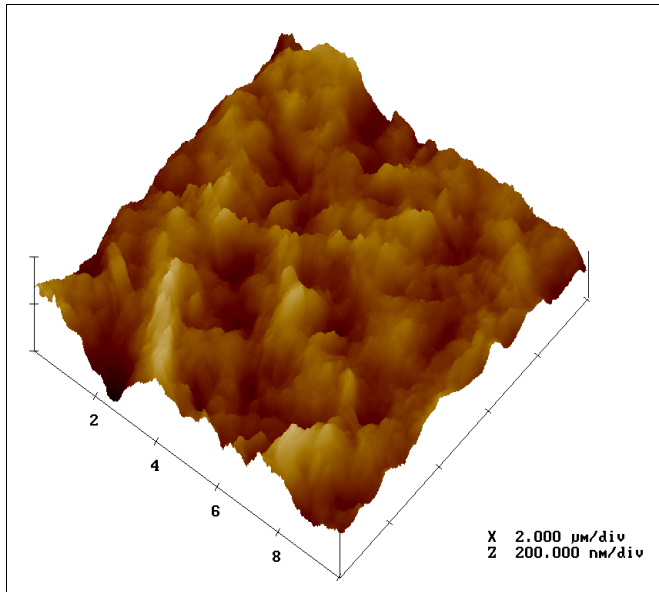


Figure 34. AFM picture of PHB (mp REF), exposed to macrophages. The area shown in the picture is $10 * 10 \mu\text{m}^2$.

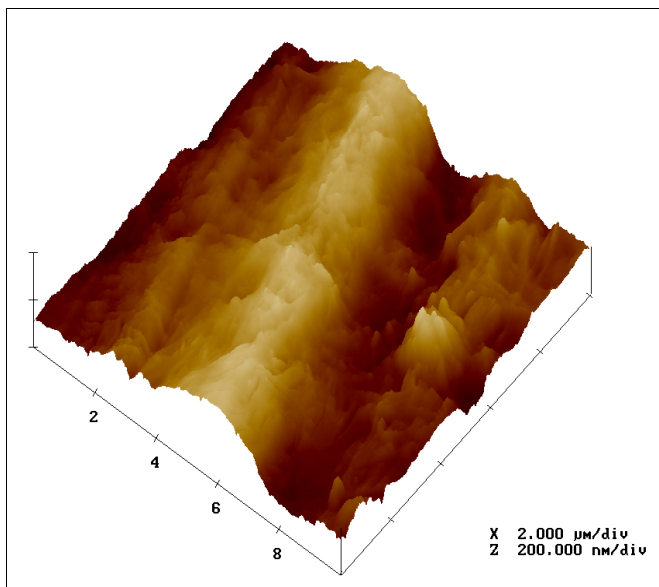


Figure 35. AFM picture of PHB (mp REF), not exposed to macrophages. The area shown in the picture is $10 * 10 \mu\text{m}^2$.

4.1.8 Coulter counter

The average diameters of the PHB and PLG particles after freeze-drying were determined and the result is shown in table 11.

Particle	Mean diameter (μm)	St.dev. (μm)
PHB	2.40	0.16
PLG	1.68	0.25

Table 11. PHB (n=5) and PLG (n=3) particle diameter based on number average diameter.

4.2 Cell experiments

4.2.1 Fibroblasts and cell adhesion

The results shown from study 1, study 2 and study 4 have been corrected with respect to NR-uptake into films of PHB, as presented in study 5. The correction was performed as

$$\bar{X}_i = \bar{a}_i - \bar{b}_i \quad \text{(Equation 18)}$$

$$S_i = \sqrt{\left(\frac{s_{i,1}^2}{n_{i,1}} + \frac{s_{i,2}^2}{n_{i,2}} \right)} \quad \text{(Equation 19)}$$

, where X_i is the average absorbancy used for each value and presented in figures and appendix, a_i the absorbancy value before subtraction of NR-uptake and b_i the absorbancy value of NR-uptake into different modified films. S_i is the pooled standard deviation used and presented in figures and appendix, $s_{i,1}$ is the standard deviation belonging to average absorbancy a_i and number of samples $n_{i,1}$. $s_{i,2}$ is the standard deviation belonging to average absorbancy b_i and number of samples $n_{i,2}$.

For all studies (except study 0 and study 5), Student's T-test (see section 3.5) has been used to analyse the data. To obtain a total probability of 95% ($p < 0.05$) for all comparisons to be true, an α -value was adjusted according to the solution of the equation: $(1-\alpha)^x = 0.95 \rightarrow \alpha = 1 - (0.95)^{1/x}$, where x

denotes the number of comparisons performed in a study. All data from the T-tests can be found in appendix 6.

All types of modified films were compared to the reference film (s.e or m.p, respectively) or TCPS (where possible) for every studied time. In addition, the absorbancy values at 1 hour and 72 hours were compared (where possible) for every type of film.

In addition to the presented results, fibre patches of PHB were incubated with the fibroblasts. These results are not shown due to very low or negative fibroblast adhesion when applying Neutral Red or MTS viability tests. "Blank" patches with no cells were studied and the results were subtracted from patches incubated with cells. A large uptake of medium or Neutral Red into the patches made studies hard to conduct.

Study 0

The results can be found in appendix 7. All curves presenting the absorbancy as a function of adhesion time have been fitted polynomially (2nd degree) to the values.

In order to observe maximal differences in absorbancy values, an initial adhesion time should be chosen where the slope of the curves are the steepest. This occurs at a time of approximately 60 minutes for the three highest initial cell concentrations. Thus, an initial adhesion time of 1h is used in subsequent studies (study 1, 2, 3 and 4).

An initial cell concentration is chosen to $2.5 \cdot 10^4$ cells/cm² ($5.0 \cdot 10^4$ cells/ml) for study 1, 2 and 3. This is based on the curve for 60 minutes adhesion, where only the highest initial concentration deviates below the fitted line. In other studies, fibroblast seeding concentrations of $9 \cdot 10^3$ – $1 \cdot 10^5$ cells/cm², have been used, with the most common being approximately $1 \cdot 10^4$ cells/cm².^{29,30,31,34,56}

Study 1, NR

Since a total of 13 comparisons were made, Student's T-test was performed on a confidence level of 99.6% ($p < 0.004$).

No positive control by cultivating cells in empty TCPS wells was performed.

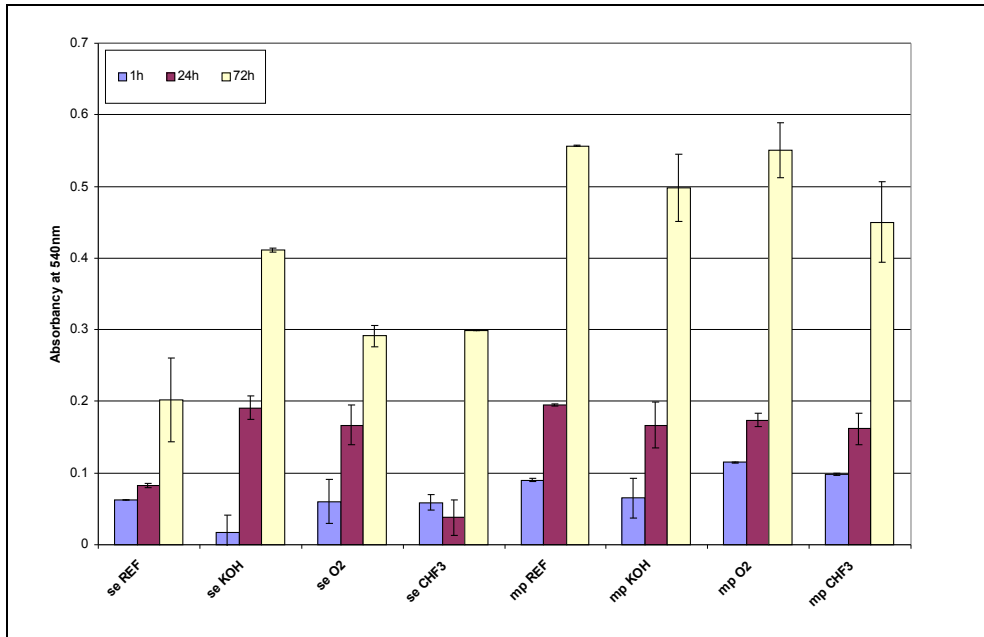


Figure 36. Adhesion of fibroblasts, study 1. Adhesion tested with NR-staining. $N = 2$ (or 1). Standard deviations shown.

Data can be found in appendix 8.

The solvent evaporated (se) films show no significant ($p < 0.004$) differences between various types of surface modifications. Though, figure 36 indicates that se KOH displays the highest adhesion among the solvent evaporated films. The elevation of adhesion between 1h and 72h is statistically significant ($p < 0.004$) for se KOH.

The melt pressed (mp) films do not show the same differences as se films do. The type of surface modification seems to be of less importance for fibroblast adhesion. They do display a higher adhesion in general though, compared to se films, at least for the measurements after 72h.

Study 2, NR

Since a total of 32 comparisons were made, Student's T-test was performed on a confidence level of 99.8% ($p < 0.002$).

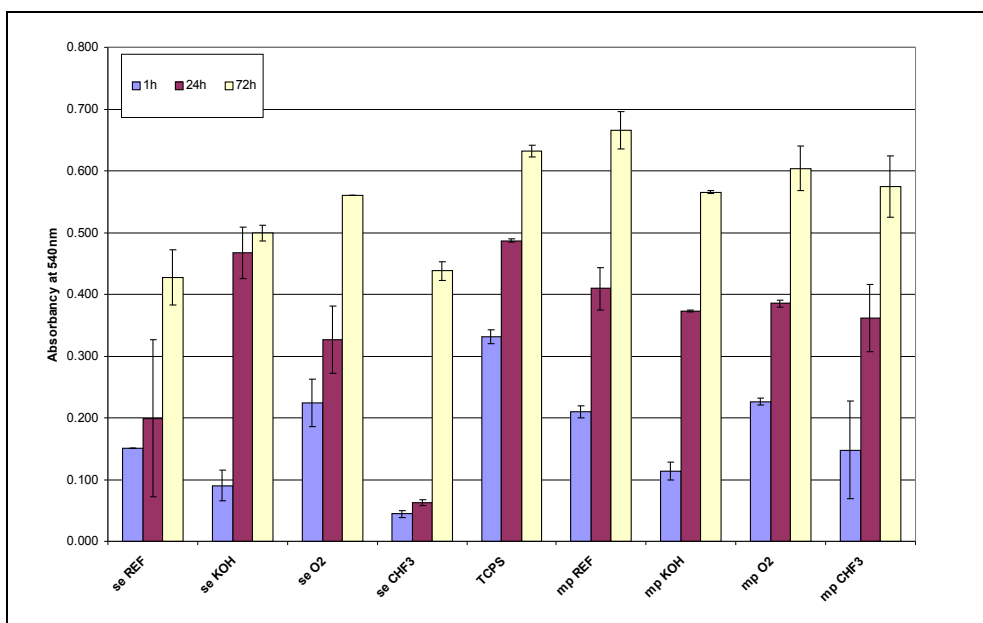


Figure 37. Adhesion of fibroblasts, study 2. Adhesion tested with NR-staining. $N = 4$ (TCPS), 2 (or 1). Standard deviations shown.

Data can be found in appendix 8.

The differences among the solvent evaporated (se) films that could be indicated in study 1 are not that evident in this study. Se CHF₃ seems to depress cell adhesion after 1h and 24h in comparison to other modifications. After 72h incubation this difference is not seen. Indeed, se CHF₃ shows a significant increase ($p < 0.002$) in cell adhesion between 1h and 72h cultivation, as also noted in study 1, figure 36. Se CHF₃ is significantly ($p < 0.002$) lower than TCPS at all times.

The melt pressed films generally have a higher cell adhesion compared to solvent evaporated films. There are no tendencies among the different modifications to favour cell adhesion.

TCPS shows a significant ($p < 0.002$) increase in cell adhesion among the cultivation times. The cells proliferate to a lesser degree on the TCPS control surfaces the last time-interval (24h to 72h), when comparing 1h to 24h with 24h to 72h. In fact, the elevations are 47% respective 30% (not with respect to the different times).

Cell adhesion for the different PHB-films, expressed as percentage of control TCPS, can be seen in figure 38. For se films in general, the levels of cell adhesion at 1h are comparable with the levels at 24h. An increase compared to TCPS between 24h and 72h of cultivation is observed. The exception is se KOH, which displays a huge comparative increase between 1h and 24h and a small decrease in adhesion thereafter to 72h.

The cell adhesions to the melt pressed films show tendencies to increase in comparison to TCPS, for all modifications.

Note that the lines drawn in figure 38 are present to visualise trends in cell adhesion between different culturing times. We do not know the actual behaviour of cell adhesion between the set times (1h, 24h and 72h), why a straight line might be misleading.

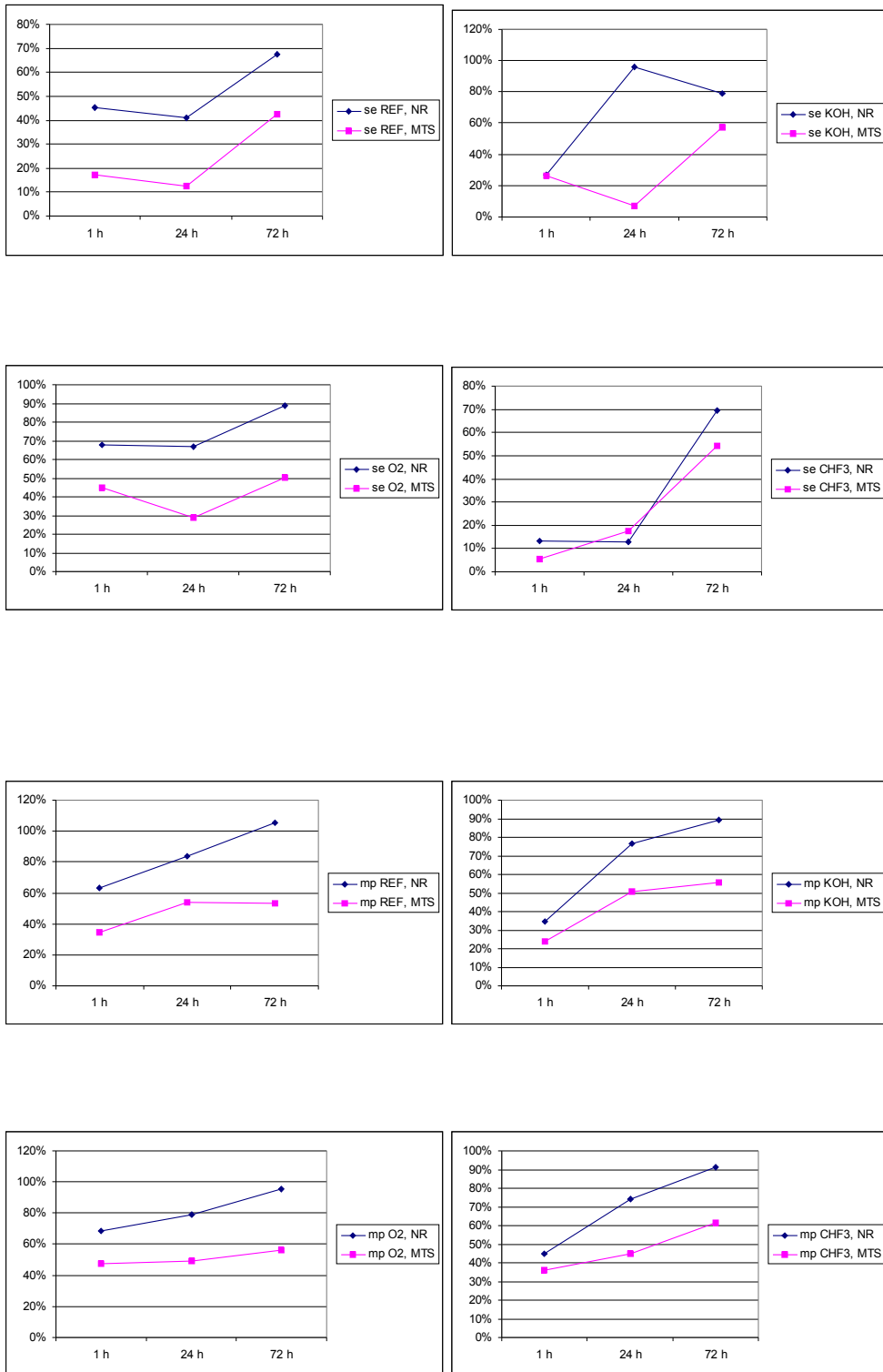


Figure 38. Adhesion of fibroblasts expressed as percentage of TCPS (positive control). $N=3, 2,$ or 1 for the films. $N=4$ for TCPS. Study 2 and study 3 displayed in the same figure. NR=Study 2, MTS=Study 3.

Study 3, MTS

Since a total of 34 comparisons were made, Student's T-test was performed on a confidence level of 99.8% ($p < 0.002$).

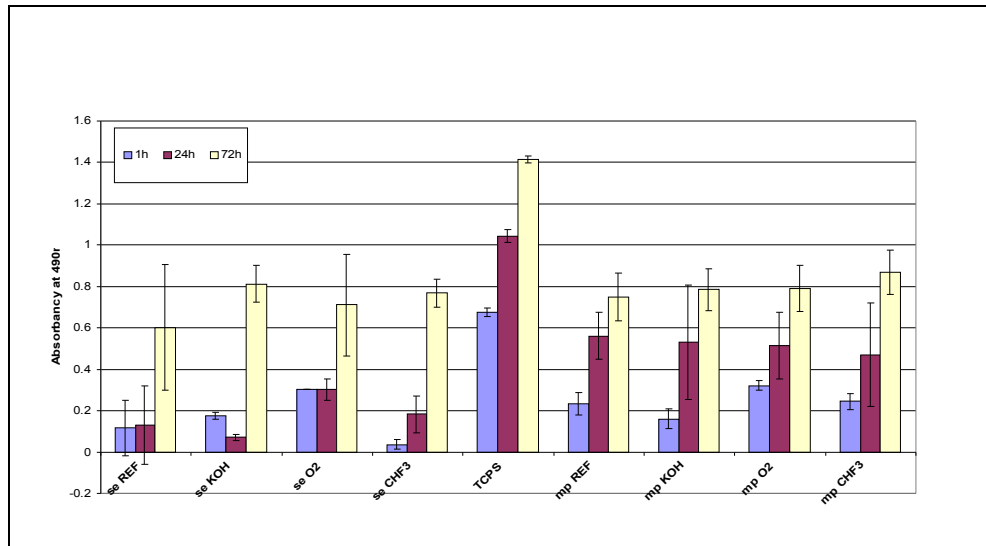


Figure 39. Adhesion of fibroblasts, study 3. Adhesion tested with MTS. $N = 4$ (TCPS), 3, or 2 (s.e. KOH). Standard deviations shown.

Data can be found in appendix 8.

No common tendency can be seen among the solvent evaporated (se) films to favour cell adhesion for a certain type of modification. They all display a tendency in increased cell adhesion between 24h and 72h of incubation. Compared to TCPS, cell adhesion to se films is significantly ($p < 0.002$) lower for all types of modifications except se REF 1h, se REF 72h and se O2 72h.

The melt pressed (mp) films generally have a tendency to higher cell adhesion compared to se films at 1h and 24h incubation. Nearly all mp films are significantly ($p < 0.002$) lower in cell adhesion at all occasions, compared to TCPS.

TCPS shows a significant ($p < 0.002$) increase in cell adhesion among the cultivation times. The cells proliferate to a lesser degree on the TCPS control surfaces the last time-interval (i.e. between 24h and 72h), the increases are 54% respective 35% (not with respect to the different times).

Cell adhesion for the different PHB-films, expressed as percentage of control TCPS, can be seen in figure 37. All types of se films show tendencies to increase their comparative adhesion between 24h and 72h of

incubation. The cell adhesions on the melt pressed films show tendencies to increase in comparison to TCPS, for all modifications.

Study 4, double cell concentration

Since a total of 8 comparisons were made, Student's T-test was performed on a confidence level of 99.4% ($p < 0.006$). When comparing these values (study 4), expressed as percentage of TCPS, to respective values (at 1 hour) from study 2 and 3, a total of 23 comparisons were made. This gives a confidence level of 99.8% ($p < 0.002$).

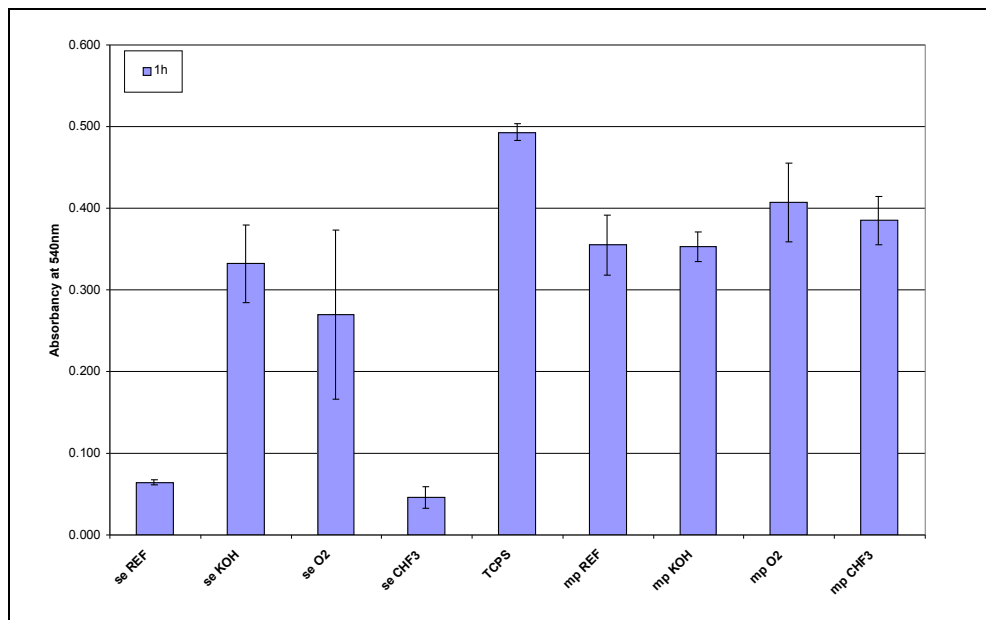


Figure 40. Adhesion of fibroblasts, study 4. Adhesion tested with NR. $N = 2$. Standard deviations shown.

Data can be found in appendix 8.

The fibroblast adhesion after 1h to the solvent evaporated (se) films se KOH and se O2 is comparable ($p < 0.006$) to that to TCPS. Se REF and se CHF3 are significantly ($p < 0.006$) lower in fibroblast adhesion than TCPS.

The cell adhesions of melt pressed films, except mp KOH, are comparable with the cell adhesion to TCPS. Mp KOH shows significantly ($p < 0.006$) lower fibroblast adhesion, when compared with that of TCPS.

Fibroblast adhesion results from study 2, study 3 and study 4 differ from each other. The cell adhesion for se CHF3 and mp KOH is significantly lower ($p < 0.002$) compared to that of TCPS in all three experiments.

Study 5, NR uptake into films

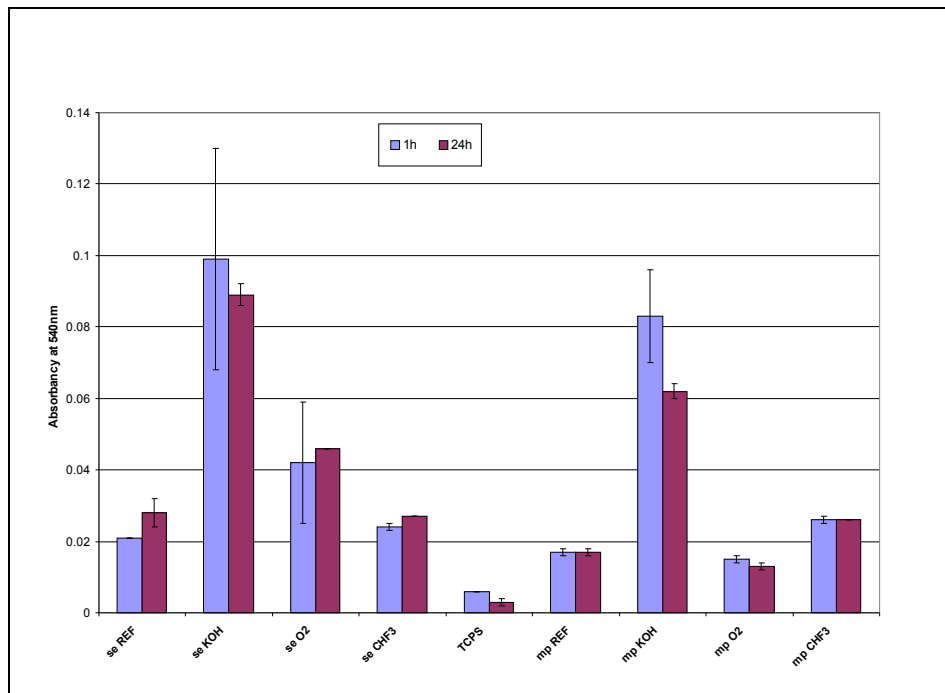


Figure 41. Absorbance arising from NR- or medium-uptake into the films, study 5. $N = 2$. Standard deviations shown.

The results shown in figure 41 show differences among the films. Highest absorbance values, and thus NR-uptake (or medium-uptake) into the films are found for the chemically modified films, se KOH and mp KOH. The uptake of Neutral Red by PHB films seems to level out after 24 hours of medium incubation, see figure 41.

The absorbance values obtained in study 5 are subtracted from the values in previous studies (1,2,4), regarding different modifications and different times. The absorbance values at 72 hours in the other studies (1,2,4) will be decreased by the value from 24 hours in this study, as no general

increase in absorbancy can be observed between 1 hour and 24 hours of incubation from this study.

Light microscopy

Solvent evaporated PHB-films with fibroblasts were studied in light microscopy. Generally, all types of modifications displayed the same amount and morphology of the cells. One representative picture is shown in figure 42.

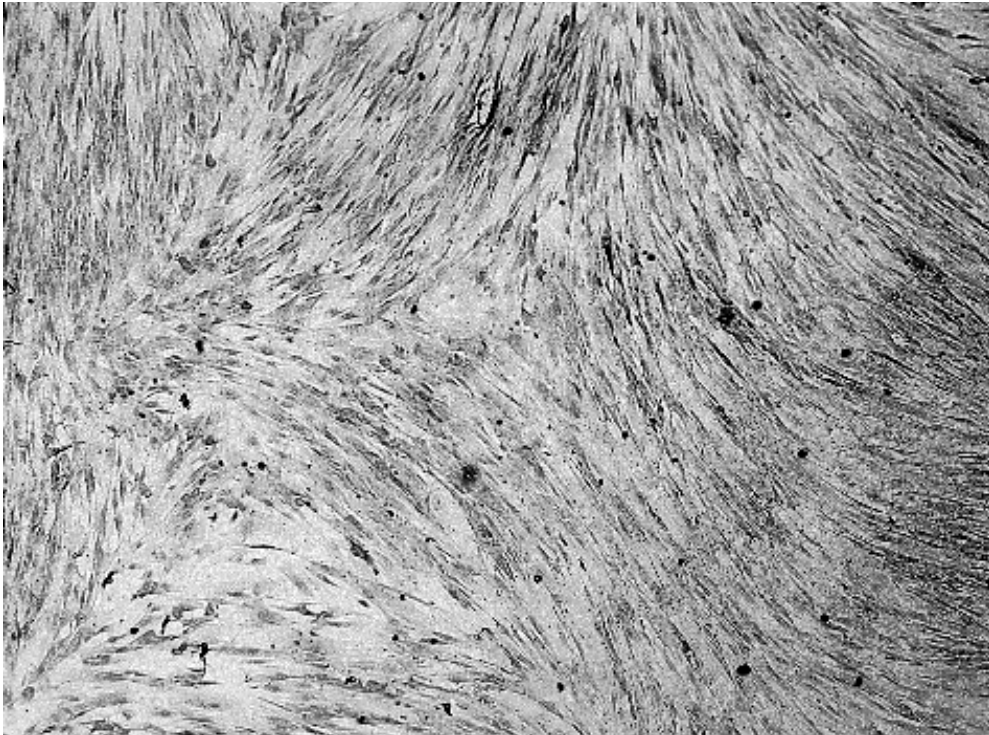


Figure 42. *Fibroblasts incubated for 3 days on se O2. Magnification 50x.*

Melt pressed PHB films were not studied in light microscopy, since not enough light could penetrate the films.

4.2.2 Macrophages and cell activation

Cytokine production

The cytokine responses of the 8 different types of PHB films, PHB fibre patch and the positive control were compared to the negative control using Student's T-test on 95% confidence level ($p < 0.05$). Since 40 comparisons were performed on each type of cytokine, the α -value was adjusted according to the solution of the equation: $(1-\alpha)^{40} = 0.95 \Rightarrow \alpha = 0.0013$. This α -value secures that the probability is 95% that all 40 comparisons are true. It was only the positive control that showed significantly different (larger) cytokine production compared to the negative control.

Some types of PHB films, showed high scores in the T-test performed. The scores were, however, not high enough to be statistically significant when performing 40 comparisons. When just comparing one type of PHB film to the negative control, significant differences can be obtained in some measurement points. The comparison was made on the four measurement points, 6h, 24h, 46h and 54h. In this case the α -value was adjusted according to the solution of the equation: $(1-\alpha)^4 = 0.95 \Rightarrow \alpha = 0.012$. However, no type of film showed significant differences in all four measurement points.

Therefore, the overall result is that the PHB films and the PHB fibre patch did not induce any cytokine response in the differentiated THP-1 cells. They produced the same amount of cytokines as the negative control did. The differentiated THP-1 cells responded to LPS treatment (positive control) by the production of TNF- α , IL-1 β and IL-6, indicating that the cells were able to produce cytokines upon activation. Data is found in the appendix 9. Some typical graphs are shown in this section, see figure 43, 44 and 45.

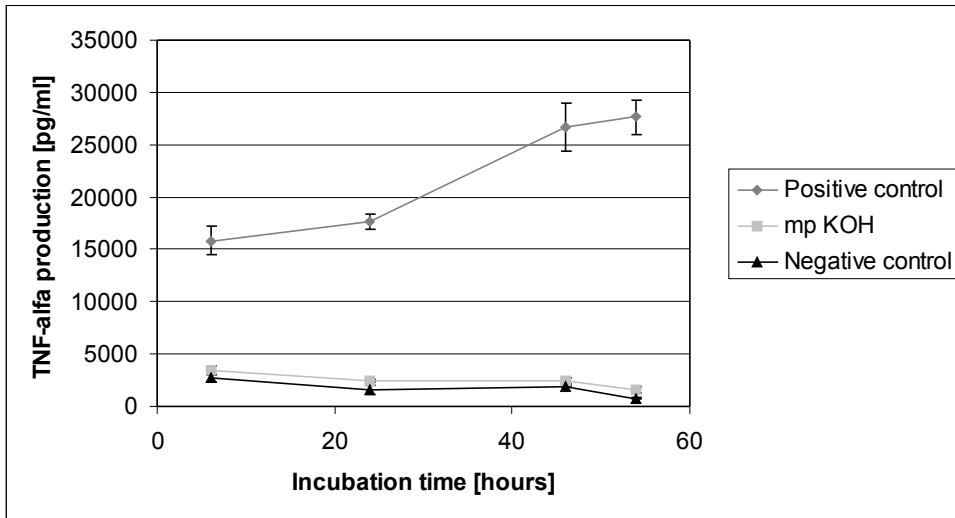


Figure 43. *TNF- α* production in positive control (n=4), PHB mp KOH (n=3) and negative control (n=4). Error bars indicate ± 1 standard deviation.

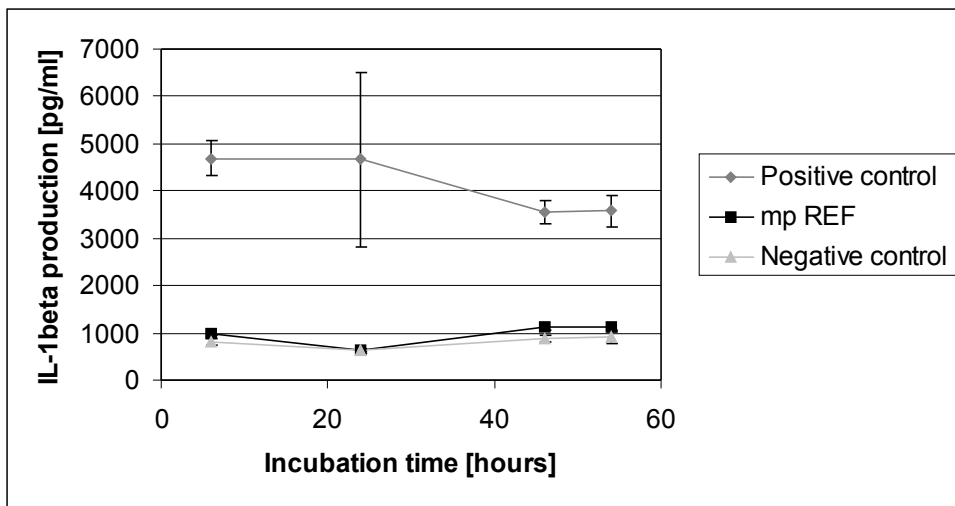


Figure 44. *IL-1 β* production in positive control (n=4), PHB mp REF (n=3) and negative control (n=4). Error bars indicate ± 1 standard deviation.

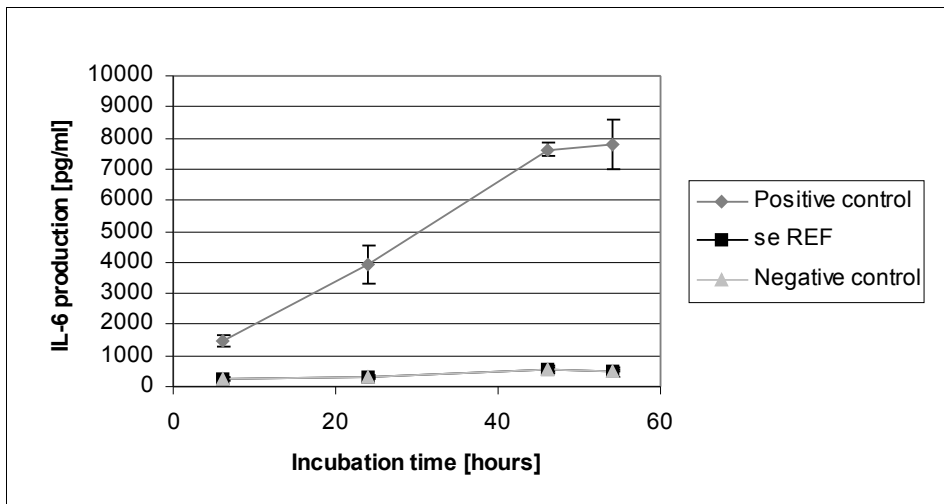


Figure 45. IL-6 production in positive control ($n=4$), PHB se REF ($n=3$) and negative control ($n=4$). Error bars indicate ± 1 standard deviation.

Light microscopy

Solvent evaporated PHB films incubated with differentiated THP-1 (macrophages) were studied in light microscopy. The same macrophage response was observed on all different PHB films. Cells were attached one by one and they were sometimes spread on the surface. No foreign body giant (FBG) cells were seen. One representative picture is shown in figure 46.

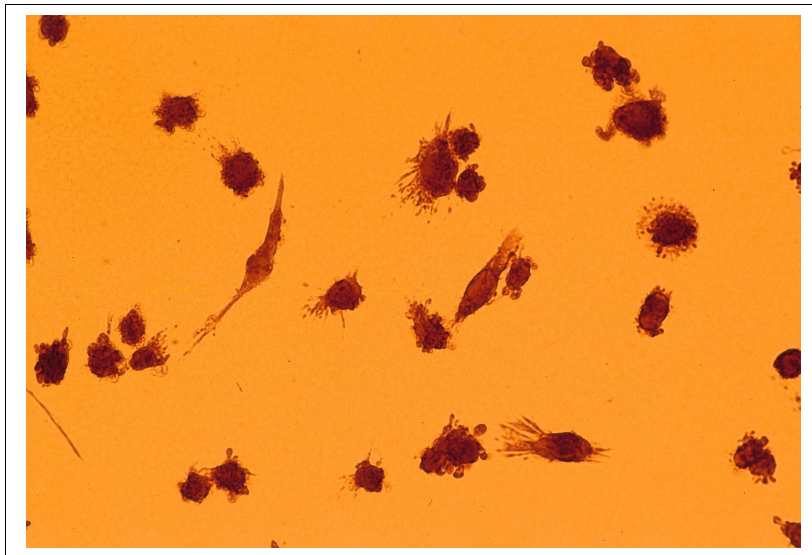


Figure 46. Macrophages incubated 5 days on a PHB film (se CHF3). Magnification 400x.

Melt pressed PHB films were not studied in light microscopy, since not enough light could penetrate the films.

5 Discussion

Viscosimetry

Viscosimetry results before radiation indicate that PHB fibre patches processed by solvent evaporation exhibit no notable degradation. This type of processing is thus useful when the \overline{M}_w of PHB is to be retained. PHB fibre patches processed by melt pressing seem to be degraded significantly. This indicates that the heat and pressure used in melt pressing affect the \overline{M}_w of PHB. It should be considered if this kind and degree of degradation is desirable.

Results after radiation shows that the \overline{M}_w of PHB can be lowered in a desired manner by irradiation with high-energy β -radiation. Though, none of the types of PHB studied obtained the desired value (65000 g/mole). This can be due to several things including inaccurate formulas when calculating the radiation dose, inaccurate dose obtained and different susceptibility to radiation for differently processed polymer types. Compared to the desired value, patches seem to be more degraded, whereas films seem to become less degraded.

Contact angle and surface energy

The contact angle results led to 8 PHB surfaces with different surface energy. Plasma modification with O_2 resulted in hydrophilic surfaces, while plasma modification with CHF_3 resulted in hydrophobic surfaces. Plasma treatment with O_2 leads to an increase in functional groups containing oxygen, e.g. hydroxyl-groups and carboxyl-groups. Thus, the contact angle to water should decrease. This is also the case, even if the decrease is relatively small. A larger decrease may be achieved by prolonged plasma treatment. Fluorocarbon surfaces have characteristically high water and methylene iodide contact angles and low surface energies. The main reason is the large size of the $-CF_2-$ groups compared to $-CH_2-$ groups. Since fewer $-CF_2-$ groups can be packed into a given area of the solid, the

free energy of liquid adhesion is less and the contact angles are thus greater.²² Chemical modification with KOH also increases the number of functional oxygen groups. In this case, a larger decrease in contact angle can be observed compared to plasma modification with O₂.

Differences between solvent evaporated (se) and melt pressed (mp) surfaces with the same modification, might be due to the surface roughness. In a rough solid, the liquid fills up and penetrates most of the hollows and pores. The result is a plane surface, part solid and part liquid. Since the contact angle between liquid and liquid is equal to zero, the resulting contact angle decreases. The method used to prepare the solid may also affect the contact angle. Penetration and entrapment of traces of e.g. water in the surface layer leads to a lower contact angle.²² However, the general trends for solvent evaporated and melt pressed surfaces are the same.

Fourier transform infrared spectroscopy (FTIR)

The results obtained from FTIR do not show any differences between the different types of modified PHB films. The detection depth of a few micrometers is probably too large to study the surface. Signs of spectra changes after cell incubation, caused by e.g. biodegradation, are also absent. This indicates that no bulk biodegradation has occurred.

Electron spectroscopy for chemical analysis (ESCA)

ESCA results from PHB surfaces before cell exposure show that plasma modification with CHF₃ has worked out properly. Concerning chemical modification with KOH and plasma modification with O₂, se KOH and se O₂ surfaces show indications of greater oxygen contents compared to se REF. The melt pressed films do not show any evident signs of surface modifications. The origin of contaminations (nitrogen and calcium) is not clear.

The results after cell incubation indicate that both macrophages and fibroblasts degrade the PHB surface, since the surface layer of fluorine is absent after incubation. The fluorine has left the surface during cell incubation and not during the washing program after incubation. This can be concluded since a comparison to a surface not exposed to cells but treated with the same washing program was made. Nitrogen and sulphur contents on the cell-incubated surfaces are probably due to attached biological materials.

Gel permeation chromatography (GPC)

The GPC results show that no big changes in molecular weights (\overline{M}_w and \overline{M}_n) have occurred during cell incubation. Smaller differences can be observed, but since only two injections were made on each type of PHB film, no biodegradation can be statistically secured. Some indications of decreasing molecular weights can be observed. However, in some cases the molecular weight increases during cell incubation. Therefore, the changes might be due to measurement uncertainty. It should be pointed out that GPC mainly analyses the bulk, since a whole piece of PHB is dissolved in chloroform before analysis. Therefore, biodegradation may have occurred on the PHB film surfaces. Longer incubation time or thinner PHB films might reveal biodegradation.

Since the PHB and PLG particles were not dissolved in chloroform, no molecular weights were obtained. A probable reason might be that polyvinylalcohol from the particle formation remained at the particle surface.

Scanning electron microscopy (SEM)

The solvent evaporated surface displays pores with an approximate diameter of 1 μm . These probably arise from the evaporation of the solvent when processed. The melt pressed surface does not show the same porosity. Rather does it have a topography different from the solvent evaporated film, with a wave-like structure. This is probably originating from the structure of the teflon-plates used in melt pressing. Note that the SEM-pictures are displayed with different magnifications, the solvent evaporated being 100x more magnified. When magnifying the melt pressed surface (not shown) to the same extent as the solvent evaporated, no pores could be seen.

The surface of the PHB particles does not seem to have been affected by the macrophages. The PLG particles are very round and smooth before cell incubation. After incubation they are not perfectly rounded and some of the particles show pores. These pores might be due to biodegradation.

Atomic force microscopy (AFM)

The AFM results indicate that macrophages have affected the PHB film surface. The number of peaks and valleys seems to increase during macrophage incubation. The results can be compared to AFM-experiments performed by Rouxhet et al. on surfaces of poly(hydroxybutyrate-co-

hydroxyvalerate). In their experiments, alkaline hydrolysed surfaces showed an increase in peaks and valleys, compared to non-hydrolysed.⁴³ Their series of pictures resemble the pictures in this report.

Cell adhesion

The TCPS controls show an increase in cell adhesion during cultivation. This indicates that the cells are viable and capable to proliferate.

No significant differences in cell adhesion can be observed among the different types of modified films, except for the most hydrophobic solvent evaporated film, se CHF3. This film has a tendency to reduce cell adhesion in comparison to other films after 1 hour and 24 hours of incubation. After 72 hours, this difference is not seen. Se CHF3 has a surface energy of 35 mN/m and a water contact angle of 83 degrees. Surface energies below 50 mN/m have been proposed to reduce cell spreading.¹ Tamada and Ikada showed a reduced fibroblast adhesion after 22 hours of incubation to different hydrophobic surfaces (water contact angle 92 – 116 degrees) compared to more hydrophilic ones.³¹ Ho Lee et al. grew fibroblasts on polycarbonate (PC) surfaces with different wettabilities. They observed a reduced adhesion after 1 day and 2 days of incubation to surfaces with contact angles between 75 and 85 degrees, compared to more hydrophilic surfaces.³⁴ Tamada and Ikada also noted a more active biosynthesis of collagen *per cell* on the hydrophobic surfaces, implying that cells on surfaces unsuitable for adhesion modify their local environment more actively than cells on favorable surfaces. Collagen is associated with cell proliferation.³¹ Cells on relative hydrophobic surfaces may have a prolonged lag-phase during which the collagen synthesis is active, after which they proliferate extensively owing to high accumulated amounts of collagen. On the contrary in our study, mp CHF3, which has a surface energy of 27 mN/m and a water contact angle of 88 degrees, do not show any tendencies to reduce cell adhesion in comparison to the other melt pressed films.

Solvent evaporated films generally display lower cell adhesions at 1h and 24h of incubation compared to those of melt pressed films. This might be due to differences in surface structure, the surfaces of solvent evaporated films being rough due to pores of 1 μm in diameter. All melt pressed films had smooth surfaces without any pores, see figures 28 and 29. Lee et al. showed a dependence on cell adhesion with surface topography, implying that adhesion and growth were progressively inhibited by large pores (8 μm) compared to small pores (0.2 μm).³⁴ On the contrary, other studies have shown optimal cell adhesion and growth for surfaces with pore sizes of 1-2

μm .¹ In this study, the differences between solvent evaporated films and melt pressed films more likely arise from the handling of the films. Solvent evaporated films are much more fragile than melt pressed and it is thus more difficult to ensure similar treatment for all films.

All melt pressed films showed the same level of fibroblast adhesion after 1h when an initial cell concentration of 10^5 cells/ml was used (study 4). Though the surface energies of the melt pressed films ranged from 63 to 27 mN/m, the fibroblast adhesion levels were comparable. The surface smoothness rather than the surface energy seems to influence 1h fibroblast adhesion to melt pressed films. A possible reason for the significantly ($p < 0.006$) lower fibroblast adhesion to melt pressed (mp) KOH, can be that the chemical treatment with 2.5M KOH might increase the roughness of the polymer film. The fibroblast adhesion to se KOH and se O2 is comparable ($p < 0.006$) to that to TCPS after 1h. One reason to this might be that these solvent evaporated surfaces show low water contact angles, 41° and 52° respectively. That is, they have hydrophilic surfaces.

One reason to differences in initial fibroblast adhesion when comparing study 2, 3 and 4 might be the influence on cell concentration on cell adhesion. In study 4, the cell concentration was twice as high as in study 2 and study 3. Another reason might be the low number of samples, affecting the statistical significance level. In all three studies, though, se CHF3 and mp KOH are significantly lower in fibroblast adhesion. They have water contact angles of 83° and 45° and surface energies of 32 mN/m and 59 mN/m, respectively. This indicates that there might be other surface properties besides water wettability and surface energy that influence fibroblast adhesion. One property might be the surface topography. Hydrolysis with KOH results in etched surfaces of poly(hydroxybutyrate-co-hydroxyvalerate), as reported earlier.⁵⁷ This might be true for melt pressed films too. As the surface roughness increases the cell adhesion during the first hour is influenced.

When compared to TCPS, the cell adhesion for all surfaces (study 2 and 3) increases during cultivation. The cells cultured on TCPS might be approaching confluency, leading to reduction in apparent comparative adhesion. After 24h incubation, all melt pressed films exhibit values in the range of 49-54% (MTS-test) or 74-84% (NR-test) of cell adhesion to TCPS. Saad et al. have in two separate reports studied fibroblast adhesion to polyesters/polyethers respectively polyesterurethanes. These studies propose good biocompatibility for materials with fibroblast adhesion of 60% respectively 50-85% of TCPS control.^{32,56} This indicates that PHB in our study, at least in the form of melt pressed films, shows biocompatibility in terms of good fibroblast adhesion.

The studies using Neutral Red for adhesion tests generally display higher values of cell adhesion in percentage of control TCPS, than the study using MTS for adhesion tests. This might once again be due to the handling of the films, since the MTS-test involves the transfer of viable cells from one well to another. This can affect the cells negatively.

The differences observed in NR-uptake into films (study 5) can only be speculated about. No literature describing the phenomena has been found. Perhaps the NR-adsorption is coupled to the chemical structure of the surfaces in a direct way, or indirect through selective protein adsorption from the medium.

Light microscopy studies show that the fibroblasts are attached and well spread on the PHB surfaces. Different types of modified PHB surfaces did not induce different alignment, number or morphology of the fibroblasts. These observations indicate that the surfaces are biocompatible, concerning adhesion, to fibroblasts.

Cell activation

The cytokine concentrations in the negative controls are relatively large, compared to other experiments performed at AstraZeneca. These experiments showed that non-stimulated THP-1 cells do not produce cytokines to the same extent as in this study. In the AstraZeneca studies, the cells were differentiated in the wells of a tissue culture plate. Thus, the trypsin/EDTA treatment was not needed in order to remove the cells from a culture flask to a well.

A probable explanation to the large cytokine responses is therefore that trypsin activates the cells. In the present study the cells treated with trypsin/EDTA were diluted 10 times in culture medium before use. In screening studies, the dilution of trypsin/EDTA was about 5 times. This led to even larger cytokine responses of the negative control. However, a dilution of 10 times does not seem to be sufficient. In order to dilute the trypsin/EDTA even more, the suspension has to be centrifuged and the cells resuspended in culture medium again. This way around was tested but led to cell aggregates, i.e. non single-cell suspension. Thus, the number of cells in a given well would be hard to control. Besides, even if the centrifuge step would have been done, the initial 15 minutes trypsin/EDTA incubation still remains. This treatment probably plays a role in the activation of THP-1. Another way around the problem with pre-activation is to differentiate the THP-1 cells in the wells of a culture plate, where PHB films already have been applied. However, the differentiation takes some

time and the main interest is to study polymer-macrophage interactions and not polymer-monocyte interactions.

The positive controls for TNF- α , IL-1 β and IL-6, show large activation. This indicates that the cells are able to be activated and are not damaged in any essential way.

The PHB films and PHB fibre patch did not induce any cytokine response compared to the negative control. Thus, no correlation between cell activation and surface energy was shown. These results are similar to results reported by Saad et al. They have investigated the TNF- α responses from macrophages exposed to different block co-polyesters with about 40% (w/w) poly(hydroxybutyrate-co-hydroxyvalerate) (HB/HV 95/5). The TNF- α levels were equal for negative control (TCPS) and the polymers. No correlation between contact angle to water and cell adhesion was observed.⁴⁸

Furthermore, DeFife et al. have also reported lack of correlation between macrophage activation and surface energy. They have studied interactions between monocytes and silicon rubber (SR) with different coatings. The materials exhibited water contact angles between 25 and 100 degrees. TNF- α and IL-1 β concentrations were measured in the supernatant of the cells, that were exposed to the different materials. Typical cytokine levels were about 1000 pg/ml. No positive control was included in this experiment. No correlation between contact angle to water and cell activation was observed.⁴⁷

Light microscopy studies show that the macrophages are attached one by one at the PHB surfaces. No signs of FBG cells are seen and the cells are sometimes spread on the surface. Different types of modified PHB surfaces did not affect the macrophages according to size, morphology et cetera. These observations indicate that the surfaces are biocompatible to macrophages.

6 Conclusions

- PHB films with different surface structures, surface energies and molecular weights are possible to fabricate and to characterise.
- PHB films are biocompatible materials in terms of good fibroblast adhesion.
- Hydrophilic solvent evaporated PHB films promote initial fibroblast adhesion, compared to more hydrophobic solvent evaporated PHB films.
- PHB films and PHB fibre patch do not activate macrophages to produce the cytokines TNF- α , IL-1 β and IL-6. There is no correlation between macrophage activation and surface energy.
- PHB film surface degradation occurs during short time (3 to 5 days) fibroblast or macrophage exposure.
- No PHB film bulk degradation occurs during short time (3 to 5 days) fibroblast or macrophage exposure.
- The surface of PHB particles is not affected by short time (5 days) macrophage exposure.

7 Future directions

- Further studies should focus on one or two types of surface modified PHB films, in order to increase the statistical significance. A future study should be planned according to the statistical demands.
- Co-culturing of several cell types, including for example fibroblasts, macrophages and neutrophils, on PHB, should be performed in order to detect occurrence of cell – cell interactions.
- Degradation of PHB should be studied during a prolonged (weeks) cell incubation time.
- Further extensive studies on initial serum protein (e.g. fibronectin and C3b) deposition to PHB surfaces need to be performed.
- The treatment of the PHB film pieces during cell experiments needs to be evaluated. In order to avoid the need for moving the pieces of film between wells, larger pieces of films that cover the whole bottom area of a cell culture well should be employed.

8 Acknowledgements

We would like to thank the following people:

Andrea Schmid, our supervisor at Astra Tech.

Anders Peterson, our supervisor at AstraZeneca.

Fredrik Andersson, Astra Tech, for his help with pictures to the report.

Bruno Becker, for his help with the MTS-viability assay.

Marie Björklund, CTH, for her help with GPC analyses.

Herbert Helander, for help with fixation.

Jan Karlsson, IFP, for his help with plasma modification and contact angle analyses.

Anette Larsson, Lisbeth Caous and Susanna Abrahmsén-Alami, AstraZeneca, for their help with the particles.

Nadereh Poorkhalkali, for common help with lab.equipment at AstraZeneca.

Staffan Schantz, AstraZeneca, for his help with contact angle analyses.

Sten Sturefeldt, AstraZeneca Draco, for his help with SEM analyses.

Ann Wendel, CTH, for her help with ESCA analyses.

Kerstin Wiklander, AstraZeneca, for her help with statistics.

All@AstraTech R&D for their help, encouragement and Friday cakes.

9 References

1. Ratner, B.D. et al., *Biomaterials science, an introduction to materials in medicine*, 1996, Academic press, ISBN 0-12-582461-0.
2. Tortora, G.J. and Grabowski, S.R., *Principles of anatomy and physiology*, 5th ed., 1996, Biological Sciences Textbook Inc., ISBN 0-673-99354-X.
3. Andersson F. *Impurities in poly[(R)-3-hydroxybutyrate] (PHB)*, 1999, Department of Physics and Measurement Technology, University of Linköping, Sweden.
4. Holmes, P.A., *Biologically produced (R)-3-hydroxyalkanoate polymers and copolymers*, *Developments in Crystalline Polymers*, 2nd ed., 1988, Basset D.C., Elsevier, London, p.1 - 65, ISSN 0263-6204.
5. Hankemeyer, C.R. and Tjeerdema, R.S., *Polyhydroxybutyrate: plastic made and degraded by microorganisms*, *Rev. Environ. Contam. Toxicol.* 159, 1999, p.1 - 24, Springer-Verlag.
6. Reusch, R.N. et al., *Transport of poly-beta-hydroxybutyrate in human plasma*, *Biochimica et Biophysica Acta.* 1123, 1992, p. 33 - 40.
7. In-house report, Astra Tech AB.
8. Hyperlink: <http://www.fontijne.nl/site/index.html> //appliances/platen presses, page visited 000114.
9. Chasin, M. and Langer, R., *Biodegradable polymers as drug delivery systems*, 1990, Marcel Dekker, Inc.
10. Gangrade, N. and Price, J.C., *Poly(hydroxybutyrate-hydroxyvalerate) microspheres containing progesterone: preparation, morphology and release properties*, *J. Microencapsulation*, 1991, Vol. 8, No. 2, 185-202.
11. *Plasma technology briefing note*, Plasma Ireland Ltd., Cork, Ireland. Available at hyperlink: <http://www.plasma-ireland.com/Plasmas/index.html>.
12. Rudie, B., *Hydrophilicity and Hydrophobicity*, hyperlink: <http://osmonics.com/products/Page772.htm>, page visited 000114.

13. McLaughlin, W.L. et al., *Dosimetry for radiation processing*, 1989, Taylor&Francis, ISBN 0-85066-740-2.
14. *Sterilization of health care products – Requirements for validation and routine control – Radiation sterilization*, International Standard, ISO 11137:1995(E)
15. Rosen, S.L., *Fundamental principles of polymeric materials*, 1982, John Wiley & Sons, Inc., p.57 – 58, ISBN 0-471-08704-1.
16. Billmeyer, F.W., Jr., *Textbook of polymer science*, 3rd ed., 1984, John Wiley & Sons, Inc., p. 211.
17. *Operating instructions, Ubbelohde-Viskosimeter*, Schott Geräte, Version 910103M
18. In-house report, Astra Tech AB
19. Fatigh, A., *Adhesion mellan nylon 6,6 och tre olika tryckkänsliga adhesiv som är baserade på akrylat, silikon och EVA*, 1997, Institutionen för polymerteknologi, Chalmers Tekniska Högskola, Sweden.
20. Wu, S., *Polymer interface and adhesion*, 1982, Marcel Dekker Inc., p. 178 - 181, ISBN 0-8247-1533-0.
21. Skoog and Leary, *Principles of Instrumental analysis*, 4th ed., 1992 Saunders College Publishing, ISBN 0-03-023343-7.
22. Shaw, D.J., *Introduction to colloid & surface chemistry*, 4th ed., 1992, Butterworth-Heinemann, Oxford, ISBN 0 7506 1182 0.
23. Brandrup and Immergut, *Polymer handbook*, 3rd ed., 1989, John Wiley & Sons, p. VII/15, ISBN 0-471-81244-7.
24. *Instructions for SEM*, FTS, AstraZeneca Mölndal, BIOLLO/991012
25. Hyperlink: <http://www.zurich.ibm.com/Technology/Atomic/atomic.force.html>: IBM Zurich Research Laboratory, page visited 000108.
26. Hyperlink: <http://enuxsa.eas.asu.edu/~vuppu/tmaf.html>, Research at the Arizona State University, page visited 000108.
27. Hyperlink: <http://www.coulter.com/Coulter/PC/SS000104.ASP>, page visited 000104.
28. Alberts et al., *Molecular biology of the cell*, 3rd ed., 1994, Garland Publishing, Inc., New York and London, ISBN 0-8153-1620-8.
29. Peluso, G. et al., *The differential effects of poly(2-hydroxyethyl methacrylate) and poly(2-hydroxyethyl methacrylate)/poly(caprolactone) polymers on cell proliferation and collagen synthesis by human lung fibroblasts*, Journal of Biomedical Materials Research, 1997, Vol. 34, p. 327 – 336.

30. Steele J.G. et al., *Mechanism of initial attachment of corneal epithelial cells to polymeric surfaces*, *Biomaterials* 18, 1997, p.1541 - 1551.
31. Tamada, Y. and Ikada, Y., *Fibroblast growth on polymer surfaces and biosynthesis of collagen*, *Journal of Biomedical Materials Research*, 1994, Vol. 28, p. 783 – 789.
32. Saad, B. et al., *Multiblock copolyesters as biomaterials: in vitro biocompatibility testing*, *Journal of materials science: Materials in medicine* 8, 1997, p. 497 - 505.
33. Rihova, B., *Biocompatibility of biomaterials: hemocompatibility, immunocompatibility and biocompatibility of solid polymeric materials and soluble targetable polymeric carriers*, *Advanced Drug Delivery Reviews* 21, 1996, p. 157 - 176.
34. Ho Lee, J. et al., *Interaction of fibroblast on polycarbonate membrane surfaces with different micropore sizes and hydrophilicity*, *J. Biomater. Sci. Polymer Edn.*, 1999, Vol. 10, No. 3, p. 283 – 294.
35. Ho Lee, J. et al., *Interaction of different types of cells on polymer surfaces with wettability gradient*, *Journal of Colloid and Interface Science* 205, 1998, p. 323 – 330.
36. Brocchini, S. et al., *Structure-property correlations in a combinatorial library of degradable biomaterials*, *Journal of Biomedical Materials Research*, 1998, Vol. 42, p. 66 – 75.
37. Elliott, W.M. and Auersperg, N., *Comparison of the Neutral Red and Methylene Blue Assay to Study Cell Growth in Culture*, *Biotechnic & Histochemistry*, 1993, Vol. 68, No. 1.
38. *CellTiter 96® AQueous Non-Radioactive Cell Proliferation Assay*, Promega Technical Bulletin, No. 169.
39. Bernatchez, S.F et al., *Interactions of macrophages with fibrous materials in vitro*, *Biomaterials*, 17, 1996, p. 2077 - 2086.
40. Takahashi, K. et al., *Development and heterogeneity of macrophages and their related cells through their differentiation pathways*, *Pathology International*, 46, 1996, p. 473 - 485.
41. Defife, K.M. et al., *Spatial regulation and surface chemistry control of monocyte/macrophage adhesion and foreign body giant cell formation by photochemically micropatterned surfaces*, *Journal of biomedical materials research*, 45, 1999, p. 148 - 154.
42. Axelsson, B., *Introduktion till immunologi*, 1994, Avd. För immunologi, Wennergrens Institut, Stockholms universitet.

43. Rouxhet, L. et al. *Interactions between a biodegradable polymer, poly(hydroxybutyrate-hydroxyvalerate), proteins and macrophages*, Macromolecular Symposium 130, 1998, p. 347 - 366.
44. Jirouskova, M. et al., *Comperative study of human monocyte and platelet adhesion to hydrogels in vitro – effect of polymerstructure*, Journal of materials science: Materials in medicine, 8, 1997, p. 19 - 23.
45. Garbassi et al., *Polymer Surfaces, from physcics to technology*, John Wiley & Sons Ltd., 1994, ISBN 0-471-93817-3.
46. Rice, J.M. et al., *Macrophage-polymer interactions*, Journal of Biomaterials science, Polymer edition, Vol 9, No. 8, 1998, p. 833 - 847.
47. Defife, K.M. et al., *Effects of photochemically immobilized polymer coatings on protein adsorption, cell adhesion, and the foreign body reaction to silicone rubber*, Journal of biomedical materials research, 44, 1999, p. 298 - 307.
48. Saad, B. et al., *Characterization of the cell response of cultured macrophages and fibroblasts to particles of short-chain poly[(R)-3-hydroxybutyric acid]*, Journal of biomedical materials research, Vol. 30, 1996, p. 429 - 439.
49. Johansson, G., *Macrophage and monocyte stimulating activity of PHB*, 1998, Astra Tech report, RP-RR-0086-A.
50. Zhou, Z., *Evaluation of 90:10 poly(D,L.lactide-co-glycolide) microspheres containing norethisterone: drug release and biodegradation*, Biomat., art. Cells & immob. Biotech., 41(4), 1993, p. 475 - 486.
51. Johnsson, E., *Patcher från ICI Zeneca*, Astra Tech report IQ02213-B
52. Shanbhag, A.S. et al., *Macrophage/particle interactions: Effect of size, composition and surface area*, Journal of biomedical materials research, 1994, Vol 28, p. 81 - 90.
53. Harris, D.C., *Quantitative chemical analysis*, 4th ed., 1995, W.H. Freeman and company, New York, ISBN 0-7167-2508-8.
54. Wallström, F., *Enzymatisk nedbrytning av PHB*, 1998, Institutionen för kemiteknik, Chalmers Lindholmen, Sweden.
55. Foster, L.J.R. and Tighe, B.J., *The degradation of gel-spun poly(β -hydroxybutyrate) wool*, Journal of Environmental Polymer Degradation, 1994, Vol. 2, No. 3, p. 185-194.
56. Saad, B. et al., *Development of degradable polyesterurethanes for medical applications: In vitro and in vivo evaluations*, Journal of Biomedical Materials Research, 1997, Vol. 36, p. 65 – 74.
57. Rouxhet, L., *Macromol. Symp.* 130, 1998, p. 347-366.

58. Råde och Rudemo, *Sannolikhetslära och statistik*, 1984, Biblioteksförlaget, Stockholm.

10 Appendices

- Appendix 1 *Harmonic-mean method and Gauss' approximation formula*
- Appendix 2 *Standard curves for GPC*
- Appendix 3 *Results from viscosimetry*
- Appendix 4 *FTIR-spectra*
- Appendix 5 *GPC data*
- Appendix 6 *Results from Student's t-test on fibroblast adhesion*
- Appendix 7 *Graphs from study 0, fibroblast adhesion*
- Appendix 8 *Results from fibroblast adhesion studies 0, 1, 2, 3, 4 and 5*
- Appendix 9 *Cytokine responses*

Appendix 1**1 (3)***Harmonic-mean method and Gauss' approximation formula*

The Harmonic-mean method uses the contact angles of two testing liquids, Young's equation and the harmonic-mean equation. In order to achieve the surface energy ($\gamma_s^D + \gamma_s^P$) of the solid, a system of equations has to be solved, see equations *i* and *ii*.

$$0.25(1+\cos\theta_1)\gamma_1 = (\gamma_1^d \gamma_s^d / (\gamma_1^d + \gamma_s^d)) + (\gamma_1^p \gamma_s^p / (\gamma_1^p + \gamma_s^p)) \quad (\text{eq. } i)$$

$$0.25(1+\cos\theta_2)\gamma_2 = (\gamma_2^d \gamma_s^d / (\gamma_2^d + \gamma_s^d)) + (\gamma_2^p \gamma_s^p / (\gamma_2^p + \gamma_s^p)) \quad (\text{eq. } ii)$$

where $\gamma = \gamma^d + \gamma^p$ and the subscript 1 and 2 refers to the testing liquids 1 and 2, respectively. If γ_j^d and γ_j^p for the testing liquids ($j = 1$ and 2) are known, the dispersion and polar components of solid surface tension (γ_s^d and γ_s^p) can be obtained from the contact angles, θ_1 and θ_2 , by solving the two equations. Water and metylene iodide are two convenient testing liquids, whose preferred γ^d and γ^p values are known. Subscript 1 refers to water and subscript 2 refers to metylene iodide.²⁰

$$\gamma_1^d = 22.1 \text{ mN/m}$$

$$\gamma_1^p = 50.7 \text{ mN/m}$$

$$\gamma_2^d = 44.1 \text{ mN/m}$$

$$\gamma_2^p = 6.7 \text{ mN/m}$$

The system of equations was solved using the following steps:

Set:

$$R = 0.25(1+\cos\theta_1) \text{ and } T = 0.25(1+\cos\theta_2)$$

$$A = \gamma_1, B = \gamma_1^d, C = \gamma_1^p, D = \gamma_2, E = \gamma_2^d \text{ and } F = \gamma_2^p$$

$$X = \gamma_s^d \text{ and } Y = \gamma_s^p$$

Solve X as a function of Y and Y as a function of X, see equations *iii* and *iv*.

Appendix 1**2 (3)**

$$X = (ABCR+(ABR-CB)Y) / (BC-ACR+(B+C-AR)Y) \quad (\text{eq. } iii)$$

$$Y = (DFET+(DFT-EF)X) / (EF-DET+(E+F+DT)X) \quad (\text{eq. } iv)$$

Set:

$$M = ABCR, N = ABR-CB, O = BC-ACR \text{ and } P = B+C-AR$$

$$Q = DEFT, S = DFT-EF, U = EF-DET \text{ and } V = E+F-DT$$

Insert the new variables (M, N, O, P, Q, S, U and V) in equations *iii* and *iv*, see equations *v* and *vi*.

$$X = (M+NY) / (O+PY) \quad (\text{eq. } v)$$

$$Y = (Q+SX) / (U+VX) \quad (\text{eq. } vi)$$

Equation *vi* inserted in equation *v* gives equation *vii*.

$$X = - (OU+QP-MV-SN) / 2(OV+SP) \pm [((OU+QP-MV-SN) / 2(OV+SP))^2 + (MU+QN)/(OV+SP)]^{0.5} \quad (\text{eq. } vii)$$

if $OV+SP \neq 0$

Set the surface energy = $SE = X$ (dispersion component) + Y (polar component)

In order to calculate the variance of the surface energy and its polar and dispersion component, Gauss' approximation formulas were used.⁵⁸ For this purpose the partial derivatives $\partial SE/\partial\theta_1$, $\partial SE/\partial\theta_2$, $\partial X/\partial\theta_1$, $\partial X/\partial\theta_2$, $\partial Y/\partial\theta_1$ and $\partial Y/\partial\theta_2$ are needed. Those were simulated for a given pair of $[\theta_1=a, \theta_2=b]$ by equations *viii* and *ix* (a and b are the means of measured values and their variances are denoted var a and var b).

$$\partial SE/\partial\theta_1 \Big|_{a,b} = [SE(a+\delta a, b) - SE(a-\delta a, b)] / 2*\delta a \quad (\text{eq. } viii)$$

$$\partial SE/\partial\theta_2 \Big|_{a,b} = [SE(a, b+\delta b) - SE(a, b-\delta b)] / 2*\delta b \quad (\text{eq. } ix)$$

Appendix 1

3 (3)

where $\delta a = \delta b = 0.001$. Smaller δa and δb were evaluated but did not give different results.

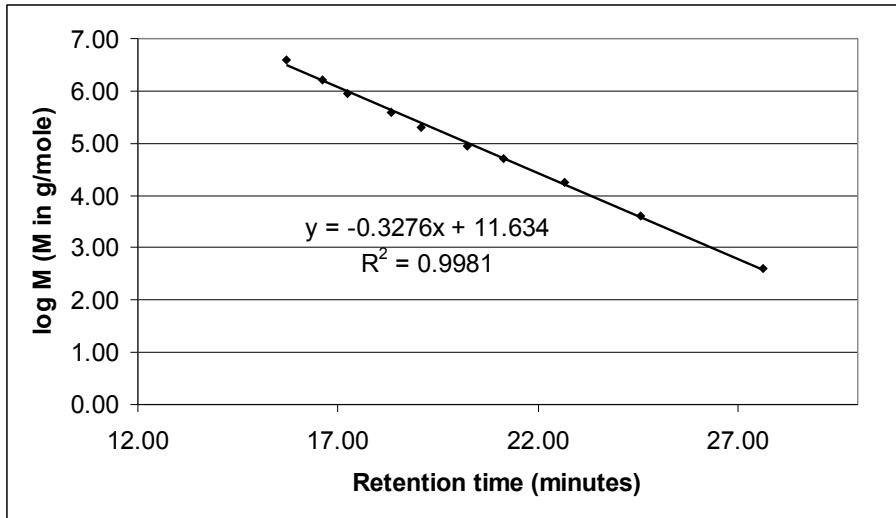
$\partial X/\partial\theta_1$, $\partial X/\partial\theta_2$, $\partial Y/\partial\theta_1$ and $\partial Y/\partial\theta_2$ were simulated in the same way.

Gauss' approximation formula gives, see equation x.

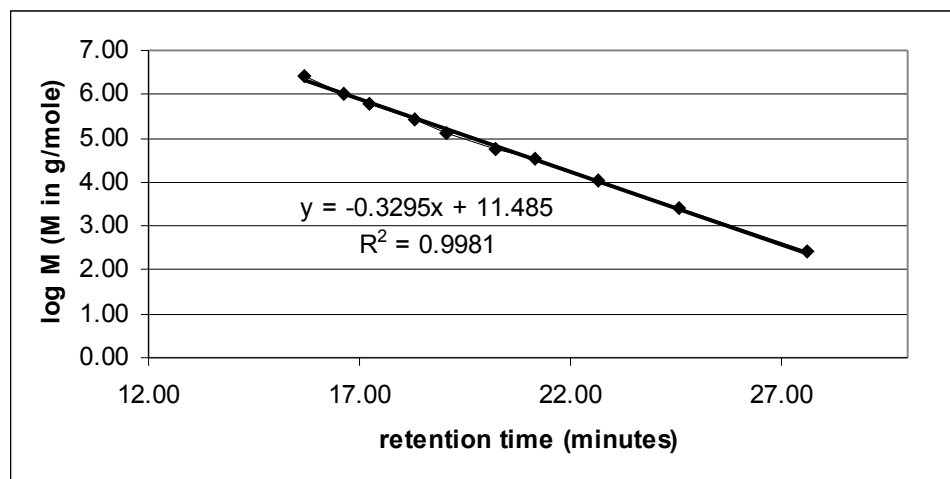
$$\text{var}[\text{SE}(a,b)] \approx (\partial\text{SE}/\partial\theta_1|_{a,b})^2 * \text{var } a + (\partial\text{SE}/\partial\theta_2|_{a,b})^2 * \text{var } b \quad (\text{eq. x})$$

$\text{var}[X(a,b)]$ and $\text{var}[Y(a,b)]$ were calculated in the same way.

Standard curves for GPC



PS standard curve for GPC.



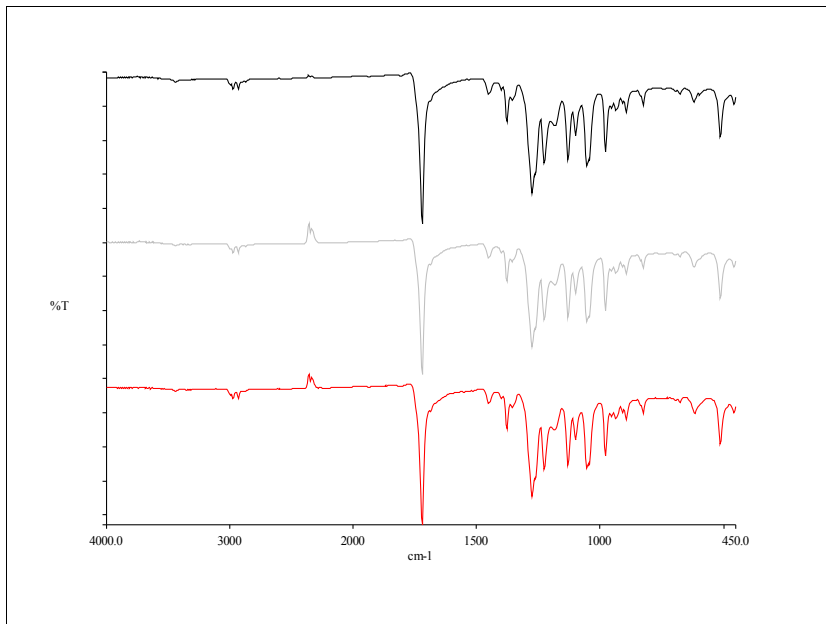
PHB standard curve for GPC.

Results from viscosimetry

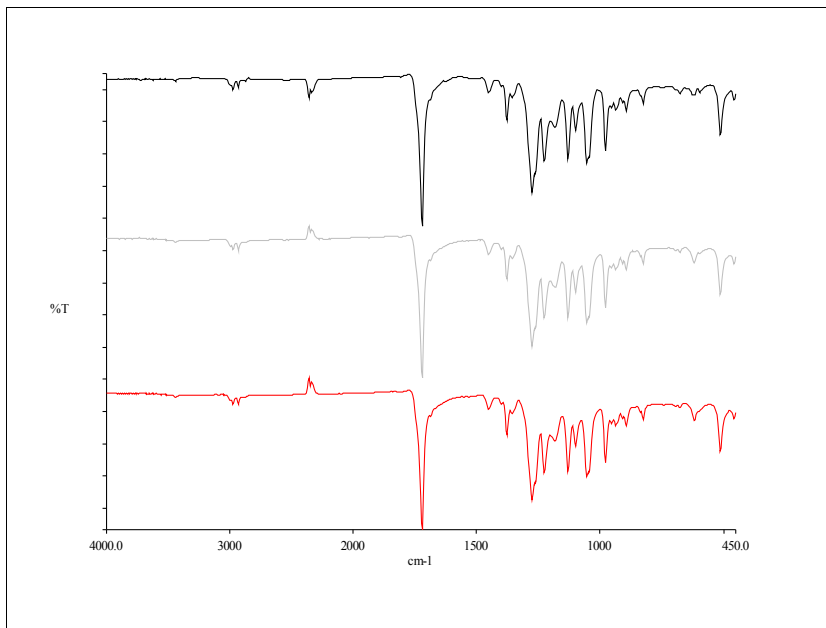
K=viscosimeter constant [mm²/s²], t= time [s],
 Mw = weight average molecular weight [g/mole]
 Each t-value is an average from three measurements.

Before radiation				After radiation		
	K [mm ²]	t [s]	Mw [g/mole]	K [mm ²]	t [s]	Mw [g/mole]
Fiber patch	0.005840	183.7	474982	0.005840	83.05	60009
	0.005947	179.5	471462	0.005947	81.34	59131
	0.005840	183.1	472426			
	0.005947	178.5	467025			
se REF	0.005947	176.1	456920	0.005947	83.79	69390
	0.005369	194.9	456493	0.005840	86.54	74399
	0.005947	174.5	450146	0.005947	84.82	73743
	0.005369	197.2	464934	0.005840	86.37	73698
se KOH	0.005947	176.5	458697	0.005947	83.47	68074
	0.005369	198.0	468181	0.005840	86.04	72365
	0.005947	177.9	464758	0.005947	84.67	73099
	0.005369	197.3	465490	0.005840	86.96	76145
mp REF	0.005947	110.9	183320	0.005947	84.63	72945
	0.005369	122.6	182343	0.005369	94.15	74495
	0.005947	109.5	177274	0.005947	84.66	73057
	0.005369	121.2	177023	0.005369	95.89	81066
mp KOH	0.005947	111.9	187463	0.005947	85.63	77144
	0.005369	123.4	185464	0.005369	96.01	81546
	0.005947	112.3	188989	0.005947	84.96	74317
	0.005369	123.5	185552	0.005840	87.59	78756

FTIR spectra



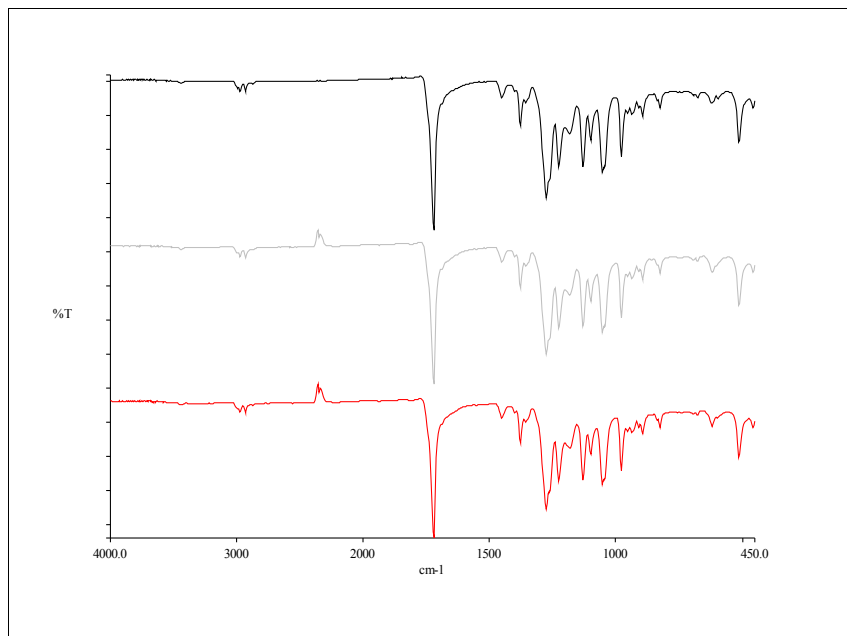
FTIR spectra of mp KOH, from above: before cell incubation, after fibroblast incubation and after macrophage incubation.



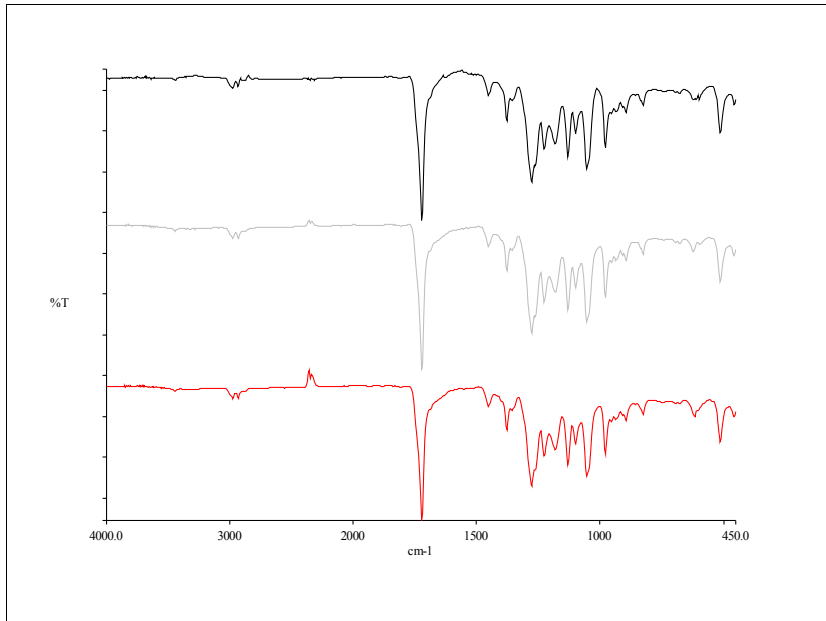
FTIR spectra of mp O2, from above: before cell incubation, after fibroblast incubation and after macrophage incubation.

Appendix 4

2 (4)



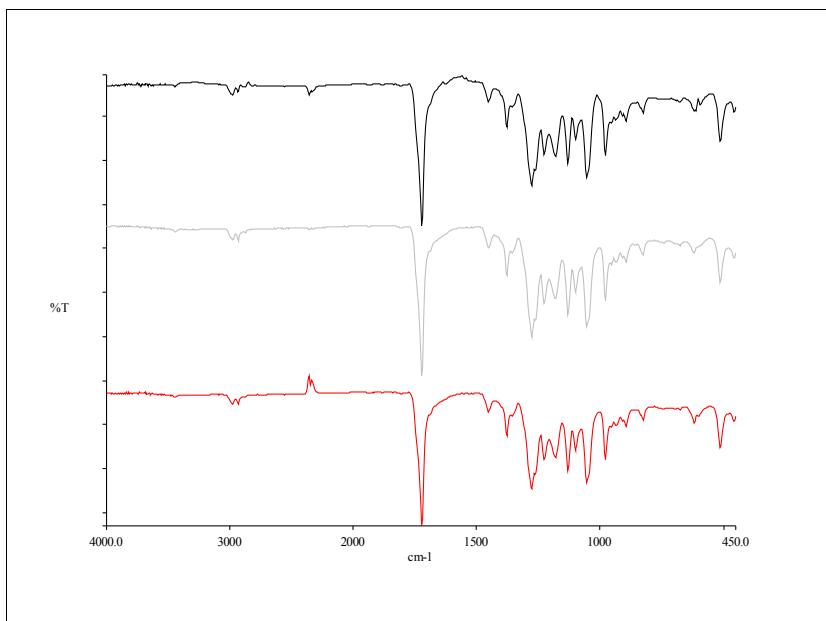
FTIR spectra of mp CHF3, from above: before cell incubation, after fibroblast incubation and after macrophage incubation.



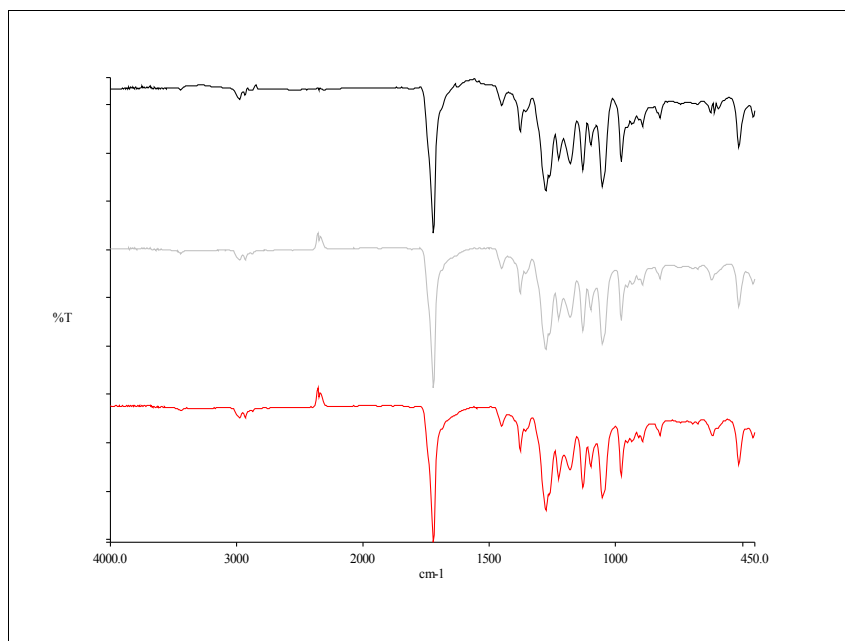
FTIR spectra of se KOH, from above: before cell incubation, after fibroblast incubation and after macrophage incubation.

Appendix 4

3 (4)



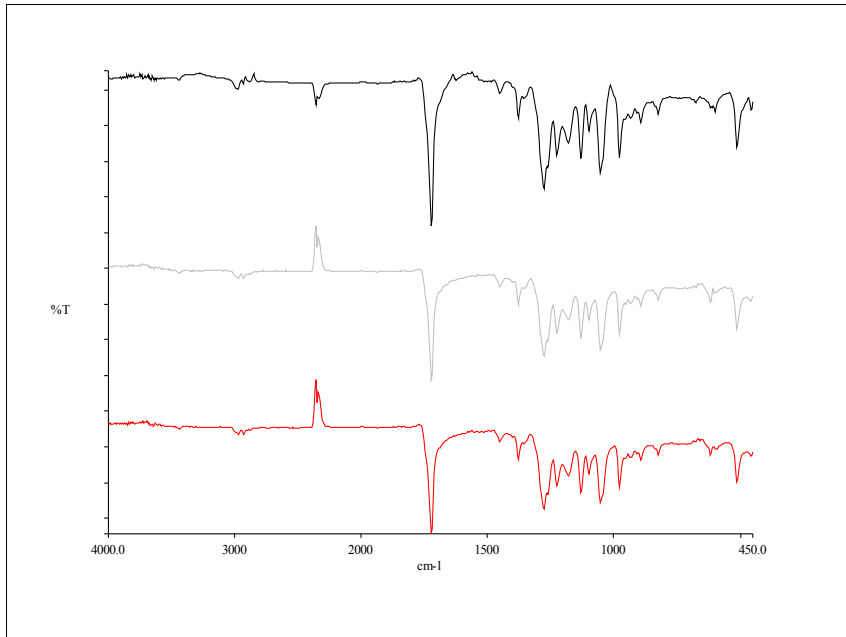
FTIR spectra of se O2, from above: before cell incubation, after fibroblast incubation and after macrophage incubation.



FTIR spectra of se CHF3, from above: before cell incubation, after fibroblast incubation and after macrophage incubation.

Appendix 4

4 (4)



FTIR spectra of PHB fibre patch, from above: before cell incubation, after fibroblast incubation and after macrophage incubation.

Appendix 5

1 (1)

GPC data

2 injections/sample

$$R = M_w / M_n$$

A = average peak area

m = mass PHB dissolved in 5 ml chloroform

THP-1 = incubated 5 days with THP-1 cells (macrophages)

MRC-5 = incubated 3 days with MRC-5 cells (fibroblasts)

Sample	Mn (g/mole)		Mw (g/mole)		R avg	A/m
	Mean	St.dev	Mean	St.dev		
se ref	25870	678	73678	3589	2.8	0.69
se KOH	21407	5011	71336	2325	3.4	0.78
se O2	26015	198	72198	3019	2.8	0.81
se CHF3	24170	484	67888	54	2.8	0.79
mp ref	29239	209	80084	761	2.7	0.73
mp KOH	27806	78	80967	173	2.9	0.74
mp O2	29201	957	81474	964	2.8	0.75
mp CHF3	30692	1	80180	1330	2.6	0.72
Patch	20336	697	56820	70	2.8	0.78
THP-1 se ref	25936	2255	70799	1139	2.7	0.78
THP-1 se KOH	21468	1421	70957	45	3.3	0.89
THP-1 se O2	25526	355	72229	4546	2.8	0.89
THP-1 se CHF3	26619	733	72070	623	2.7	0.73
THP-1 mp ref	27293	265	74909	1592	2.7	0.72
THP-1 mp KOH	27645	343	77051	438	2.8	0.66
THP-1 mp O2	28065	885	78635	1146	2.8	0.76
THP-1 mp CHF3	28381	45	76596	726	2.7	0.71
THP-1 Patch	21377	1894	55821	1701	2.6	0.73
MRC-5 se ref	28627	4965	69646	422	2.5	0.73
MRC-5 se KOH	17542	479	65034	1020	3.7	0.78
MRC-5 se O2	24968	3351	72293	556	2.9	0.79
MRC-5 se CHF3	25792	472	64827	5838	2.5	0.8
MRC-5 mp ref	26932	1589	80648	386	3.0	0.74
MRC-5 mp KOH	26541	134	80453	846	3.0	0.75
MRC-5 mp O2	27651	1375	78868	1426	2.9	0.77
MRC-5 mp CHF3	27805	680	78065	646	2.8	0.73
MRC-5 Patch	23191	1853	70365	2290	3.0	0.74

Appendix 6

1 (4)

Results from Student's t-test on fibroblast adhesion

Study 1

████████ = significant difference at level p(a)
████████ = no significant difference at level p(a)
 [blank] = can't be measured due to failed pieces; reason subjected next to data

a = number of t-tests performed
 n = number of samples

NR-viability test. No TCPS.
 n=2 if not else subjected
 a = 13; p(a) < 0,0039; 99,6% confidence interval

Tested vs. reference surface at all times				
	1h	24h	72h	
se KOH				1h, 24h se REF; n=1 72h se CHF3; n=1
se O2				
se CHF3				
mp KOH				72h mp REF; n=1
mp O2				
mp CHF3				

Tested 1h vs. 72h of the same type of piece		
se REF		1h se REF; n=1 72h se CHF3; n=1
se KOH		
se O2		
se CHF3		
mp REF		72h mp REF; n=1
mp KOH		
mp O2		
mp CHF3		

Appendix 6

2 (4)

Study 2

████████ = significant difference at level $p(a)$
████████ = no significant difference at level $p(a)$
 [blank] = can't be measured due to failed pieces; reason submitted next to data

a = number of t-tests performed
 n = number of samples

NR-viability test.
 n=4 for TCPS and 2 for all others, if not else submitted
 a = 32; $p(a) < 0,0016$; 99,8% confidence interval

Tested vs. TCPS surface at all times			
	1h	24h	72h
se REF			
se KOH			
se O2			
se CHF3			
mp REF			
mp KOH			
mp O2			
mp CHF3			

1h se REF; n=1

Tested 1h vs. 72h of the same type of piece			
	1 vs 72		
se REF			
se KOH			
se O2			
se CHF3			
mp REF			
mp KOH			
mp O2			
mp CHF3			
		1 vs. 24	24 vs. 72
TCPS	(no test)		

1h se REF; n=1

Appendix 6

3 (4)

Study 3

= significant difference at level p(a)
 = no significant difference at level p(a)
 [blank] = can't be measured due to failed pieces; reason submitted next to data

a = number of t-tests performed
 n = number of samples

MTS-viability test.
 n=4 for TCPS and 3 for all others, if not else submitted
 a = 34; p(a) < 0,0015; 99,8% confidence interval

Tested vs. TCPS surface at all times				
	1h	24h	72h	
se REF				1h se REF, KOH, O2; n=2
se KOH				24 h se KOH, O2, CHF3; n=2
se O2				72h se KOH; n=2
se CHF3				
mp REF				1h mp O2; n=2
mp KOH				72h mp O2; n=2
mp O2				
mp CHF3				

Tested 1h vs. 72h of the same type of piece			
1 vs 72			
se REF			
se KOH			
se O2			
se CHF3			
mp REF			
mp KOH			
mp O2			
mp CHF3			
		1 vs. 24	24 vs. 72
TCPS	(no test)		

Appendix 6

4 (4)

Study 4; double cell concentration

 = significant difference at level p(a)
 = no significant difference at level p(a)
 [blank] = can't be measured due to failed pieces; reason submitted next to data

a = number of t-tests performed
 n = number of samples

NR-viability test.
 n=4 for TCPS and 2 for all others, if not else submitted
 a = 8; p(a) < 0,0064; 99,4% confidence interval

Tested vs. TCPS surface at 1h	
1h	
se REF	
se KOH	
se O2	
se CHF3	
mp REF	
mp KOH	
mp O2	
mp CHF3	

Adhesion; comparison of week 2, 3 and double cell concentration

 = significant difference at level p(a)
 = no significant difference at level p(a)
 [blank] = can't be measured due to failed pieces; reason submitted next to data

a = number of t-tests performed
 n = number of samples

NR-viability test.
 n=4 for TCPS and 3 or 2 for all others, if not else submitted
 a = 23; p(a) < 0,0022; 99,8% confidence interval

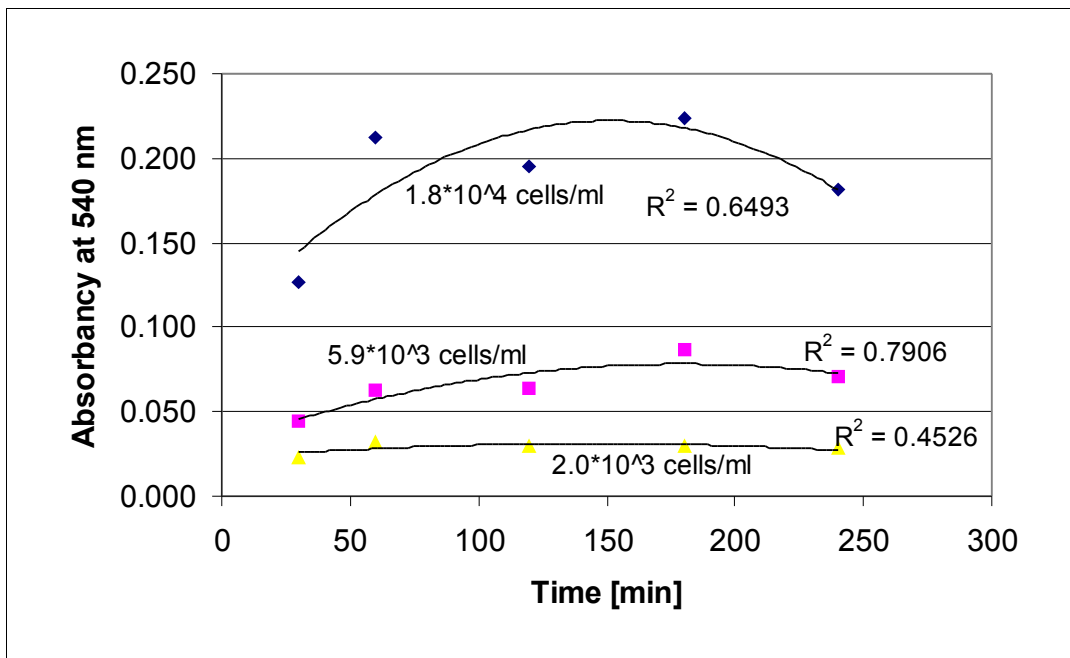
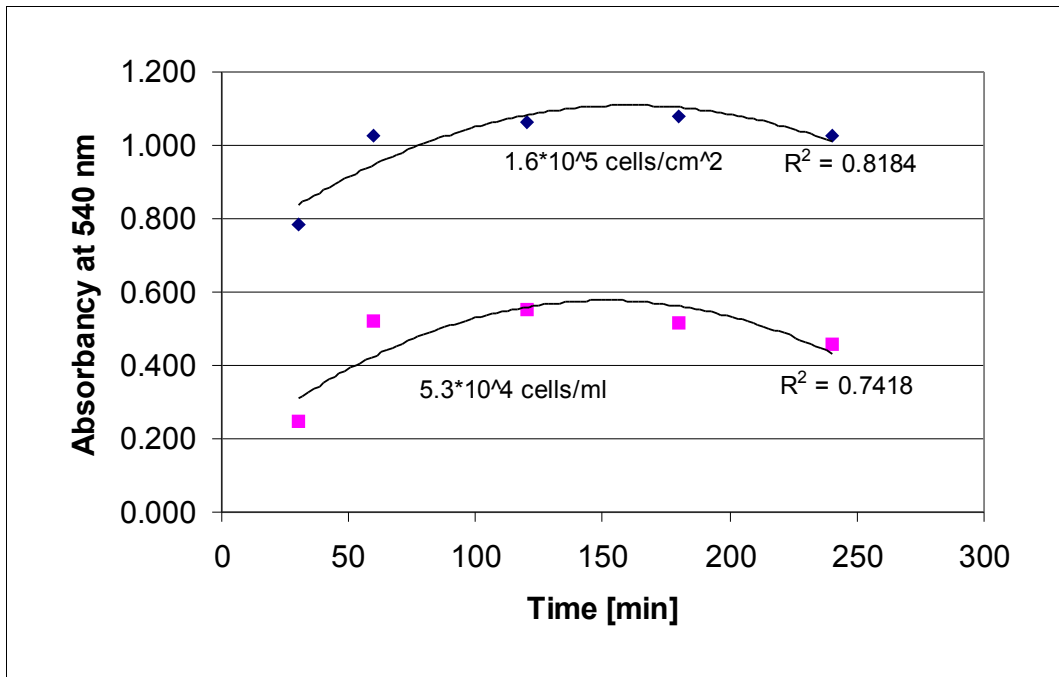
Tested vs. TCPS surface at 1h			
	week 2	week 3	double
se REF			
se KOH			
se O2			
se CHF3			
mp REF			
mp KOH			
mp O2			
mp CHF3			

1h se REF, week 2; n=1

Appendix 7

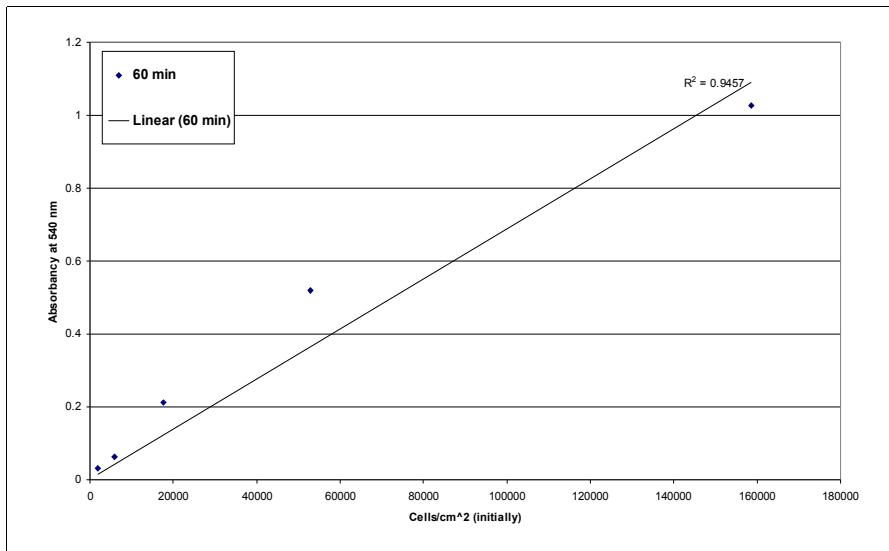
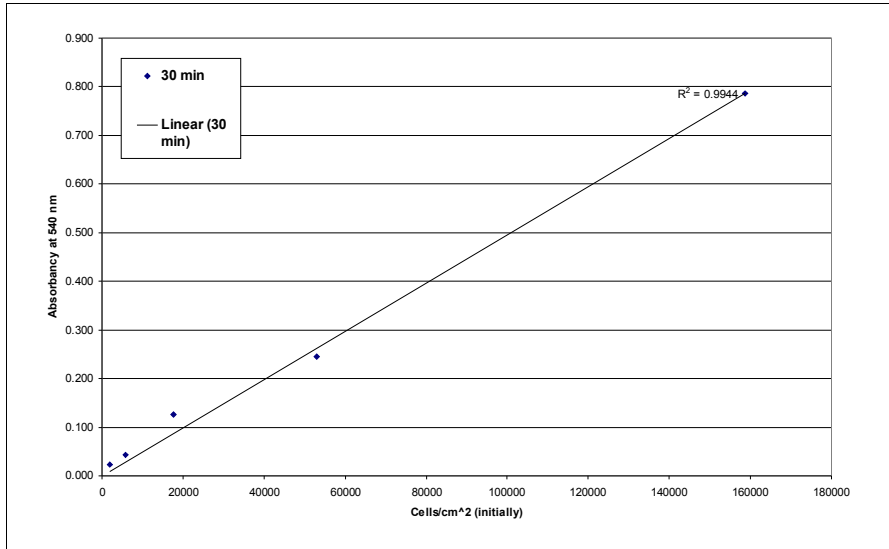
1 (3)

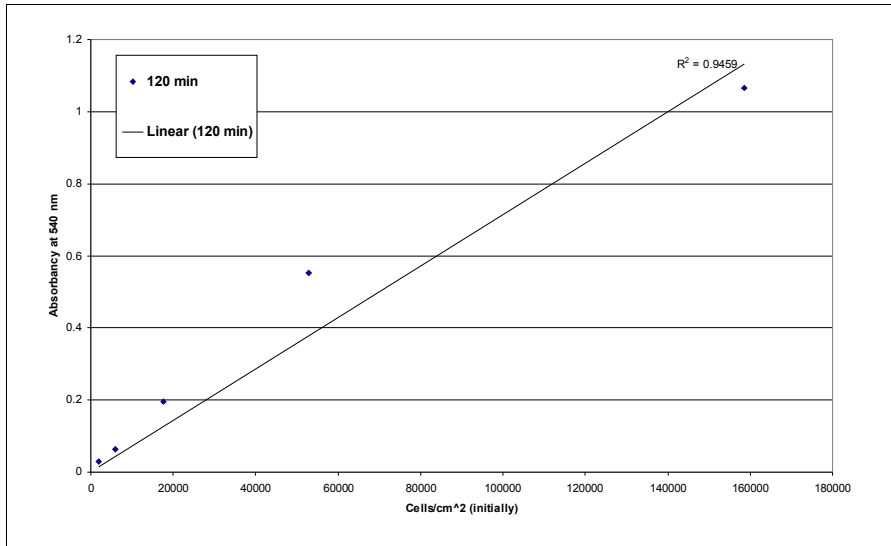
Graphs from study 0, fibroblast adhesion

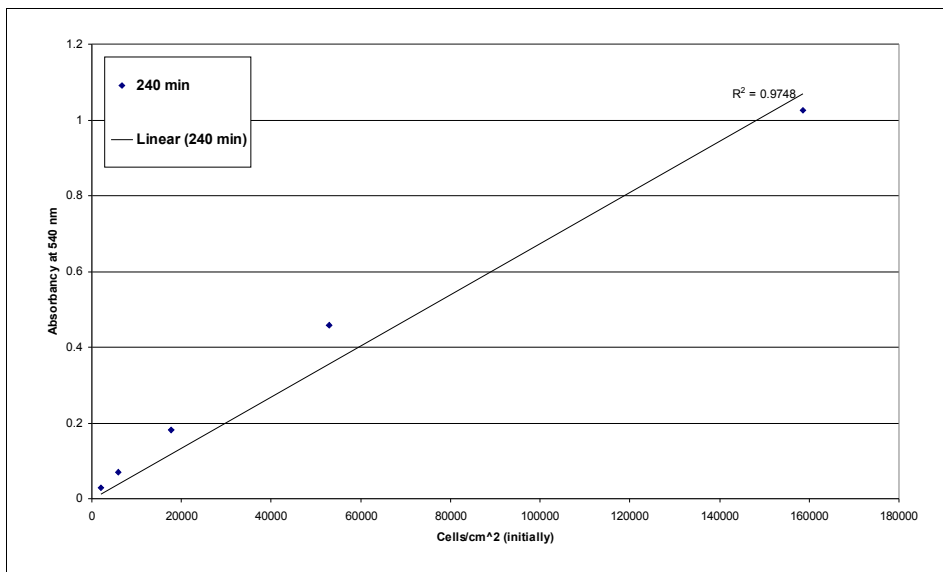
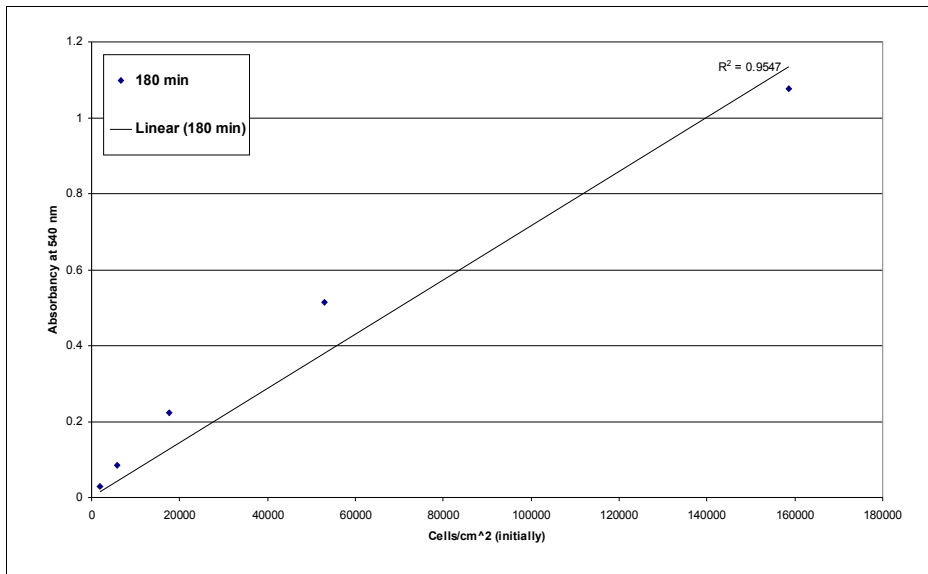


Appendix 7

2 (3)







Appendix 8

1 (3)

Results from fibroblast study 0,1, 2, 3, 4 and 5

Study 0

Unit: Absorbancy units (AU)

N=3

		Cells/ cm ²					
		158667		52889		17630	
Minutes	Abs	St. dev.	Abs	St. dev.	Abs	St. dev.	
30	0,786	0,091	0,246	0,064	0,127	0,040	
60	1,028	0,026	0,519	0,044	0,213	0,010	
120	1,065	0,046	0,553	0,022	0,195	0,047	
180	1,076	0,181	0,513	0,017	0,224	0,007	
240	1,026	0,197	0,457	0,037	0,182	0,006	
		Cells/ cm ²					
		5877		1959			
Minutes	Abs	St. dev.	Abs	St. dev.			
30	0,044	0,004	0,023	0,002			
60	0,063	0,006	0,032	0,001			
120	0,064	0,014	0,030	0,008			
180	0,086	0,004	0,029	0,007			
240	0,070	0,006	0,028	0,004			

Study 1

Unit: Absorbancy units (AU)

N=2 (or 1).

Results shown have been reduced with the results from study 5.

		se REF		se KOH		se O2		se CHF3	
Hours	Abs	St. dev.	Abs	St. dev.	Abs	St. dev.	Abs	St. dev.	
1	0,062	0,000	0,017	0,024	0,060	0,031	0,059	0,011	
24	0,082	0,003	0,191	0,016	0,167	0,028	0,038	0,025	
72	0,202	0,058	0,411	0,003	0,291	0,016	0,299	0,000	
		mp REF		mp KOH		mp O2		mp CHF3	
Hours	Abs	St. dev.	Abs	St. dev.	Abs	St. dev.	Abs	St. dev.	
1	0,090	0,002	0,065	0,028	0,115	0,001	0,098	0,002	
24	0,195	0,001	0,167	0,032	0,174	0,009	0,162	0,022	
72	0,557	0,001	0,498	0,047	0,551	0,038	0,450	0,056	

Appendix 8

2 (3)

Study 2

Unit: Absorbance units (AU)

N=2 (or 1) for PHB and n=4 for TCPS

Results shown have been reduced with the results from study 5.

	se REF		se KOH		se O2	
Hours	Abs	St. dev.	Abs	St. dev.	Abs	St. dev.
1	0,150	0,000	0,090	0,025	0,224	0,038
24	0,199	0,127	0,467	0,042	0,326	0,054
72	0,427	0,045	0,499	0,013	0,560	0,001
	se CHF3		TCPS		mp REF	
Hours	Abs	St. dev.	Abs	St. dev.	Abs	St. dev.
1	0,044	0,006	0,331	0,012	0,210	0,010
24	0,062	0,005	0,487	0,003	0,409	0,034
72	0,438	0,016	0,632	0,009	0,666	0,030
	mp KOH		mp O2		mp CHF3	
Hours	Abs	St. dev.	Abs	St. dev.	Abs	St. dev.
1	0,114	0,014	0,226	0,006	0,148	0,080
24	0,373	0,002	0,385	0,006	0,361	0,054
72	0,565	0,003	0,604	0,035	0,575	0,049

Study 3

Unit: Absorbance units (AU)

N=3 (or 2) for PHB and n=4 for TCPS

	se REF		se KOH		se O2	
Hours	Abs	St. dev.	Abs	St. dev.	Abs	St. dev.
1	0,116	0,134	0,177	0,016	0,305	0,000
24	0,132	0,190	0,072	0,014	0,303	0,051
72	0,602	0,303	0,813	0,088	0,711	0,246
	se CHF3		TCPS		mp REF	
Hours	Abs	St. dev.	Abs	St. dev.	Abs	St. dev.
1	0,037	0,024	0,676	0,020	0,234	0,055
24	0,182	0,088	1,044	0,030	0,561	0,114
72	0,769	0,067	1,413	0,017	0,750	0,115
	mp KOH		mp O2		mp CHF3	
Hours	Abs	St. dev.	Abs	St. dev.	Abs	St. dev.
1	0,160	0,047	0,322	0,024	0,244	0,038
24	0,531	0,278	0,513	0,161	0,470	0,249
72	0,785	0,100	0,792	0,112	0,868	0,108

Appendix 8

3 (3)

Study 4

Unit: Absorbance units (AU)

N=2 for PHB and n=4 for TCPS

Results shown have been reduced with the results from study 5.

	se REF		se KOH		se O2	
Hours	Abs	St. dev.	Abs	St. dev.	Abs	St. dev.
1	0,064	0,003	0,332	0,048	0,270	0,103
	se CHF3		TCPS		mp REF	
Hours	Abs	St. dev.	Abs	St. dev.	Abs	St. dev.
1	0,046	0,013	0,493	0,010	0,355	0,037
	mp KOH		mp O2		mp CHF3	
Hours	Abs	St. dev.	Abs	St. dev.	Abs	St. dev.
1	0,353	0,018	0,408	0,048	0,385	0,030

Study 5

Unit: Absorbancy units (AU)

N=2 for PHB and n=3 (1h) or 4 (24h) for TCPS

	se REF		se KOH		se O2	
Hours	Abs	St. dev.	Abs	St. dev.	Abs	St. dev.
1	0,021	0,000	0,099	0,031	0,042	0,017
24	0,028	0,004	0,089	0,003	0,046	0,000
	se CHF3		TCPS		mp REF	
Hours	Abs	St. dev.	Abs	St. dev.	Abs	St. dev.
1	0,024	0,001	0,006	0,000	0,017	0,001
24	0,027	0,000	0,003	0,001	0,017	0,001
	mp KOH		mp O2		mp CHF3	
Hours	Abs	St. dev.	Abs	St. dev.	Abs	St. dev.
1	0,083	0,013	0,015	0,001	0,026	0,001
24	0,062	0,002	0,013	0,001	0,026	0,000

Appendix 9

1 (3)

Cytokine responses

TNF- α responses

Unit: pg/ml

N = 3 for PHB samples and n = 4 for positive and negative controls

	Negative control		mp ref		mp KOH	
Hours	C average	St dev	C average	St dev	C average	St dev
6	2687	344	2829	964	3474	465
24	1606	449	1991	588	2485	154
46	1887	93	1505	588	2433	243
54	751	72	1077	612	1599	292
	mp O2		mp CHF3		Patch	
Hours	C average	St dev	C average	St dev	C average	St dev
6	3282	221	3296	218	2604	73
24	1677	701	2321	77	1677	329
46	1724	244	2441	276	1344	567
54	1016	383	1771	113	791	402
	se ref		se KOH		se O2	
Hours	C average	St dev	C average	St dev	C average	St dev
6	2604	177	1888	568	2363	306
24	3027	479	2282	320	2241	133
46	4271	691	2905	525	3219	720
54	3102	1235	1863	307	2641	769
	se CHF3		Positive control			
Hours	C average	St dev	C average	St dev		
6	2527	376	15817	1381		
24	2185	262	17598	717		
46	2544	764	26659	2306		
54	2233	650	27654	1644		

Appendix 9

2 (3)

IL-1 β responses

Unit: pg/ml

N = 3 for PHB samples and n = 4 for positive and negative controls

	Negative control		mp ref		mp KOH	
Hours	C average	St dev	C average	St dev	C average	St dev
6	804	71	969	30	1029	131
24	632	29	619	62	639	60
46	870	65	1128	58	1128	29
54	908	125	1112	58	1145	132
	mp O2		mp CHF3		Patch	
Hours	C average	St dev	C average	St dev	C average	St dev
6	929	46	919	87	1069	262
24	659	135	569	75	709	62
46	1012	126	912	76	1512	225
54	795	87	862	225	1678	153
	se ref		se KOH		se O2	
Hours	C average	St dev	C average	St dev	C average	St dev
6	849	60	819	60	829	17
24	649	46	679	17	649	46
46	1212	58	1128	115	1295	150
54	1112	153	1012	153	1278	58
	se CHF3		Positive control			
Hours	C average	St dev	C average	St dev		
6	789	79	4694	359		
24	699	90	4663	1837		
46	1178	126	3550	239		
54	1128	115	3581	329		

Appendix 9

3 (3)

IL-6 responses

Unit: pg/ml

N = 3 for PHB samples and n = 4 for positive and negative controls

	Negative control		mp ref		mp KOH	
Hours	C average	St dev	C average	St dev	C average	St dev
6	255	43	259	29	212	50
24	290	39	309	46	255	49
46	531	70	246	134	185	169
54	481	147	529	184	291	63
	mp O2		mp CHF3		Patch	
Hours	C average	St dev	C average	St dev	C average	St dev
6	215	21	252	26	312	95
24	279	25	375	15	339	15
46	485	277	663	67	468	101
54	363	135	591	63	613	175
	se ref		se KOH		se O2	
Hours	C average	St dev	C average	St dev	C average	St dev
6	242	26	252	20	205	38
24	329	25	332	10	285	29
46	563	140	591	51	418	101
54	507	42	541	136	424	190
	se CHF3		Positive control			
Hours	C average	St dev	C average	St dev		
6	182	26	1488	175		
24	225	21	3925	602		
46	341	63	7629	228		
54	335	58	7796	782		